National Library
of Canada

Acquisitions and
Bibliographic Services Branch

395 Wellington Street
Ottawa, Ontario
K1A 0N4

Bibliothèque nationale
du Canada

Direction des acquisitions et
des services bibliographiques

395, rue Wellington
Ottawa (Ontario)
K1A 0N4

NOTICE

The quality of this microform is heavily dependent upon the quality of the original thesis submitted for microfilming. Every effort has been made to ensure the highest quality of reproduction possible.

If pages are missing, contact the university which granted the degree.

Some pages may have indistinct print especially if the original pages were typed with a poor typewriter ribbon or if the university sent us an inferior photocopy.

AVIS

La qualité de cette microforme dépend grandement de la qualité de la thèse soumise au microfilmage. Nous avons tout fait pour assurer une qualité supérieure de reproduction.

S'il manque des pages, veuillez communiquer avec l'université qui a conféré le grade.

La qualité d'impression de certaines pages peut laisser à désirer, surtout si les pages originales ont été dactylographiées à l'aide d'un ruban usé ou si l'université nous a fait parvenir une photocopie de qualité inférieure.

Canada

THE DISTRIBUTION AND GEOCHEMISTRY OF PLATINUM-GROUP ELEMENTS AT THE CRETACEOUS-TERTIARY BOUNDARY

Noreen J. Evans, M.Sc.

A thesis submitted
to the School of Graduate Studies and Research
in partial fulfillment of the requirements
for the Ph.D Degree: Science

Ottawa-Carleton Geoscience Centre
University of Ottawa

ISBN 0-315-85773-0

UNIVERSITÉ D'OTTAWA
UNIVERSITY OF OTTAWA

ABSTRACT

The globally-deposited clay layer marking the Cretaceous-Tertiary boundary has been studied to determine the mineralogical carrier phases for the anomalously concentrated platinum-group elements, the affinity of these elements for organic complexes in low temperature environments, the degree of terrestrial input to the boundary clay and the usefulness of platinum-group elemental ratios in projectile identification.

Grain size separates from marine and terrestrial Cretaceous-Tertiary boundary sites were analyzed for platinum-group elements (Pt, Pd, Ru, Ir, Rh) and gold using sensitive induced coupled plasma mass spectrometry. Detection limits on a five gram sample are 0.05 ppb (Rh, Ru, Ir), 0.1 ppb (Pt, Pd) and 0.2 ppb (Au).

Platinum-group elements are concentrated in clay minerals (smectite and illite-smectite clay) formed by the alteration of the original microtektite host. There is also an ubiquitous organic carrier. Ruthenium and Ir were found to be least susceptible to be fixed in organics. This fact, combined with the geochemical coherence of Ru and Ir makes them more suitable than the other platinum-group elements for estimating the terrestrial platinum-group element input to the boundary clay and for identifying the projectile.

The Ru/Ir ratio of marine sections (1.77 $\pm$ 0.53) is statistically different from that of the terrestrial sites (0.92 $\pm$ 0.28), and each represents a relatively coherent group. The marine Ru/Ir ratios are chondritic (1.48 $\pm$ 0.09), but the terrestrial ratios are not. Fractionation of Ru and Ir during condensation from the ejecta cloud may account for the broad differences between marine and terrestrial sites. Post-sedimentary alteration, remobilization or terrestrial PGE input may be responsible for the Ru/Ir ratio variations within the groups of marine and terrestrial sites studied. Modelling indicates that the marine ratios could also be attained if $\approx$ 15% of the boundary metals were contributed by Deccan Trap emissions. However, volcanic emissions could not have been the principal source of platinum-group elements in the boundary clay because mantle PGE ratios and abundances are inconsistent with those measured in the clay. The Ru/Ir values for pristine Tertiary mantle xenoliths (2.6 $\pm$ 0.48), picrites (4.1 $\pm$ 1.8) and for the Deccan Trap basalt (3.42 $\pm$ 1.96) are all statistically distinct from those measured in the Cretaceous-Tertiary boundary clay.

Several Canadian impact craters, believed to have been formed by the impact of chondritic projectiles, were analyzed for platinum-group elements in order to test if the interelement ratios identify the chondrite (i.e., the nature of the impactor). However, the dirth of literature data for various types of meteorites, the overall similarity in their platinum-group element ratios, the unknown fractionation effect upon meteorite volatilization and condensation, and the post-depositional alteration and remobilization of platinum-group elements all hamper application of the technique. Consequently, platinum-group elements cannot be readily utilized for identifying impactors beyond broad groups of meteorites (e.g., chondrite vs. iron). Nevertheless, they can often be used as supporting geochemical evidence, along with other elements (e.g., with Ni, Cr, Co abundance and ratios). This is the case at the K-T boundary, where Ru/Ir ratios, mineralogical and geochemical evidence all support a chondritic nature for the impactor.

RESUMÉ

La répartition mondiale de l'horizon d'argile marquant la transition Crétacé-Tertiaire (K-T) a été étudiée pour déterminer: les phases minéralogiques ayant une concentration anormale d'élements du groupe platinoïde, l'affinité de ces éléments pour les complexes organiques dans des environnements à basse température, et l'utilité des rapports des éléments platinoïdes pour l'identification du type de projectile.

Des échantillons de la transition K-T provenant de milieux marins et terrestres ont été séparés suivant leurs granulométries et analysés pour l'or et les éléments du groupe platinoïdes (Pt, Pd, Ru, Ir, Rh). Les analyses ont été effectuées en utilisant un spectromètre de masse par plasma à couplage inductif de haute sensibilité dont les limites de détection sur des échantillons de 5 grammes sont 0.05 ppb (Rh, Ru, Ir), 0.1 ppb (Pt, Pd) et 0.2 ppb (Au).

Les éléments du groupe platinoïdes sont concentrés dans les minéraux argileux: smectite et illite-smectite. Ces minéraux sont les produits d'altération des microtectites, à l'origine hôtes des platinoïdes. De plus, un porteur organique est omniprésent. Les recherches démontrent que le Ru et l'Ir sont les moins susceptibles à former des complexes organiques. Ce comportement du Ru et Ir associé à leur cohérence géochimique les rendent plus appropriés que les autres éléments platinoïdes pour estimer l'ajout d'éléments platinoïdes à l'horizon marqueur, et aider à l'identification du type de projectile.

Le rapport Ru/Ir des sections marines (1.77+0.53) se distingue statistiquement de celui des sections terrestres (0.92+0.28), et chacun représente un groupe relativement cohérent. Les rapport marins Ru/Ir sont chondritiques (1.48+0.09), tandis que les rapports terrestres ne le sont pas. Le fractionnement du Ru et Ir durant la condensation du nuage d'éjecta pourrait expliquer les variations entre les sites marins et terrestres. L'altération post-sédimentaire, la remobilisation ou un ajout par des platinoïdes terrestres pourraient être la cause des variations des rapport Ru/Ir des groupes d'échantillons marins et terrestres. Un modèle conceptuel propose que si ≈15% des métaux de l'horizon marqueur provenaient des émissions volcaniques de Deccan, le rapport Ru/Ir de sites marins pourrait être également atteint. Cependant, des émissions volcaniques n'auraient pu être la source principale des éléments platinoïdes dans l'horizon marqueur, puisque les rapports et les quantités de platinoïdes dans le manteau ne correspondent pas à ceux de l'horizon marqueur argileux. Les valeurs Ru/Ir, pour des xénolithes du manteau Tertiaire (2.6±0.48), pour des picrites (4.1±1.8) et pour des basaltes "Deccan Trap" (3.42±1.96), sont toutes statistiquement distinctes de celles analysées dans l'horizon argileux de la transition K-T.

Plusieurs cratères canadiens, dont l'origine semble être le résultat d'un impact par un projectile chondritique, ont été analysés pour les éléments du groupe platinoïdes afin de déterminer si les rapports inter-éléments peuvent identifier la chondrite (i.e. la nature du projectile). Cependant, le manque de données disponibles dans la littérature sur les différents types de météorites, les effets inconnus du fractionnement durant la

volatilisation et la condensation du météorite, la similarité générale dans le rapport d'éléments platinoïdes, ainsi que l'altération post-dépositionnelle et la remobilisation des éléments du groupe platinoïde rendent douteuse l'application de cette technique. En conséquence, les éléments du groupe platinoïde ne peuvent pas être directement utilisés pour identifier le type de projectile, mais seulement pour l'identification générale du type de météorite (i.e. chondritique vs. ferreux). Néanmoins, ils peuvent être souvent utilisés avec d'autres éléments (e.g. les quantités et rapport de Ni, Cr et Co) comme évidences géochimiques additionelles pouvant aider à cerner le type de projectile. Ainsi, concernant la transition K-T, les rapports Ru/Ir de même que les évidences minéralogiques et géochimiques suggèrent un projectile de nature chondritique.

ACKNOWLEDGEMENTS

The following people supplied sample material for this study; R.R. Brooks, C. Orth, F.Fleming, J. Nichols, J. Smit, J. Lerbekmo, A. Montanari, S.F. Sethna, R.K. Srivastava, S.S. Desjmukh, A.T. Rao, B. Baragar, I. Jonasson, D. Francis, J.H. Crocket and R.A.F. Grieve. All these donations are most gratefully acknowledged. I thank Yars Bodnaruk for his aid in the field in Europe. Brent McInnes provided valuable advice and help with sample collection in the U.S.A. and New Zealand. H. Stradner and A Preisinger are sincerely thanked for their guidance to the Austrian sections and their gracious hospitality during my stay in Austria. H. Hansen is acknowledged for his able guidance to the Stevns Klint site. H. Geldsetzer, C. Orth, G. Izett and J. Smit provided written guidance to other K-T sites and are warmly acknowledged. M. Wotton is thanked for preparation of initial 3-D diagrams. I am grateful to Caroline Duchesne for preparing tables and to Alex Langshur for translation of the abstract. I thank K. Besso for XRD analysis performed at CANMET and D. Riedel for XRD performed at the Ruhr University, Bochum, Germany. Mike Villeneuve, Laura Radburn and David Walker are thanked for SEM analysis at the Geological Survey of Canada. R. Kretz provided critical review of early drafts for which I thank him. Norman Miles contributed greatly through his guidance in the laboratory at Agriculture Canada and through his ongoing support. R.A.F. Grieve provided critical review of the thesis and manuscript drafts, for which I thank him. I am grateful to Digby McLaren for his help in setting up the project and many fruitful discussions. D.C. Gregoire is warmly thanked for performance of ICP-MS analyses, many consultations during chemical preparations, and for his undying sense of humor when it was needed most. W.D. Goodfellow was an integral part of this work, coordinating and supporting the project through the Geological Survey of Canada, organizing the committee and always providing stimulating criticism of ideas and written work. J. Veizer provided financial support for the project, critical assessment of all written work and is sincerely thanked for going out on a limb to support both me and this project. The financial support was provided by an NSERC postgraduate scholarship to the author and an NSERC Operating Grant to J. Veizer. Finally, I want to thank my husband, Brent for being my sounding board, my inspiration and my partner.

"Simple solutions come only from
detailed understanding of the complications"

R.H.T. Bates, 1984.

This thesis is dedicated to my parents,
Peter and Joan Evans

TABLE OF CONTENTS

TABLE OF CONTENTS

TABLE OF CONTENTS

TABLE OF CONTENTS

List of Figures

List of Figures

List of Figures

List of Figures

List of Tables

List of Tables

CHAPTER ONE

INTRODUCTION

Sixty-five million years ago half of the biological families living on Earth became extinct. Although not the largest mass extinction in Earth history, the one paleontologically marking the Cretaceous-Tertiary (K-T) boundary has garnered much attention since evidence was found to indicate a non-terrestrial causal event (Alvarez et al., 1980). The fact that the 165 Ma long reign of the dinosaurs was terminated at the end of the Cretaceous has focussed much public interest on the K-T boundary. It is also one of the best preserved major extinction boundaries due to its relatively young age and the small amount of oceanic crust that has been subducted during the past 66 Ma (< 30%; A.G. Smith in Alvarez et al., 1982). Alvarez et al. (1980) provided evidence to support the previously suggested hypothesis (Ager, 1973; Napier and Clube, 1979) that a 5-10 km diameter meteorite impacted with the Earth and that the resulting environmental stresses led to the mass extinction. The terrestrial cratering record indicates that bolides with diameters $\geq$10 km have struck the Earth with an average frequency of one every 50 million years (Weatherill and Shoemaker, 1982). The primary evidence for a K-T impact was the discovery of anomalously high concentrations of elements, such as iridium, in thin clay layers marking the boundary at well preserved, globally distributed K-T sites (Alvarez et al., 1980). Siderophile elements, like those of the platinum-group (PGE; Pt, Pd, Ru, Ir, Rh, Os) and other noble metals (e.g., Au), are relatively concentrated in metallic iron and are therefore relatively abundant in the Earth's interior and in certain meteorites (e.g., irons, chondrites), compared to crustal rocks which typically contain <0.01 ppb (Shaw et al., 1976). During the past decade, multidisciplinary studies of the

K-T boundary have produced much additional physical evidence in support of the K-T impact hypothesis (shocked minerals: Bohor et al., 1987, Izett, 1990; soot deposits: Wolbach et al., 1986; tsunami deposits: Bourgeois et al., 1988; stishovite: McHone et al., 1989; spherules: Hildebrand and Boynton, 1990). About 95 sites with enriched PGE have been located in marine and non-marine sediments, on land and in ocean drilling cores (see Alvarez and Asaro, 1990 and McLaren and Goodfellow, 1990 and references therein).

Despite the mounting evidence which suggests that an impact did occur at the termination of the Cretaceous period, it has also been suggested that the PGE enrichment and extinctions resulted from a period of extensive, volcanism (Officer and Drake, 1983, 1985; Courtillot et al., 1986; 1988; 1990). Zoller et al. (1983), Olmez et al. (1986) and Toutain and Meyer (1989) have identified Ir in volatile phases erupting from hot spot volcanoes like Kileuea, Hawaii. The Deccan Trap flood basalts ($> 10^6$ km^3), extruded as India moved over the Reunion hot spot, have been suggested as a possible PGE source, as they were deposited during a 1-4 Ma period spanning the K-T boundary (Courtillot, 1990).

Several problems inherent to the interpretation of the anomalous PGE abundances at the K-T boundary are: (i) the poorly understood behavior of the PGE during meteoritic impact and in low temperature sedimentary environments; (ii) the difficulty in distinguishing geochemically a meteoritic from a volcanic source, and (iii) the difficulty in assessing the role that elemental mobility plays in obscuring the geochemical signature, as well as the relative timing of Ir deposition and mass extinction. The overall objective of this work is to address these issues by: (i) identifying the PGE carrier phase(s) and

assessing the possibility of PGE fractionation upon condensation from an impact ejecta cloud; (ii) using PGE interelement ratios to characterize the source, and (iii) determining the degree of PGE association with organic phases to yield a rough estimate of mobility. The evaluation of a possible causal mechanism linking the origin of the K-T PGE with the mass extinction is beyond the scope of this thesis. Exhaustive reviews are already available (e.g., McLaren and Goodfellow, 1990; Glen, 1990).

The approach taken in this study involves three phases: 1) extensive, detailed sampling of the most PGE-enriched and best preserved marine and terrestrial K-T sites, 2) separation of the boundary clay into mineralogical and organic fractions and subsequent analysis for PGE, and 3) Comparison of K-T PGE abundances and ratios with those of a broad suite of primitive igneous rocks formed in a range of geological settings, including representative samples of the Deccan Trap basalt. Impact melt rocks from various Canadian craters were also analyzed to evaluate the usefulness of PGE ratios in the identification of possible impactors.

The application of a precise analytical technique (inductively coupled plasma mass spectrometry with tellurium coprecipitation pre-concentration) has overcome the limitations of low concentration and small sample size, and has allowed previously unattainable PGE (particularly Ru) determinations on K-T clays and other common rocks.

CHAPTER TWO
ANALYTICAL METHODOLOGY

Historically, the most commonly utilized method of PGE determination has been neutron activation analysis (NAA). The short half-life of Rh (4.4 min) and the interference on Ru (from uranium fission-product Ru) meant that these elements were rarely analyzed. The majority of PGE data has been limited to Ir and Pd, but with the onset of new, sensitive techniques, such as the one employed here, the entire group can be determined at the levels found in crustal rocks.

Sample Preparation

K-T boundary samples were submersed for 2 days in, and subsequently repeatedly washed with, 4% acetic acid in order to obtain a sample for PGE analysis, free of calcium carbonate. Despite the fact that 4% acetic acid will not dissolve all carbonate minerals, stronger acid was not used due to the possibility that PGE could be selectively leached. X-ray diffractometry of pre-treated samples showed that, in some cases, the presence of dolomite cement prevented complete dissolution of carbonate minerals, with up to 12% carbonate still present (Knappengraben-K1 and Petriccio-P-1). No correction for this residual carbonate was employed since CO_2 could not be determined on individual separates due to the sample size limitations. The undissolved carbonate dilutes the PGE concentrations in size-fraction separates. It has been shown recently (Ping and Chifang, 1990) that 5% citric acid with 0.1% ascorbic acid solution (pH = 1.5) is most effective for selective dissolution of all carbonate (including dolomite) in the K-T boundary clay. This solution was successfully used here in the pre-treatment of sediments from Petriccio and Elendgraben that were analyzed for background PGE.

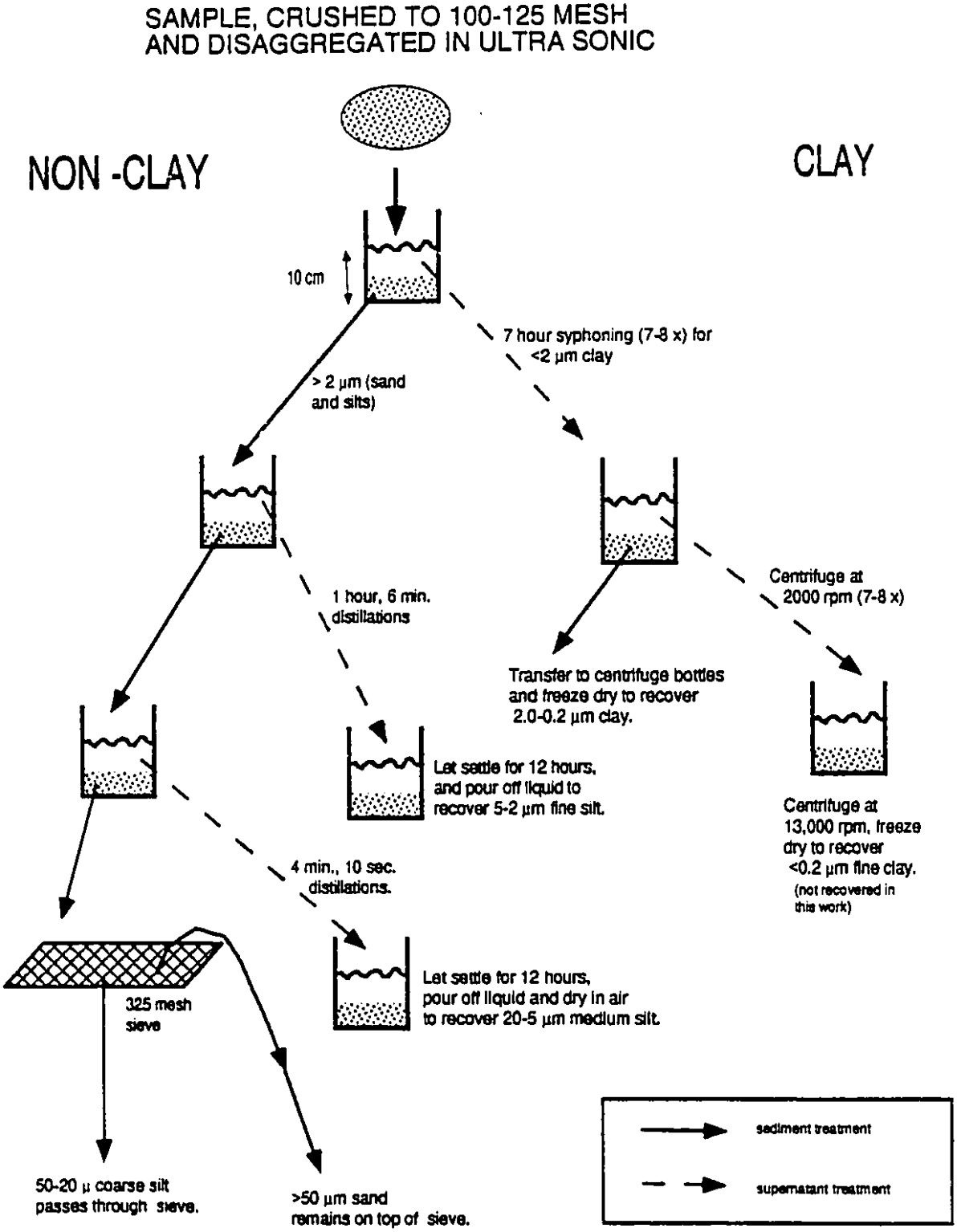

Figure 1. Flow chart of gravity grain size separation procedure employed (Jackson, 1973).

Grain-size Gravity Separation

In order to separate various minerals in the K-T boundary clay, the gravity separation procedure of Jackson (1973) was employed (Figure 1) at Agriculture Canada, Ottawa. All separations were done in distilled water and no chemicals were added. The clay minerals in terrestrial site samples dispersed instantly, however, flocculation of clay minerals in marine samples was pervasive due to the presence of salts. Dissolved salts were removed by repeated washing in distilled, deionized water. Five size-fractions were obtained; clay (<2 μm, which includes the $<$ 0.2 μm fraction), fine silt (2-5 μm), medium silt (5-20 μm), coarse silt (20-50 μm) and sand (>50 μm). Pure mineral separates are virtually impossible to obtain for samples that are composed dominantly of fine clay material. Purity of separates is indicated by the XRD results given in Tables 11 and 14a-c.

Inductively Coupled Plasma Mass Spectrometry: Isotope Dilution and External Calibration

A detailed account of the preparatory steps and analysis can be found elsewhere (Gregoire, 1988; Sen Gupta and Gregoire, 1989) and only a brief review of the procedure is given below. All pre-treatment and analysis was performed at the Geological Survey of Canada, Ottawa by the author and D.C. Gregoire, respectively.

Dissolution and digestion

An isotope spike (Pt, Pd, Ru and Ir) was added to five grams of weighed rock powder prior to digestion. Early addition of a spike ensures that the chemical state of both sample and spike PGE will be the same and, therefore, complete mixing and equilibration will occur. For each experiment, calibration standards were prepared for Rh and Au, and treated identically to samples. Reagent blanks (no spikes added) were

also prepared and treated as samples. Rh and Au were determined by external calibration due to their monoisotopic nature. All other PGE were determined by isotope dilution.

The advantage of isotope dilution is that the determination of concentration by isotope ratio (calibration isotope ratio/sample isotope ratio) yields results that are insensitive to minor loss of material during preparation or variation in machine sensitivity. External calibration necessitates preparation of a calibration curve (determined by first analysing blanks and standards) and sample concentrations are d i rmined from this curve. Although Rh analysis by inductively coupled plasma mass spectrometry (ICP-MS) is very sensitive, Rh abundance is persistently near detection limits in most crustal rocks. This, coupled with its analysis by external calibration (susceptible to those analytical problems avoided by isotope dilution), may lead to error in Rh determination by this method. The insensitivity of the mass spectrometer for Au as well as its determination by external calibration can lead to difficulty in Au determination. Since osmium volatilizes upon addition of aqua regia and does not coprecipitate with tellurium, Os analysis could not be performed by this method.

Silicates were digested with hydrofluoric acid (HF) and PGE were dissolved by aqua regia (3:1 $HCl:HNO_3$). Incomplete dissolution can occur in samples with > 1-2% chromite. These residues were treated separately as described below.

Chromite Fusion

For samples that exceeded 1% chromite (Alligator Lake xenoliths, Baffin Bay picrites, Deccan Trap samples DT 34 and 52), digestion with HF and aqua regia was not sufficient for complete dissolution. Chromite is a known carrier phase for PGE (Barnes, 1985). Platinum-group element abundances determined on unfused chromite-rich samples

represent minimum values since PGE bound in chromite is not dissolved. Such chromite-rich samples were treated as follows. Perchloric acid was heated with the washed, undissolved residue to evaporate fluorides, thereby decreasing the volume of material present for subsequent fusion. This lowers the potential for contamination by reducing the amount of sodium peroxide needed to fuse the sample. Solutions were washed in 6M HCl to dissolve the residue, and the supernatant was reserved. The chromite-bearing residue was fused with sodium peroxide in zirconium crucibles, then dissolved in dilute (6M) HCl and combined with the supernatant. Enriched isotope spike (Pt, Pd, Ru and Ir) was added to the solution and tellurium co-precipitation followed.

Separation of PGE from bulk matrix

Tellurium co-precipitation of PGE with stannous chloride (Elson and Chatt, 1983; Shazali et al., 1987) was used to separate analyte from matrix components. The efficiency of Te co-precipitation for PGE is 98-100% (Shazali et al., 1987). Filtered precipitate was dissolved in aqua regia and transferred in 5 ml of 1.5M HNO_3 solution to small centrifuge tubes for analysis.

ICP-MS analysis

Analysis of solutions from a 5 gram sample by ICP-MS (Perkin-Elmer Siex Elan Model 250) yielded detection limits of 0.1 ppb for Pt and Pd, 0.01-0.05 ppb for Rh, Ru and Ir, and 0.2 ppb for Au. Detection limits were calculated as 3 times the standard deviation for 10 reagent blanks that were treated as samples. Since blanks were included with each set of samples analysed, detection limits varied with each experiment. Maximum values are given above. When less than 5 grams of rock powder was analyzed, detection limits (3σ) were adjusted accordingly (e.g., for a 1 gram sample detection limits were 3σ x 5).

Analytical precision for research grade analysis using these methods is dependent

upon sample size, distribution of PGE within the sample and mass spectromter sensitivity. A "blanket" analytical precision for ICP-MS with Te co-precipitation for all samples analysed in this work cannot, therefore, be determined. At the ppb level, heterogeneity of PGE distribution inevitably exists and large error is therefore expected for multiplicates of rock samples in this range. Table 1 presents duplicate and triplicate analyses for PGE in a range of different rock samples, none of which are from the K-T boundary. One indication of the precision of these measurements is the standard deviation, calculated on the average difference between duplicates. Precision for the Deccan Trap basalts, as percent standard deviation are: 17% (Pt), 8% (Pd), 34% (Ru), 86% (Ir), 32% (Au), >100% (Rh). The reproducibility for Ru, Ir and Rh is quite poor since values are persistently at or below detection limits in most of the basalts analyzed. Heterogeneous distribution or remobilization of Au may explain the poor precision on its determination in these rocks. Precision determined on the melts rocks are: 20% (Pt), 10% (Pd), 3% (Ru), 13% (Ir), 70% (Au), >100% (Rh). Here, the precision on Ru and Ir determination is much improved as values are significantly above detection limits. Inhomogeneous Au distribution and low Rh concentration may account the for poor precision on determination of these elements in melt rocks. Similar precision determinations on K-T boundary clay could not be made due to sample size limitations. The low concentration of PGE in the Deccan Trap basalts, heterogeneous distribution of PGE within the melt rocks and variations in mass spectrometer sensitivity between experiments negate the confidence limits given above from being directly applicable to the K-T boundary sediments. They can, however, provide rough estimates of the limit of confidence for the K-T boundary samples.

Analytical precision calculated for non-homogenized, small samples with variable matrix is not as meaningful as that determined by repeated analysis of homogeneous material.

Table 1. Duplicate analysis (in ppb) of various igneous and impact melt rocks.

	Pt	Pd	Ru	Ir	Au	Rh
Deccan Traps						
DT-33	42.0 38.0	18.0 17.0	0.076 0.19	0.026 0.30	17 14	0.069 0.15
DT-35	9.0 10.0 11.0	17.0 16.0 17.0	0.39 0.43 0.47	0.053 0.070 0.073	12 10 10	0.046 0.071 0.10
DT-38	6.7 3.0	2.6 2.8	0.077 0.070	0.060 0.046	6.6 6.9	0.02 0.022
DT-42	11.0 9.0	5.2 5.5	0.19 0.035	0.11 0.086	12 16	0.016 0.02
DT-43	0.42 0.60	1.4 0.51	0.12 0.035	0.074 0.024	2.5 2.6	-.- -.-
DT-45	4.7 3.9	4.9 4.3	0.059 0.085	0.082 0.26	4.0 6.4	0.018 0.028
DT-46	8.8 5.3	22.0 20.0	0.27 0.24	-.- 0.056	16 6.7	0.11 0.022
DT-50	9.9 8.1	6.7 5.5	0.97 1.00	0.17 0.15	7.5 4.5	0.027 0.031
Standard Deviation	1.8	0.75	0.09	0.09	2.9	0.26
Galapagos Islands						
GR-1645-3E	1.3 3.4 1.3	0.61 0.64 0.51	0.10 0.09 0.084	0.10 0.080 0.035	-.- 2.1 1.1	-.- -.- 0.011
GR-D5	1.0 1.5 1.2	0.14 0.31 0.11	0.21 0.13 0.058	0.13 0.043 0.041	0.88 0.65 1.4	-.- -.- -.-
Melt Rocks						
New Quebec RANQ-3a	17.0 17.0	5.4 6.7	3.9 4.0	1.5 1.9	3.8 5.8	0.069 0.057
New Quebec RANQ-3b	16 13	4.3 5.4	3.3 3.5	1.7 2.0	4.8 2.4	1.0 0.029
Wanapitei MSWX-200-70	4.1 7.5	4.3 4.7	4.3 4.5	1.6 1.9	15 5.3	1.0 0.094
Brent BI-59-2781-0	15.0 21.0	8.8 8.9	7.8 7.8	3.0 2.5	11 3.2	2.2 0.095
Standard Deviation	2.7	0.62	0.13	0.27	4.5	0.88

For full sample identification, refer to Tables 16, 17, 21. All duplicate analysis was performed on portions of a single homogenized powder. -.- denotes values below the limit of detection.
Standard deviation for n similar samples, analysed in duplicate (x_1, x_2) was calculated by; $S^2 = [\Sigma(x_1-x_2)^2]/2n$.

Unfortunately, there is a lack of rock standards for PGE at the detection limits of the present technique. Precision estimated from multiple analysis of USGS standards DTS-1 (dunite) and W-1 (diabase) are given in Table 2. The high variability of PGE for DTS-1 may result from heterogeneous distribution of PGE-rich chromite (3900 ppm Cr) in the dunite. Precision as percent standard deviation for standard W-1 were the following: 13% (Pt), 7% (Pd), 6% (Ru), 0.7% (Ir), 24% (Rh). Only one Au value was determined and it is very close to the accepted value (Govindaraju, 1989). W-1 probably gives a better estimate of analytical precision for Ru, Ir and Rh than the Deccan Trap samples (Table 1), simply because it contains abundances well above the detection limits. W-1 has been homogenized during standard preparation and has a low Cr content (119 ppb; Govindaraju, 1989). However, heterogeneity may still be present as noted by Fritze and Robertson (1969) for Au and, therefore, precision determined on W-1 may also be more sample than analytically dependent.

Table 2. PGE content (in ppb) of U.S.G.S. Standards W-1 and DTS-1.

	Pt	Pd	Ru	Ir	Rh	Au
W-1	**13** 10.2 11.5 10.8 13.6	**14** 11.9 13.0 13.4 14.0	**0.2** 0.17 0.17 0.16 0.19	**0.3** 0.30 0.28 0.32 0.31	- 0.047 0.037 0.052 0.030	**4.3** 4.0
Mean (SD)	11.5 (1.5)	13.1 (0.88)	0.17 (0.01)	0.30 (0.02)	0.042 (0.01)	
DTS-1	- 47.4 18.9 - -	- 9.2 2.2 62 35.4	- 2.0 3.0 13.4 9.1	**0.69** 0.18 0.11 2.5 1.6	**0.83** 0.10 0.13 - -	**0.92** - -
Mean (SD)	33	27 (27)	6.9 (5.4)	1.1 (1.2)	0.12	

Certified values (Govindaraju, 1989) are bolded. SD = Standard Deviation. - = no data.

Organic treatment

Selective dissolution of organic material and associated platinum-group metals was accomplished using an overnight sodium hypochlorite (5% NaOCl) digestion prior to tellurium co-precipitation (Gregoire, 1985). The PGE associated with the organic fraction and the PGE in the residual mineral phases were analysed separately to determine the percentage of the elements associated with organics in the bulk sample. No estimate of the amount of organic material present could be made due to sample size limitations. An HCl, HF leaching procedure for kerogen extraction has been used previously (Schmitz et al., 1988) in a study of PGE-organic complexing at K-T boundary sites (Stevns Klint, Denmark and Caravaca, Spain). However, the high percentage of organically-bound Ir found by Schmitz et al. (1988) (>50% versus 3% determined here; Table 4) may imply some contamination of organic matter by mineralogically-bound PGE during the kerogen extraction procedure. It has been determined (Gregoire, 1985) that <0.01% to 3.4% of the Au in mineral phases is solubilized with the NaOCl treatment. No data exist for the other PGE. Stripping of PGE from mineral phases will depend on grain size and the composition of the mineral host (Gregoire, 1985).

X-Ray Diffractometry

XRD analysis was performed on all size separates in order to establish the mineralogy and aid in identification of the PGE carrier phase(s). All analysis was done on oriented samples, mounted on glass slides. Samples were run air-dried, glycolated and after heating to 540°C in order to identify various clay minerals. Diffraction analysis of marine sites was done at CANMET on a RIGAKU automated powder diffractometer with a rotating anode and copper target ($CuK\alpha_1$ = 1.54098Å). Runs were made in increments of 10° in 2ϕ/min.

Scans were from 2-90°. The terrestrial sections were analyzed at the Ruhr Universität in Bochum, Germany with the same run increments and degrees scanned. The results are given in Tables 11 and 14a-c.

Scanning Electron Microscopy

Mineral separates were examined at the Geological Survey of Canada using a Cambridge S-200 scanning electron microscope (SEM) with a Link AN10/855 energy dispersive X-ray analyser. A small amount of representative powder was mounted on double-sided tape-covered stubs and then carbon-coated. Samples were chosen for SEM on the basis of high PGE content in a hope of identifying the PGE carrier phase or of eliminating certain minerals as carrier phase candidates (e.g., ilmenite at the Elendgraben site), and also to check the purity of mineral separates. No discreet PGE-bearing grains were detected and due to the extensive mechanical disaggregation of the size-fraction separation process, no original textures were observed in the boundary clay layer(s).

CHAPTER THREE
CRETACEOUS-TERTIARY SITES: SELECTION AND STRATIGRAPHY

Site Selection

The selection of K-T boundary sites for this study (Figure 2a,b) was based on the following criteria: 1) the level of PGE enrichment from previous work, 2) well-documented detailed stratigraphy, 3) sedimentary environment (marine vs. terrestrial sites), 4) degree of preservation and exposure and, 5) accessibility and sampling opportunity.

Criterion (1) was important for two reasons. First, separation of the bulk K-T samples into grain size-fractions results in small sample size (often < 1 gram). Since PGE are not uniformly partitioned among all mineral and organic phases (Chapter 5), some fractions may have concentrations below the detection limit. Secondly, the probability of identifying the PGE carrier phase(s) using physical separation techniques or SEM methods is highest in samples having the highest PGE content. The detailed stratigraphy (2) was vital for accurate sampling of the thin (often <0.5 cm) boundary clay in extensive sections spanning the K-T boundary. Criterion (3) was essential in order to representatively document the global nature of the event. It is, however, also essential that poorly preserved or exposed sections (4) be excluded from consideration. The original discovery site for the K-T PGE anomaly was near the Italian town of Gubbio, but this section was not open to sampling at the time of field work for this study, and flooding prevented the sampling of several New Zealand sites (Flaxbourne River, Chancet Rocks, Wharanui and Waipara).

Marine K-T sites consist mainly of pelagic and hemipelagic sediments, deposited beyond continental margins in deep-water environments (McLaren and Goodfellow, 1990).

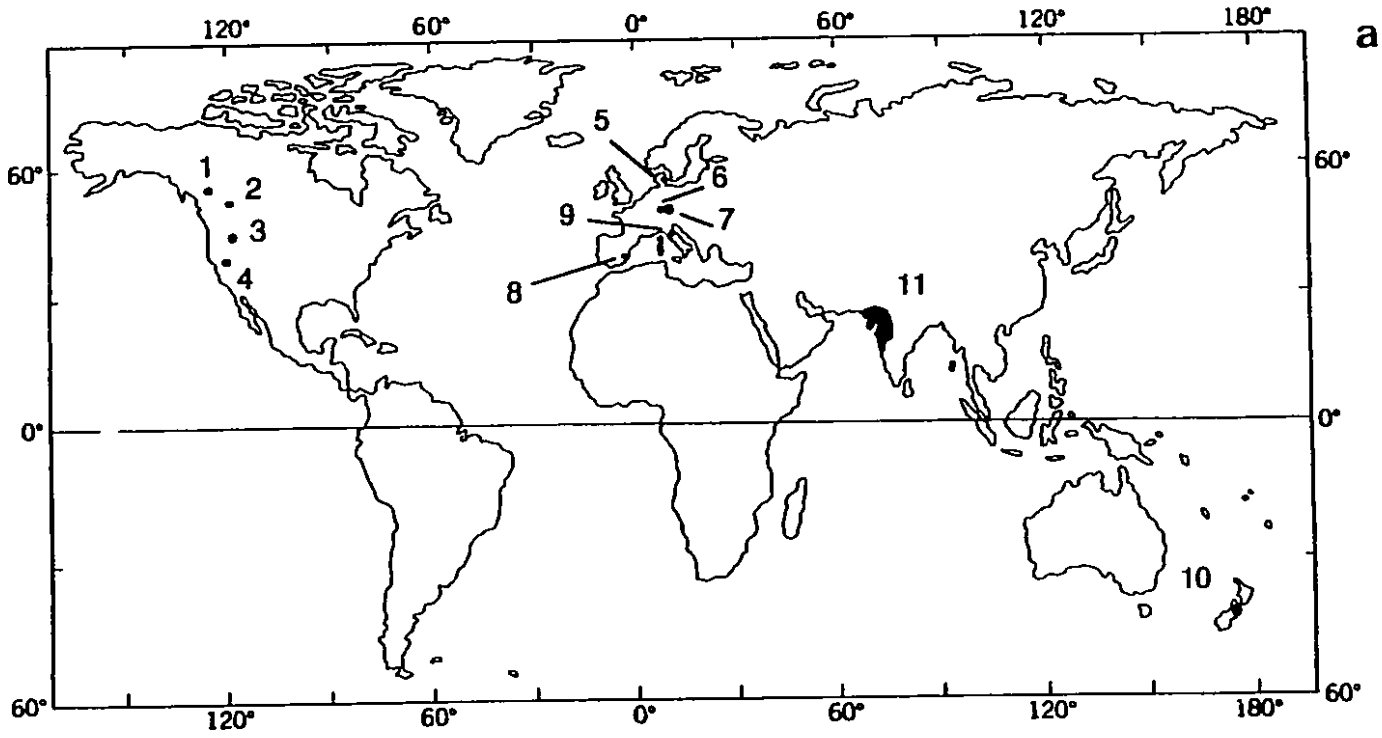

Figure 2a,b. Location map of K-T boundary sites studied; a) present continental configuration, b) continental configuration 65 Ma ago. 1 = Red Deer Valley, Alberta; 2 = Morgan Creek, Saskatchewan; 3 = Lance Creek, Wyoming; 4 = Berwind Canyon, Starkville South, Clear Creek North, Raton Basin, Colorado; 5 = Stevns Klint, Denmark; 6 = Elendgraben, Gosau Basin, Austria; 7 = Knappengraben, Gams, Austria; 8 = Agost, Spain; 9 = Petriccio, Italy; 10 = Woodside Creek, New Zealand; 11 = Deccan Trap basalt, India.

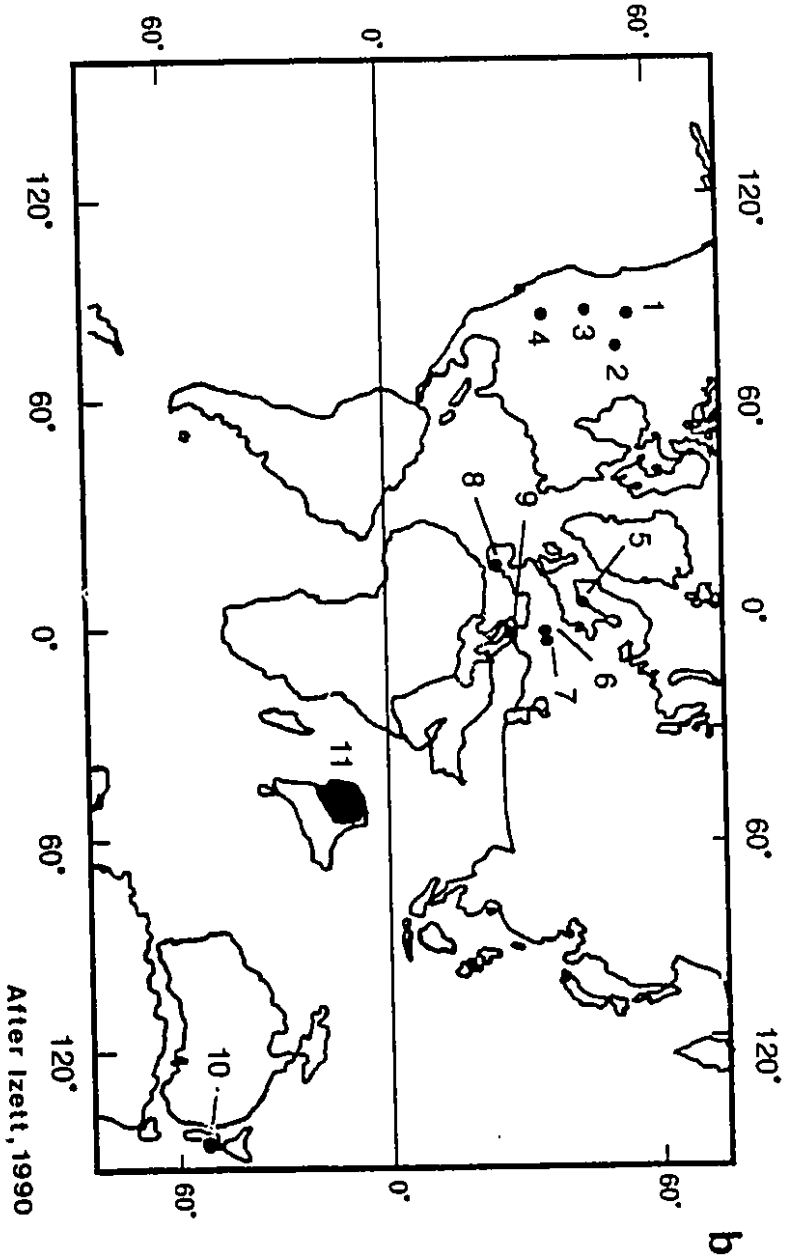

After Izett, 1990

1990). The sites studied include Petriccio, Italy (Montanari et al., 1983), Knappengraben and Elendgraben, Austria (Preisinger et al., 1986) and Agost, Spain (Smit et al., 1988; Groot et al., 1989). Continental shelf sediments are found in marine sections from Stevns Klint, Denmark (Birkelund and Hakansson, 1982) and Woodside Creek, New Zealand (Strong, 1977; Brooks et al., 1986a). The K-T boundary in non-marine sections from the Western Interior of North America is preserved in paleo-fluvial, -pond and -swamp environments. The lithologic record in the Raton Basin of Colorado (Clear Creek North; Starkville South and Berwind Canyon), Wyoming (Lance Creek), Alberta (Red Deer Valley) and in Saskatchewan (Morgan Creek) shows deposition of the boundary clay just prior to the onset of coal formation (Izett, 1990).

Sampling Methods

The K-T boundary sites sampled include Petriccio, Knappengraben, Elendgraben, Woodside Creek, Stevns Klint, Agost and the Raton Basin sites. Samples from Red Deer Valley, Morgan Creek and Lance Creek were donated by others. Once the section containing the K-T boundary had been located, the outcrop was cleared and brushed to prevent infall of soil and other debris during sampling. Where possible, the outcrop face was excavated 0.5-1 m to expose fresher material for sampling. The stratigraphic level of samples was measured from the top Cretaceous ("0 cm" horizon). Sampling tools included brushes, wallpaper scrapers, plastic knives, rock hammer and chisels. No jewelry was worn during sampling. Disposable plastic knives were used to remove, separate and clean the individual layers of the boundary clay. Samples were collected from the highest to the lowest stratigraphic level (e.g., Tertiary background sample(s),

boundary clay layers, Cretaceous background sample(s)), and each was brushed clean before being placed in a labelled plastic bag. Due to the large numbers of scientist studying the K-T boundary, the boundary clay had often been deeply excavated and it was difficult to acquire enough material of the often < 1cm boundary clay layer, particularly at Woodside Creek and Petriccio. At Stevns Klint, care had to be taken not to undercut the outcrop as large boulders of Tertiary rock had been known to fall on unsuspecting samplers (H. Hansen, pers. comm. 1988).

Generalized Stratigraphy of the K-T Boundary Interval

The correlation between the fossil-defined marine and pollen-defined terrestrial K-T boundary sequences is based on the observation that, 1) both boundaries occur in reverse polarity magnetozone 29R (Shoemaker et al., 1987) and 2) PGE and shocked mineral (Izett, 1987) spikes are restricted to a thin unit in both realms (Izett, 1990). The type sections for the marine and terrestrial K-T realms are shown schematically in Figures 3a and 5a and in photos in Figures 3b and 5b.

The marine sequence, (Figure 3a,b) described by Smit and Romein (1985), shows five lithologic units, which reflect the sequence of events across the K-T boundary. Although local details may differ, the sequence, or parts thereof, can be found in almost every well-preserved K-T marine section worldwide, indicating a globally similar sequence of events. **Unit 1** is a Late Cretaceous homogeneous sequence of hemipelagic or pelagic calcareous oozes, limestones and marls with the top 10-20 cm commonly bioturbated. This unit is overlain by **Unit 2** which contains shocked minerals, graded spherules, high siderophile (including PGE) and chalcophile element anomalies, a high

Figure 3a,b. Type section stratigraphy for a generalized marine K-T boundary interval;
a) schematic section (after Smit and Romein, 1985),
b) K-T boundary section exposed at Stevns Klint, Denmark.

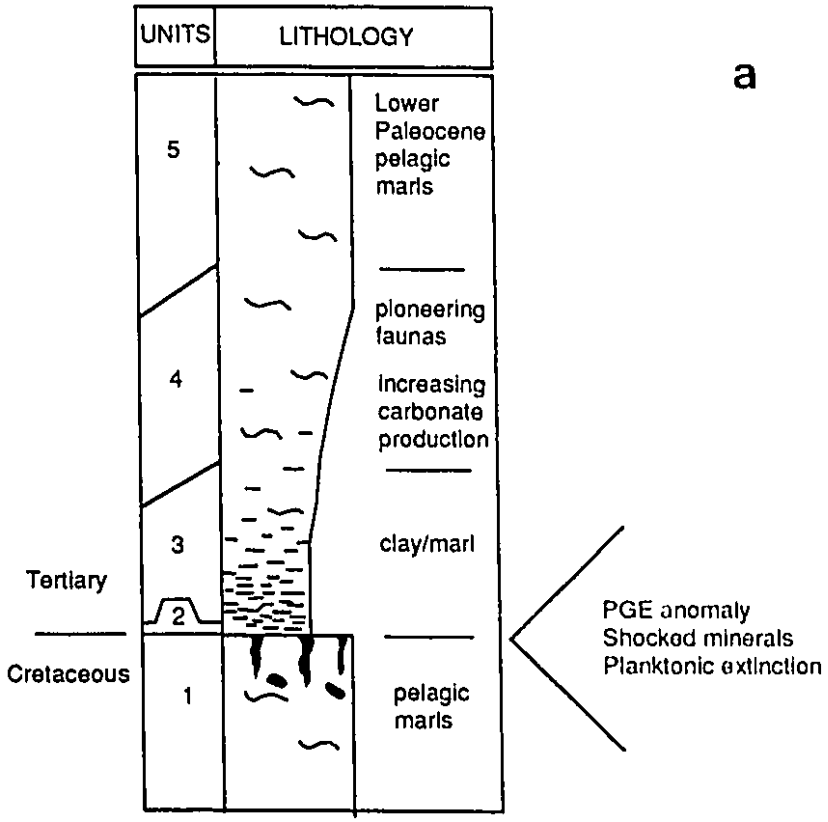
UNITS
LITHOLOGY
a
5
4
3
2
1
Lower Paleocene pelagic marls
pioneering faunas
increasing carbonate production
clay/marl
pelagic marls
Tertiary
Cretaceous
PGE anomaly
Shocked minerals
Planktonic extinction

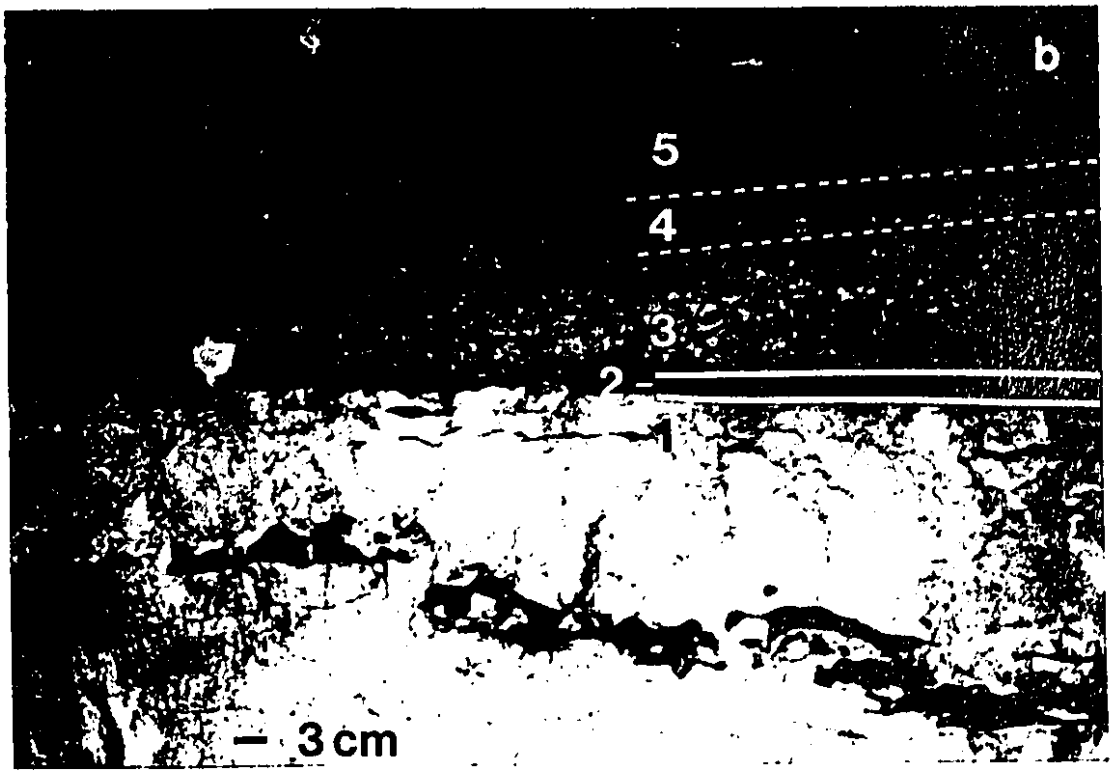
b
5
4
3
2
1
3 cm

Figure 4. Pyrite nodule altered to goethite at the Stevns Klint site, Denmark.

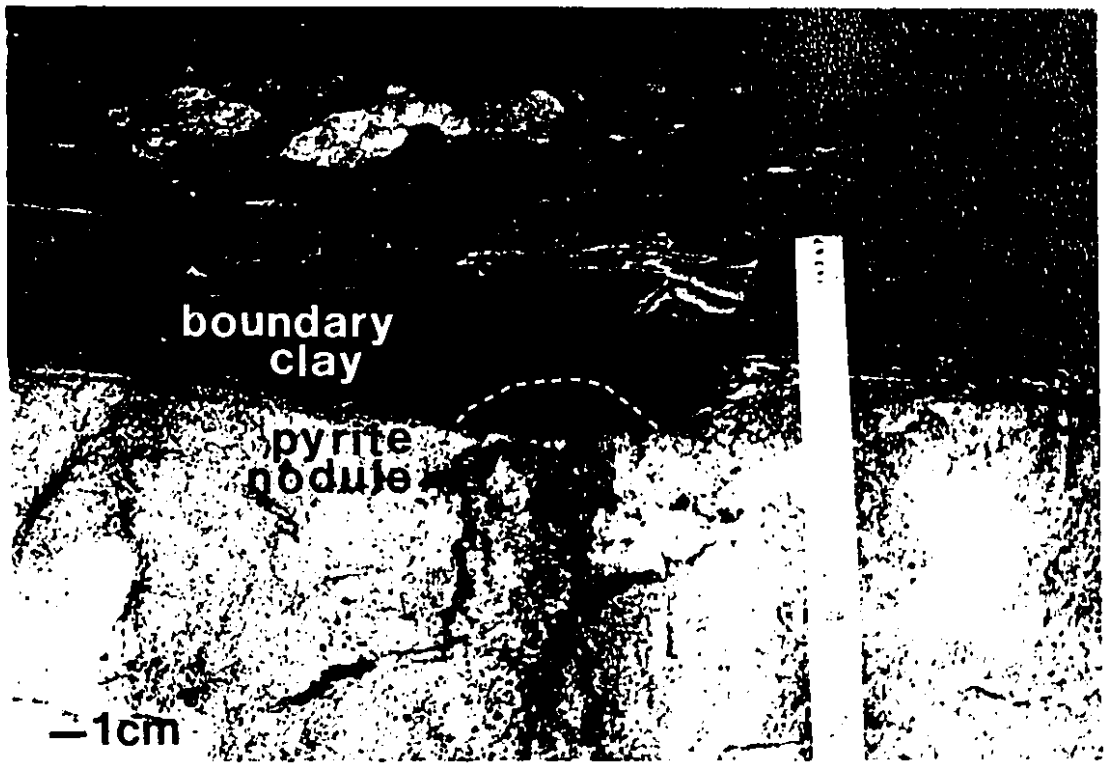
boundary
clay
pyrite
nodule
—1cm

sulphide content and almost no benthic organisms. The later two characteristics indicate anoxic conditions. The common red coloration in weathered sections is due to pyrite oxidation to goethite (Figure 4). Tsunami deposits (Bourgeois et al., 1988) or an erosional hiatus (Jones et al., 1987) can mark this horizon. **Unit 3** is a graded dark to pale grey, organic-rich layer with normal detrital clay (e.g., comparable to units 1 or 5) and with 20-40% carbonate originating from reworked species or from the few survivors. "Strangelove" conditions (low productivity following a biotic crisis; Hsü and Mackenzie, 1985) characterize this unit. An increase in carbonate productivity occurs near the pale grey top. The first Paleocene planktonic fauna appear in **Unit 4**, followed by an explosive increase in carbonate productivity and sedimentation. Normal marine sedimentation in the form of Lower Paleocene pelagic marls dominates in **Unit 5**, but with completely new planktonic biota.

For terrestrial sections (Figure 5a,b) the generalized sequence of K-T boundary layers is different to that of the marine sites (Izett, 1990). The Upper Cretaceous rocks of **Unit 1** are mudstone, carbonaceous shale, coal, impure coal or sandstone with dominant pollen of angiosperms. **Unit 2**, 1-2 cm thick, has been termed by its discoverer, C.L. Pillmore, the "K-T boundary claystone" (Izett, 1990). It is dominated by clay minerals such as microspherulitic kaolinite, illite/smectite (I/S) mixed-layer clay or smectite, and is essentially free of clastic grains. A marble cake appearance with root-like structures, plant impressions and vitrinite lamina characterize the unit, indicating inclusion of plant material during its deposition (Izett, 1990). This unit contains a small Ir anomaly (0.07-0.32 ppb), low Ni contents (<2-15 ppm; mean = 4.8 ±4.2 ppm for 8 sites; Izett, 1990) and no shocked minerals. The unit is not a blanket-like layer, but

Figure 5a,b. Type section stratigraphy for a generalized terrestrial K-T boundary interval; a) schematic section (after Izett, 1990), b) K-T boundary section exposed at Berwind Canyon site, Raton Basin, Colorado.

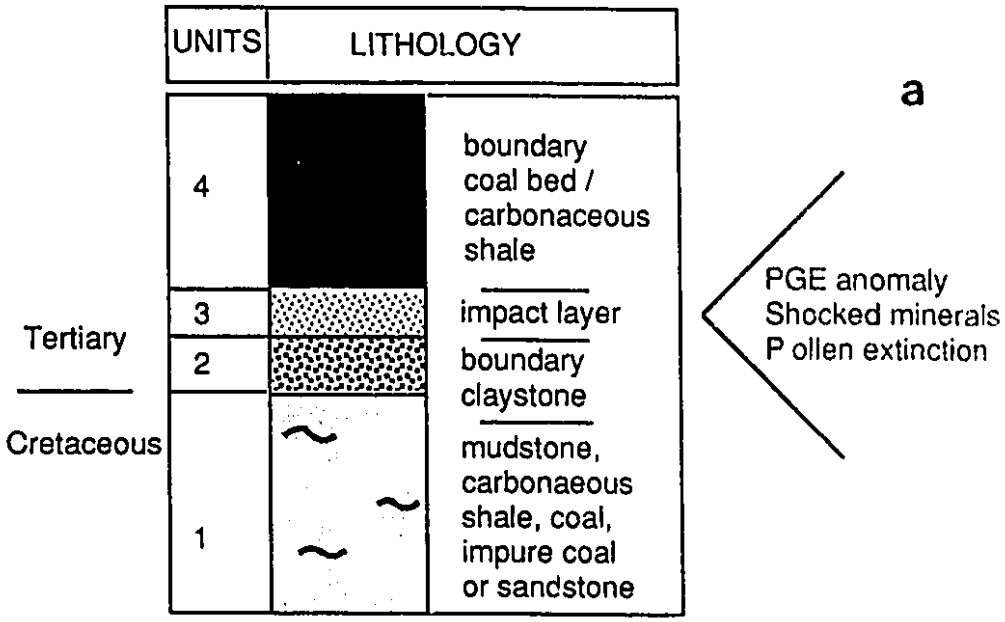
UNITS
LITHOLOGY
a
4
3
2
1
Tertiary
Cretaceous
boundary coal bed / carbonaceous shale
impact layer
boundary claystone
mudstone, carbonaceous shale, coal, impure coal or sandstone
PGE anomaly
Shocked minerals
P ollen extinction

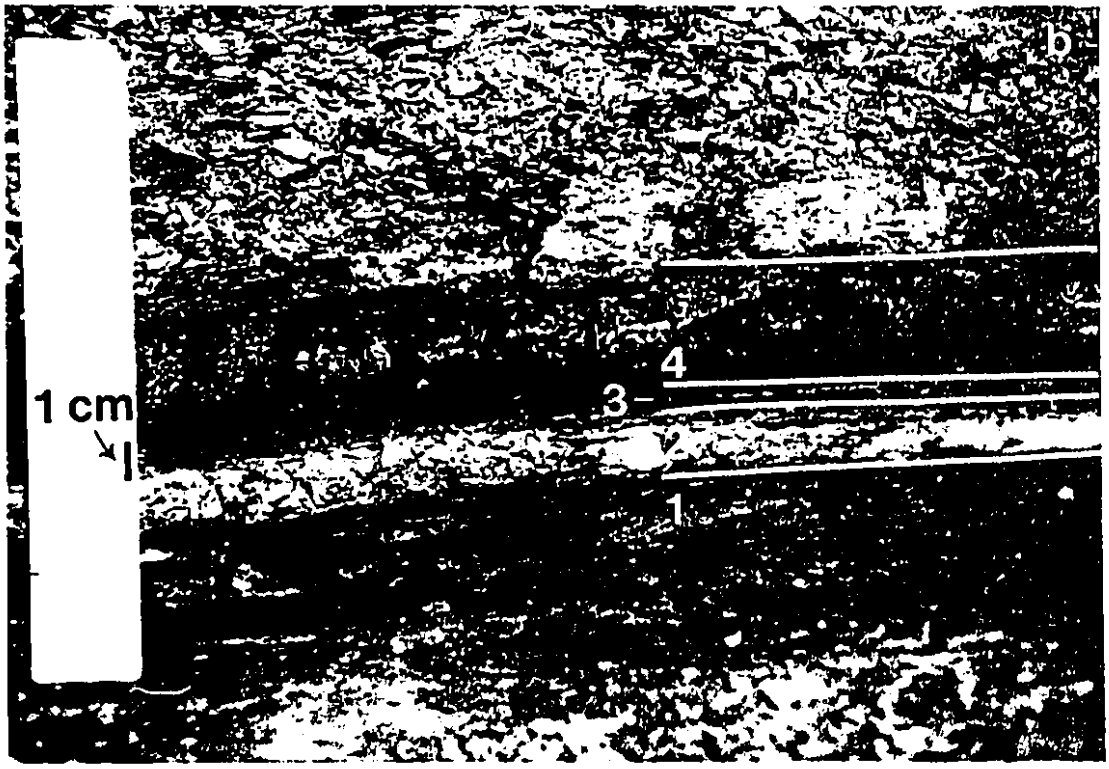
b
1 cm
4
3
1

occurs sporadically across western North America in fine-grained sediments, adjacent to coal swamps (Izett, 1990). It is not found in any of the marine sites and is interpreted by Izett (1990) as a pedogenic claystone that formed over a broad area in a tropical-temperate zone. Unit 3 has been termed the "K-T boundary impact layer" by Izett (1990). This 3-8 mm thick unit, usually in sharp contact with the boundary claystone below, is composed mainly of kaolinite and I/S mixed layer clay. The unit is microlaminated and contains planar vitrinite laminae, but is different texturally from the microspherulitic Unit 2. The boundary impact layer marks the major reduction of characteristic Cretaceous pollen genera (Tschudy and Tschudy, 1986). It concentrates shocked minerals and siderophile elements and correlates with the Unit 2 in the marine sections. Directly overlying this layer is the Unit 4, the "K-T boundary coal layer" or carbonaceous shale (Izett, 1990), which can contain almost as much Ir as the impact layer due to PGE remobilization (Nichols et al., 1986; Wallace et al., 1990). The base of the coal sequence is dominated by fern spores with a few pollen grains. Higher up in the section, the percentage of angiosperm pollen increases and the proportion of fern spores diminishes. Ten to 15 cm above the boundary, pollen once again becomes dominant (Tschudy and Tschudy, 1986).

Detailed Stratigraphy of the K-T Sites Studied

Detailed lithological sections have been published for all sites studied (Birkelund and Hakansson, 1982; Montanari et a' 1983; Montanari, 1986; Preisinger et al., 1986; Groot et al., 1989; Smit, 1977; Strong, 1977; Lerbekmo et al., 1979; Lerbekmo and St. Louis, 1986; Lerbekmo et al., 1987; Nichols et al., 1986; Bohor et al., 1987b; Izett,

1990). Description of stratigraphic sections for each site sampled in this work follow. Samples of each unit were taken in all cases, but time limitations precluded analysis of all samples. Arrows indicate samples analysed for PGE, either for boundary layer(s) abundance (Tables 9 and 14a-c) or for background analysis (Table 5).

Marine Sites

Petriccio, Italy

The Petriccio section (Figure 6)(lat 45° 36.7'N, long 12°38.7'E) in the Scaglia Rossa Formation has an abnormally thick boundary clay (2.6 cm) and is essentially free of tectonic shearing and surface contamination with younger material (Alvarez and Lowrie, 1981). The boundary clay lies between pelagic limestone beds which have been homogenized by bioturbation (Montanari et al., 1983). The clay layers, however, have not been seriously disturbed by burrowing organisms as shown by the preserved millimeter-scale laminations of red and green clay in the lower part of the clay. Oxidation in the section is reflected in variations in sediment coloration (dark pink limestone more oxidized). Peak Ir and spheroid abundances coincide in the red part of the boundary clay (Montanari et al., 1983).

Knappengraben, Elendgraben, Austria

The Knappengraben, Gams (lat 47°40'N, long 14°45'E) and Elendgraben, Gosau (lat 47°33.2'N, long 13°28.2'E) sections (Figure 7a-c) in the Austrian Alps have a relatively thin boundary clay layer (3 mm) deposited in a deep-sea environment. The adjacent sediments are a sequence of alternating sandstone, siltstone, limestone, marly

Figure 6. Stratigraphic section of the K-T boundary interval at Petriccio, Italy.

Petriccio, Italy

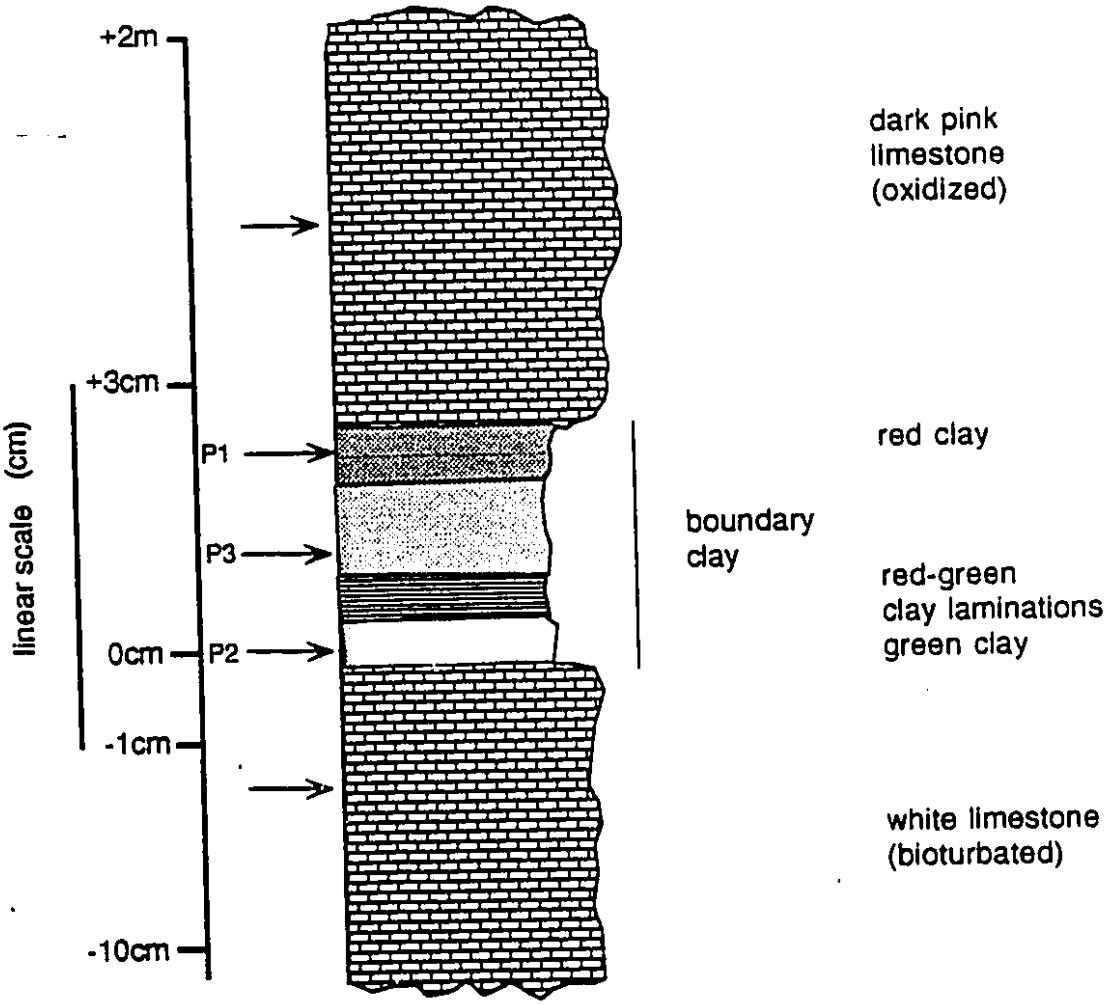

Figure 7a-c. (a) Stratigraphic section of the K-T boundary interval at Knappengraben, Gams, Austria and Elendgraben, Gosau, Austria. (b) Photo of the K-T section at Knappengraben. (c) Photo of the K-T section at Elendgraben. Boundary clay is located at the arrow. Black marks on ruler (b) are 1 cm. Hammer in (c) is 30 cm long.

a

Knappengraben and Elendgraben, Austria

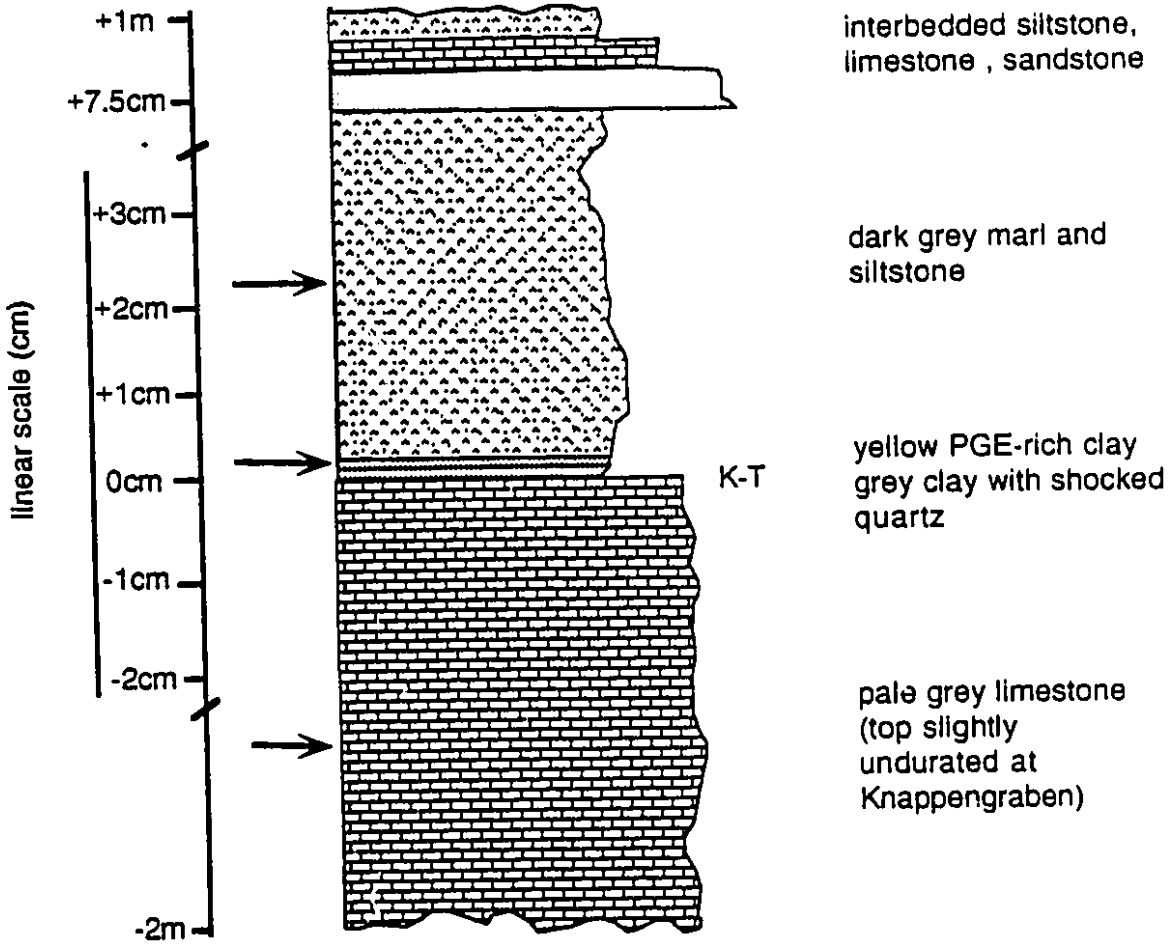


b

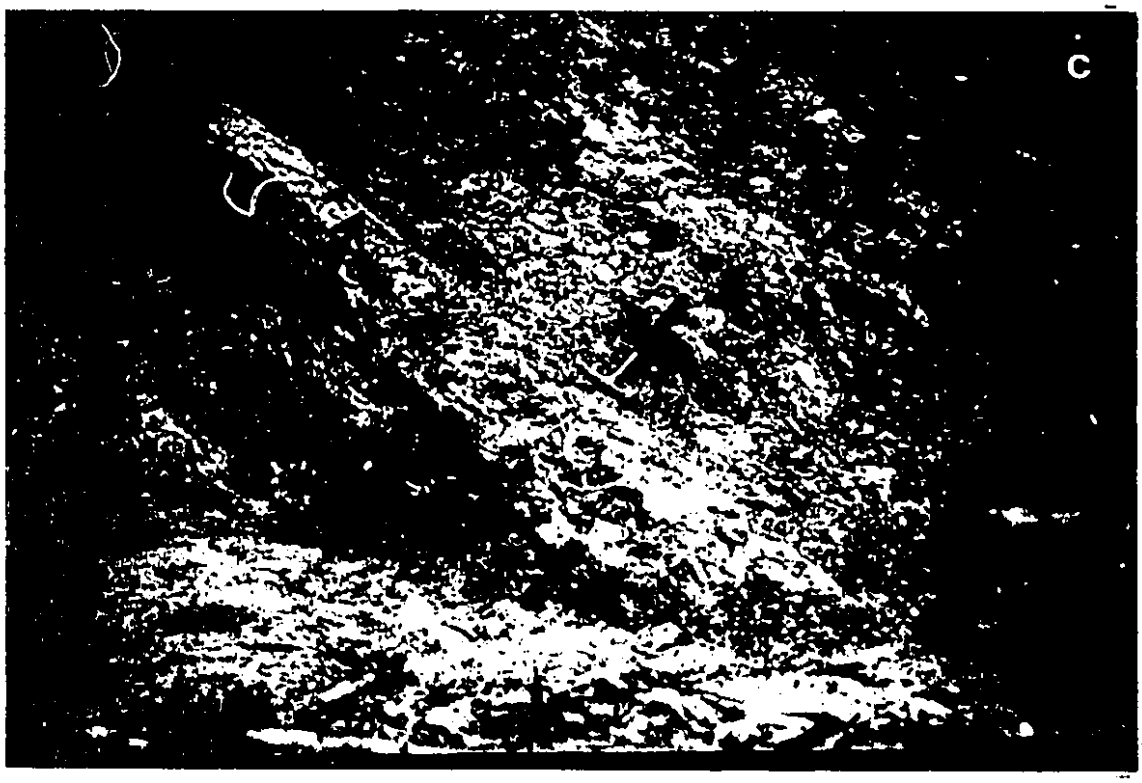
c

limestone and marls which are partly turbiditic and partly hemipelagic (Preisinger et al., 1986). The sections are very similar (both part of the Gosau Formation), but the upper Cretaceous limestone at the Elendgraben site is flatter with less induration than at Gams (H. Stradner, pers. comm., 1988). The Knappengraben section was sampled at two locations in order to assess the horizontal continuity of PGE distribution in the boundary clay. The boundary clay is composed of a thin (1 mm) layer of light grey clay where shocked quartz is concentrated and 2 mm of yellow PGE-rich clay (sample analysed here for PGE). There is no evidence of bioturbation in the boundary layer which is extremely well-preserved (Preisinger et al., 1986).

Woodside Creek, New Zealand

The Woodside Creek site, located in northeastern Marlborough Province (lat 41°57'S, long 174°03'E) has an 8 mm thick, highly weathered ferruginous clay marking the boundary (Figure 8a-c). This layer separates thinly bedded pink to cream argillaceous limestones with occasional carbonaceous clay partings (Tertiary), from underlying thickly bedded white-grey Cretaceous argillaceous limestone with flint lenses (Brooks, 1986a). Both the lowermost Tertiary and uppermost Cretaceous rocks are missing at this site and the upper Cretaceous limestone shows shallow depressions into which the boundary material has been winnowed and redeposited (Bohor, 1990b). The section is highly silicified (Brooks, 1986b).

Stevns Klint, Denmark

The site sampled (Figure 9a,b) at Stevns Klint (lat 55°16.7'N, long 12°26.5'E)

Figure 8a-c. (a) Stratigraphic section of the K-T boundary interval at Woodside Creek, New Zealand. (b) Photo of the K-T boundary interval at Woodside Creek. Boundary clay is located at the arrow. Black marks on ruler (b) are 1 cm. (c) Photo of the boundary clay at Woodside Creek. Coin is 5 mm across.

Woodside Creek, New Zealand

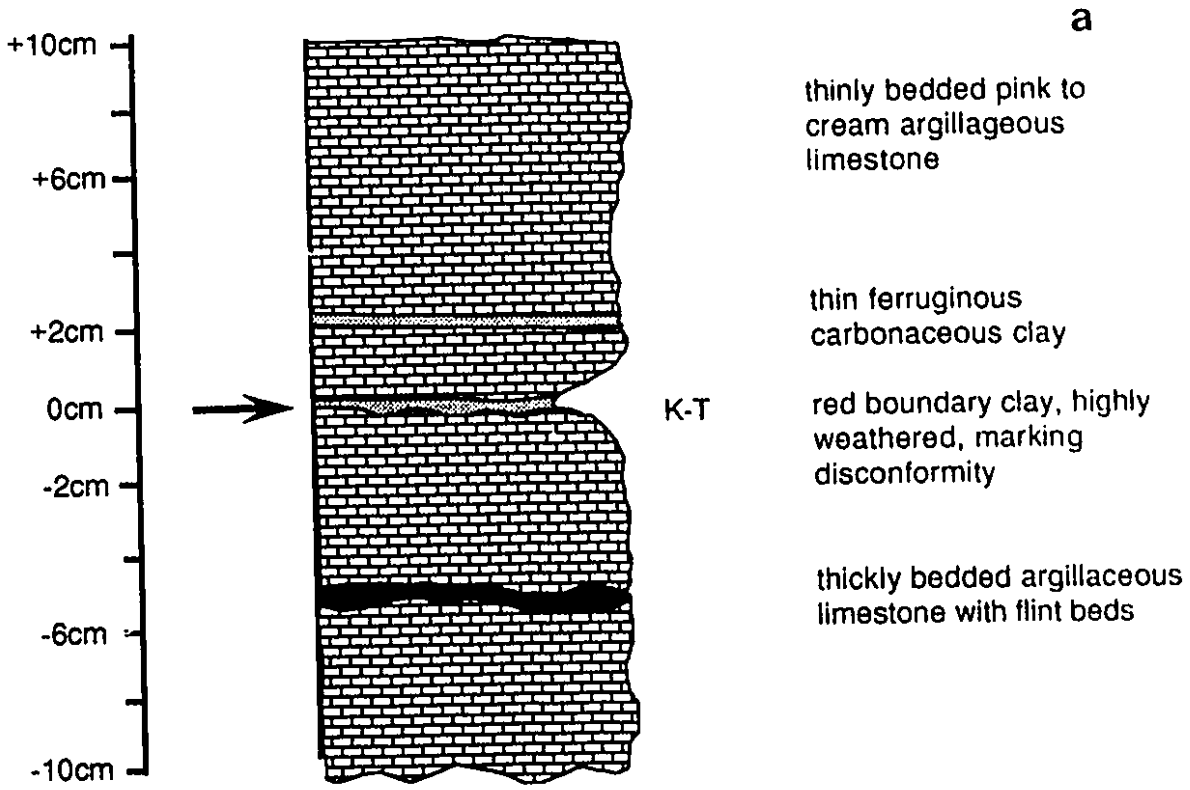

TOP

was exposed along the cliffs, about 2 km west of Hojerup church. The boundary layer is a marl overlain by thick Tertiary limestone and chalk sequences and underlain by thick (≈900 m; Elliot et al., 1989) accumulations of Cretaceous bryozoa-rich chalk containing numerous flint beds and nodules (Schmitz, 1985). The Cretaceous chalk was deposited as low mounds, as is revealed by the undulating nature of flint beds (Birkelund and Hakansson, 1982). Extensive study of this site has led to detailed description of boundary "fish clay" sub-layers (e.g., Ekdale and Bromley, 1984; Schmitz, 1985). The upper and lower boundaries of the clay are characterized by alternating marl and carbonate seams, which have been altered by solution-compaction to form a microstyolitic fabric of tiny, lenticular chalk nodules, separated by clay laminae. The microstyolitic transition is 0.5 to 2 cm thick at the lower contact (upper Cretaceous chalk and fish clay) and is more than 2 cm thick at the upper contact (fish clay and lower Tertiary limestone-chalk). The chalk trough-mound structure and microstyolitic transition has provided an uneven surface on which the fish clay was deposited (Ekdale and Bromley, 1984). The fish clay itself can be subdivided into obvious subunits (Figure 9b) (Christensen et al., 1973; Schmitz, 1985). The entire bed is thickest and most complete in interbiohermal troughs. The subunits (from Schmitz, 1985) include (from bottom to top): **Lower layer III,** 1 cm of laminated, spheroid-rich red smectitic clay with numerous burrows, microcrystalline pyrite spheroids that are partially or wholly altered to goethite and shocked quartz (Schmitz, 1985) (SK 3 in this work); **Upper layer III,** 2-3 cm of reduced, organic-rich black marl, rich in fish scales with less pyrite spheroids than the underlying red layer (SK 2 in this work): **layer IV,** 3 cm of dark to light grey laminated marl with included fragments of chalk (SK 1 in this work). Flattened burrows are

Figure 9a,b. (a) Stratigraphic section of the K-T boundary interval at Stevns Klint, Denmark with a close-up of the fish clay (b).

Stevns Klint, Denmark

a

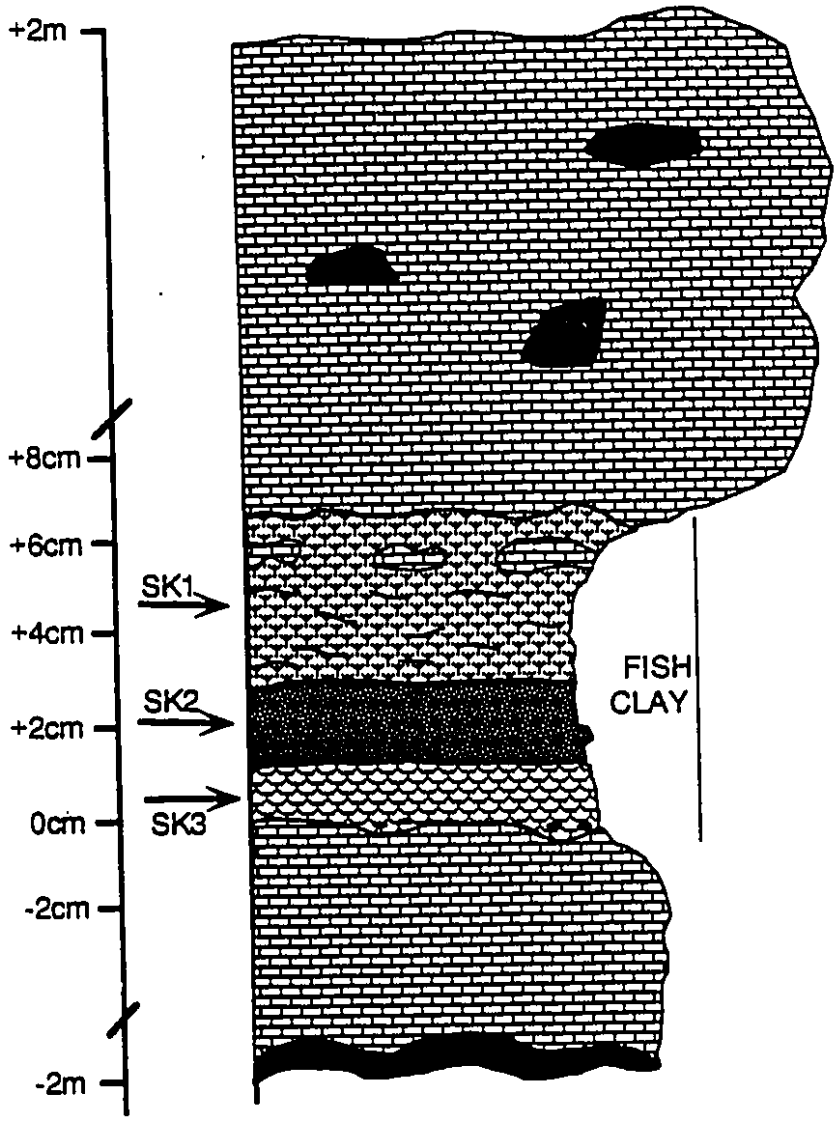

Tertiary limestone
-chalk with flint
nodules

transition phase marl-chalk
IV - dark to light grey marl
with burrows

III - black marl, some pyrite
lower III - laminated, pyrite-
rich, spherule-rich
red marl with shocked qtz.
transition phase chalk-clay

white calcareous bryozoa-
chalk with flint

b

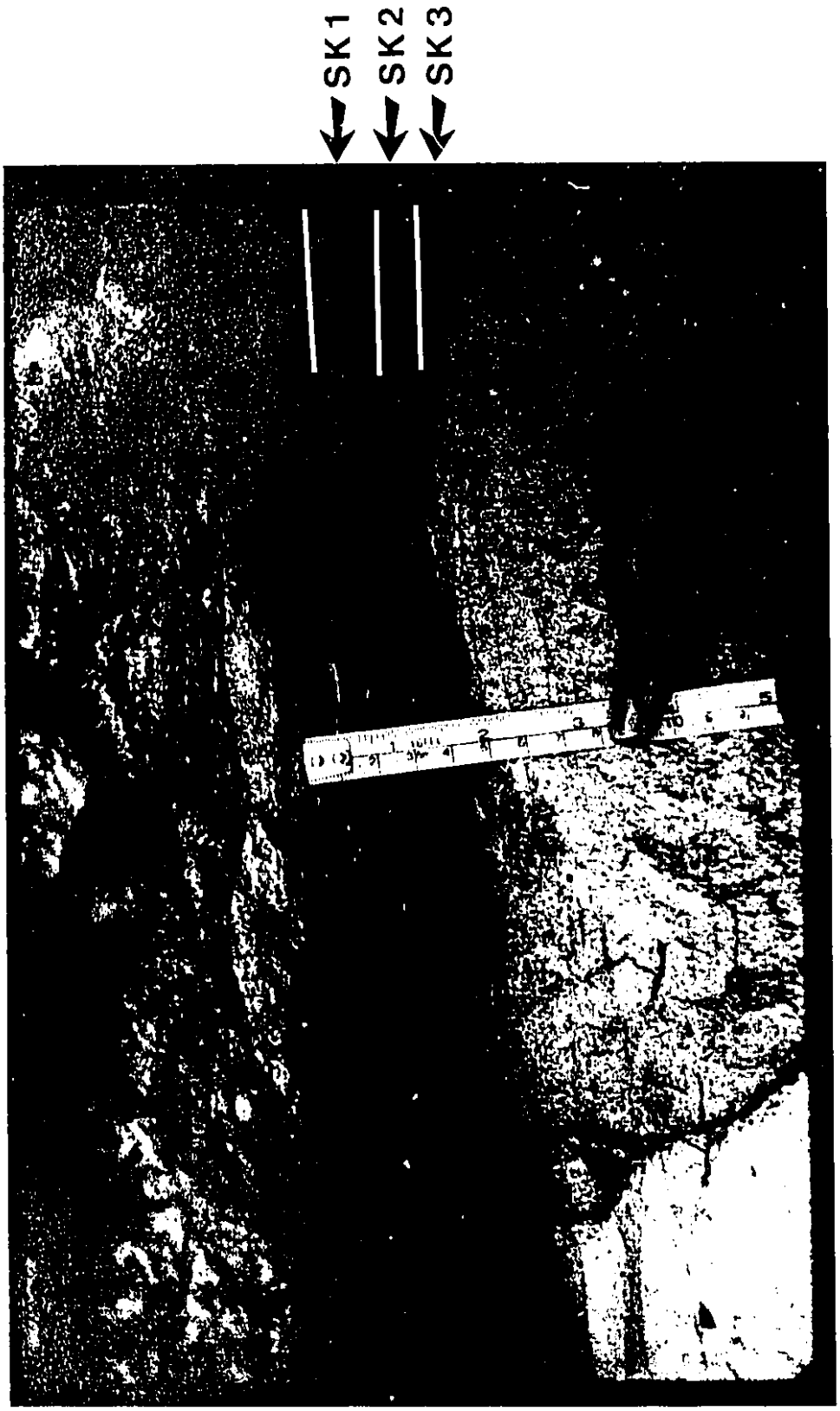

common in layer IV (Figure 9b) but are not seen in the black or red layers. The high organic content, lack of bioturbation and presence of pyrite indicate anoxic conditions existed during fish clay formation (Schmitz, 1985).

Agost, Spain

The Agost site (lat 38°26'N, long 0°36'W) occurs in the Betic Cordilleras stratigraphic unit in Spain and is almost identical lithologically, geochemically and paleontologically to the well-described Caravaca, Spain site (Groot et al., 1989), 100 km away. At Agost, however, the K-T interval is better preserved since it is not disturbed by tectonic movements and shows minimal surface weathering (Smit et al., 1988). Sedimentation is continuous and sedimentation rates are high (Smit, 1990). The 2 mm thick, unbioturbated, green boundary clay lies within a sequence of open-marine, hemipelagic, interbedded marl, limestone and turbidites (Figure 10). The upper Cretaceous unit is a clayey marl with numerous burrows and abundant planktonic foraminifera. The lowest Tertiary rocks are clay and marly clay with bioturbation returning 2 cm above the impact layer. Spherules and shocked quartz are located at the base of the boundary clay (DePaolo et al., 1983).

Terrestrial Sites

Berwind Canyon, Starkville South and Clear Creek North: Raton Basin, Colorado

The sequence at all studied Raton Basin (lat 36°54'N, long 104°27'W) sites is very similar (Figure 11a-c). The boundary clay occurs in the Raton Formation, a rock sequence deposited in freshwater swamp and flood plains. The upper Cretaceous rock

Figure 10. Stratigraphic section of the K-T boundary interval at Agost, Spain.

Agost, Spain

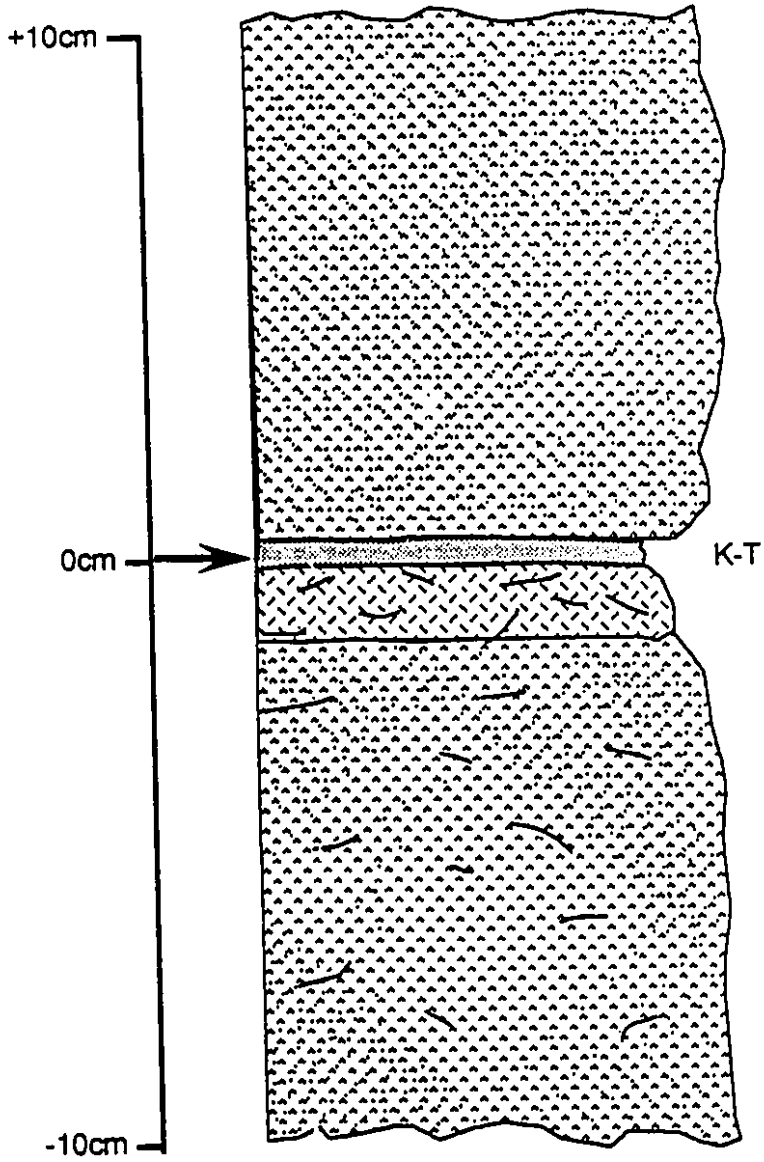
+10cm
0cm
-10cm
K-T
white clay,
marly clay
green boundary clay,
spherules & shocked
quartz at base
whitish clay,
clayey marl with
burrows

unit is typically very fine grained carbonaceous shale, often with thin, discontinuous coal beds. This unit forms a gradational contact with the overlying light grey boundary claystone, a 1-2 cm thick, uniform kaolinitic bed which underlies the ≈ 1 cm thick impact layer. The claystone contains fossil plant material, vitrinite laminae and swirls of vitrinite that may be deformed roots of plants (Izett, 1990). The Berwind Canyon section is one of the best preserved and most complete terrestrial K-T sections (G. Izett, pers. comm., 1988). At Clear Creek North (Figure 11c), shocked quartz is found in the claystone, although clastic grains do not usually occur at all in this layer (Izett, 1990). At all other sites, shocked minerals are contained in the lower part of the impact layer. Also at Clear Creek North, the boundary claystone occasionally pinches out into carbonaceous shale. At this site the boundary claystone and carbonaceous shale may have been reworked prior to deposition of the impact layer (Izett, 1990). The sample site chosen for this work was a continuous vertical sequence which included the claystone. At Berwind Canyon, the contact between the impact layer and boundary claystone is irregular on a small (<0.5 mm) scale. Indications are that desiccation-like cracks formed on top of the boundary claystone and were subsequently filled with impact layer sediment (Izett, 1990). Goyazite spherules, of non-impact origin, occur in the boundary claystone (Izett, 1990). The impact layer is a laminated claystone with pellets of cryptocrystalline kaolinite (rip-up clasts of underlying claystone layer; Izett, 1990). The lower Tertiary coal bed varies from 4-8 cm in thickness. At Starkville South (Figure 11b) a thin, impure coal bed lies directly on top of the impact layer. Fine sandstone with minor mudstone, siltstone carbonaceous shale and thin coal beds occur above the boundary coal bed.

Figure 11a-c. (a) Stratigraphic sections of the K-T boundary interval at Berwind Canyon, Starkville South and Clear Creek North, Raton Basin, Colorado. (b) Photo of the K-T boundary interval at Starkville South. (c) Photo of the K-T boundary interval at Clear Creek North. Impact layer is located at the arrow. A photo of Berwind Canyon is provided in Figure 5b.

a

Raton Basin, Colorado

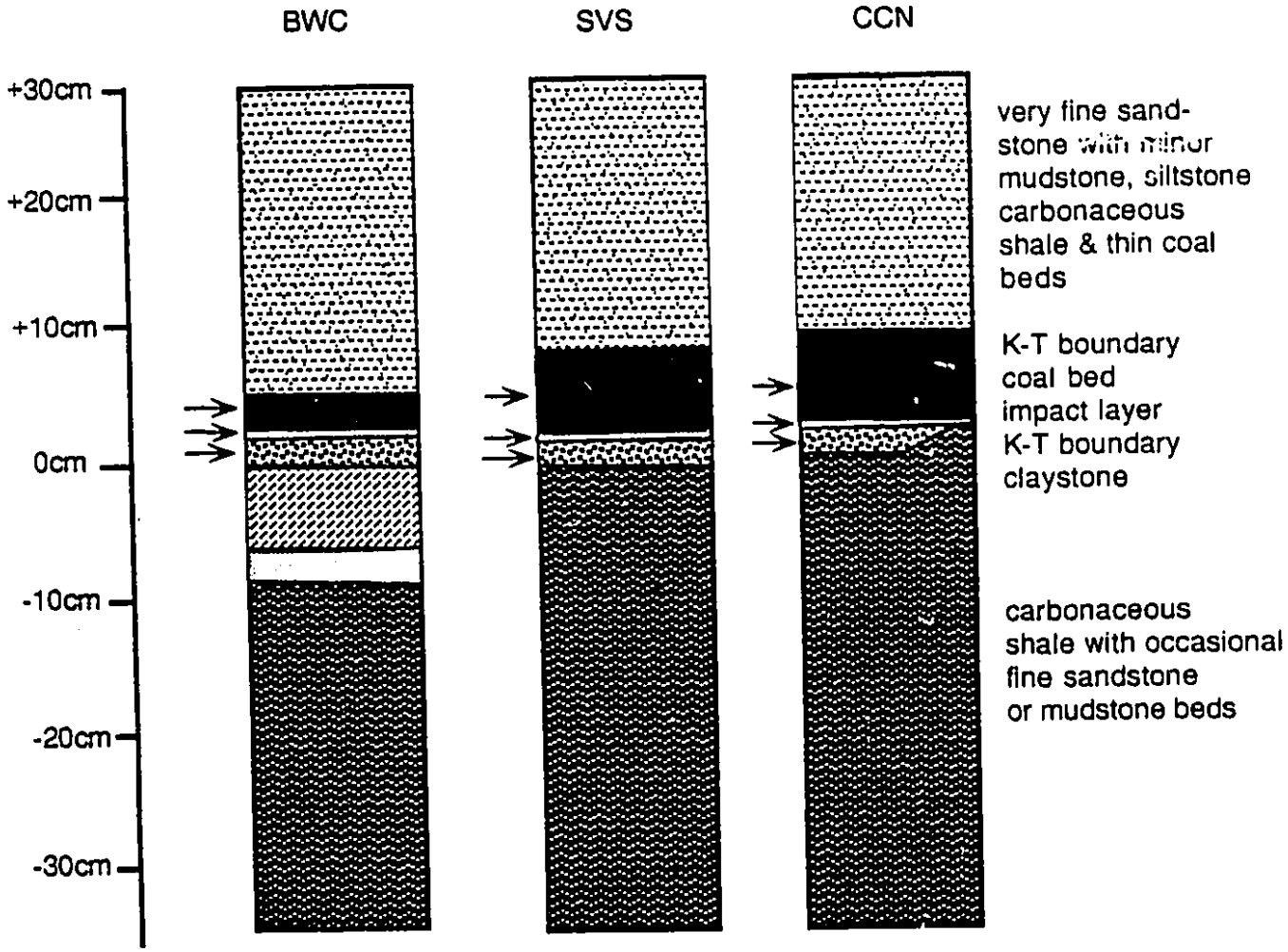


b
1cm

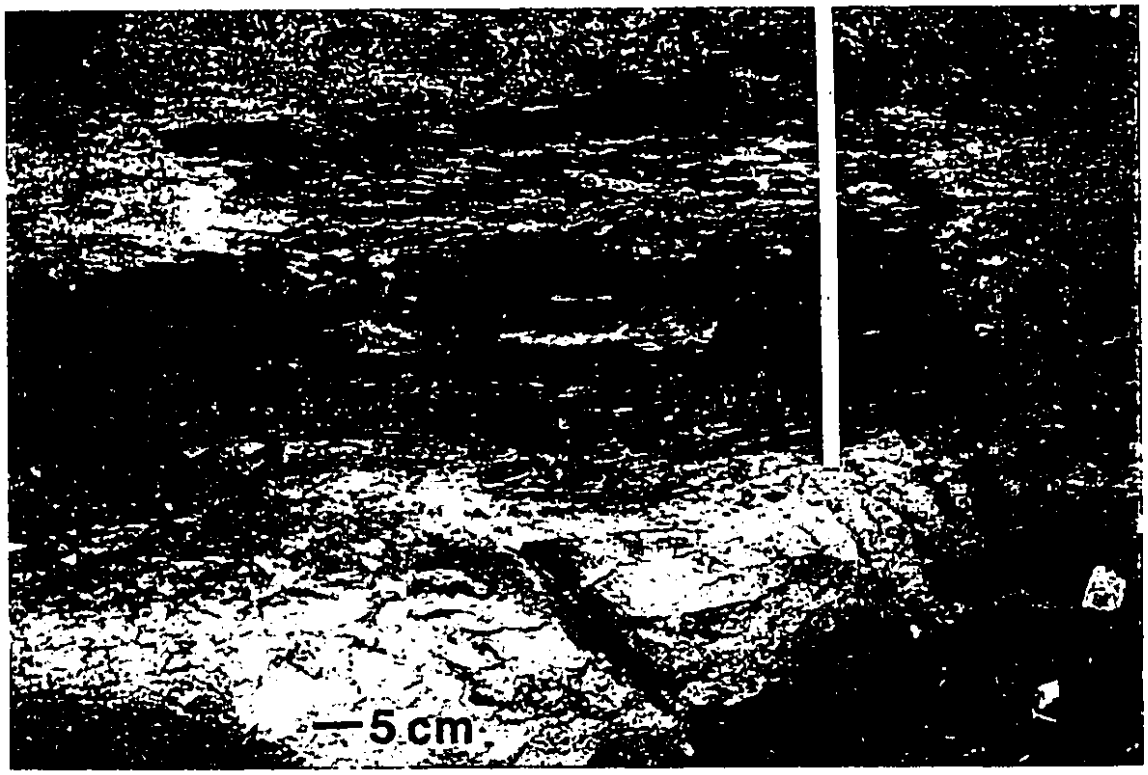
5 cm

Red Deer Valley, Alberta

The 1 cm thick boundary layer at the Red Deer Valley site (Figure 12) is found within a sequence of coal and mudstone of the Scollard Formation. The massive Nevis coal seam overlies the impact layer. The boundary claystone has been identified at this location by G. Izett, but was not analysed in this work. The upper Cretaceous rocks are mudstone. Samples of impact layer were donated by J. Lerbekmo (location given as Scollard Canyon, NE1/4, sec. 11, tp 34, rge. 22, W 4th mer.).

Morgan Creek, Saskatchewan

At the Morgan Creek site (Figure 13) (lat 49°15.8'N, long 106°19'W), the K-T boundary is located approximately at the contact between the bentonitic mudstones and siltstones of the Frenchman Formation (upper Cretaceous) and the overlying sandstone, siltstone, mudstone, carbonaceous shale and coal of the Ravenscrag Formation (lower Tertiary). These units were deposited in alluvial and lacustrine environments and the boundary clay marks the contact between coal-bearing strata (above) and dinosaur-bone-bearing strata (below). The stratigraphically-highest dinosaur bones have been found 10 m below the boundary. The 2 cm thick brown-black carbonaceous claystone impact layer is underlain by a 1.5 cm pinkish-tan boundary claystone. Shocked quartz was identified (Nichols et al., 1986) in the impact layer. A sample of the impact claystone was donated by D.J. Nichols (collected by F. Fleming).

Figure 12. Stratigraphic section of the K-T boundary interval at Red Deer Valley, Alberta (after Lerbekmo and St. Louis, 1986).

Red Deer Valley, Alberta

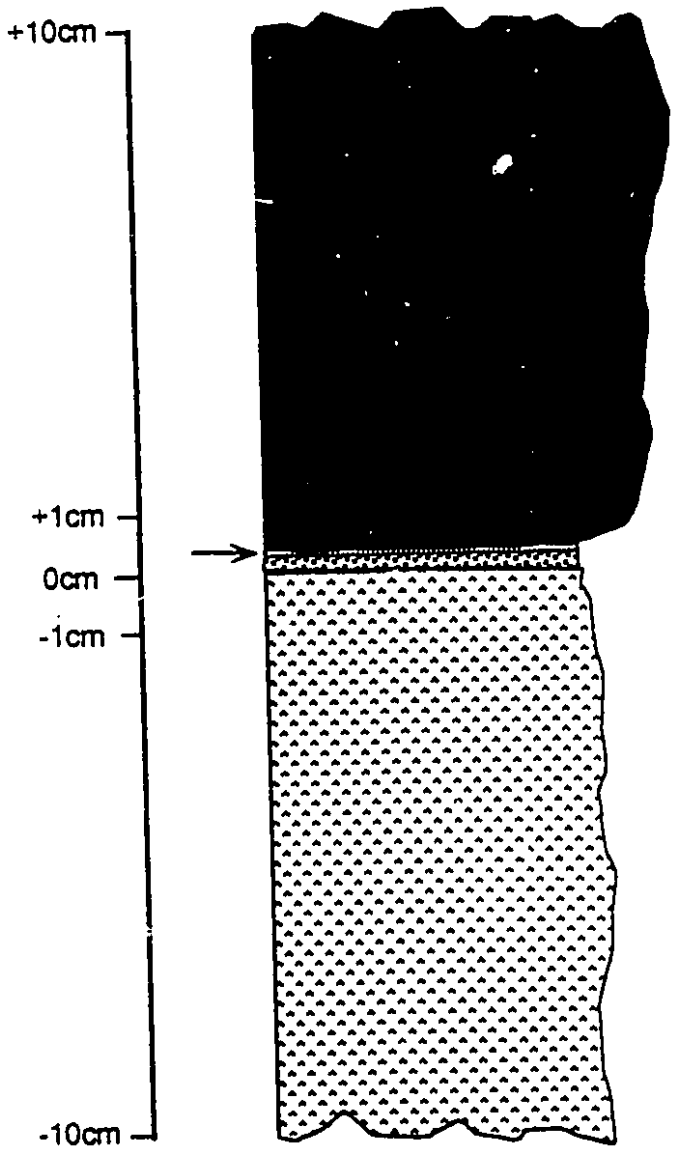

Figure 13. Stratigraphic section of the K-T boundary interval at Morgan Creek, Saskatchewan (after Nichols et al., 1986).

Morgan Creek, Saskatchewan

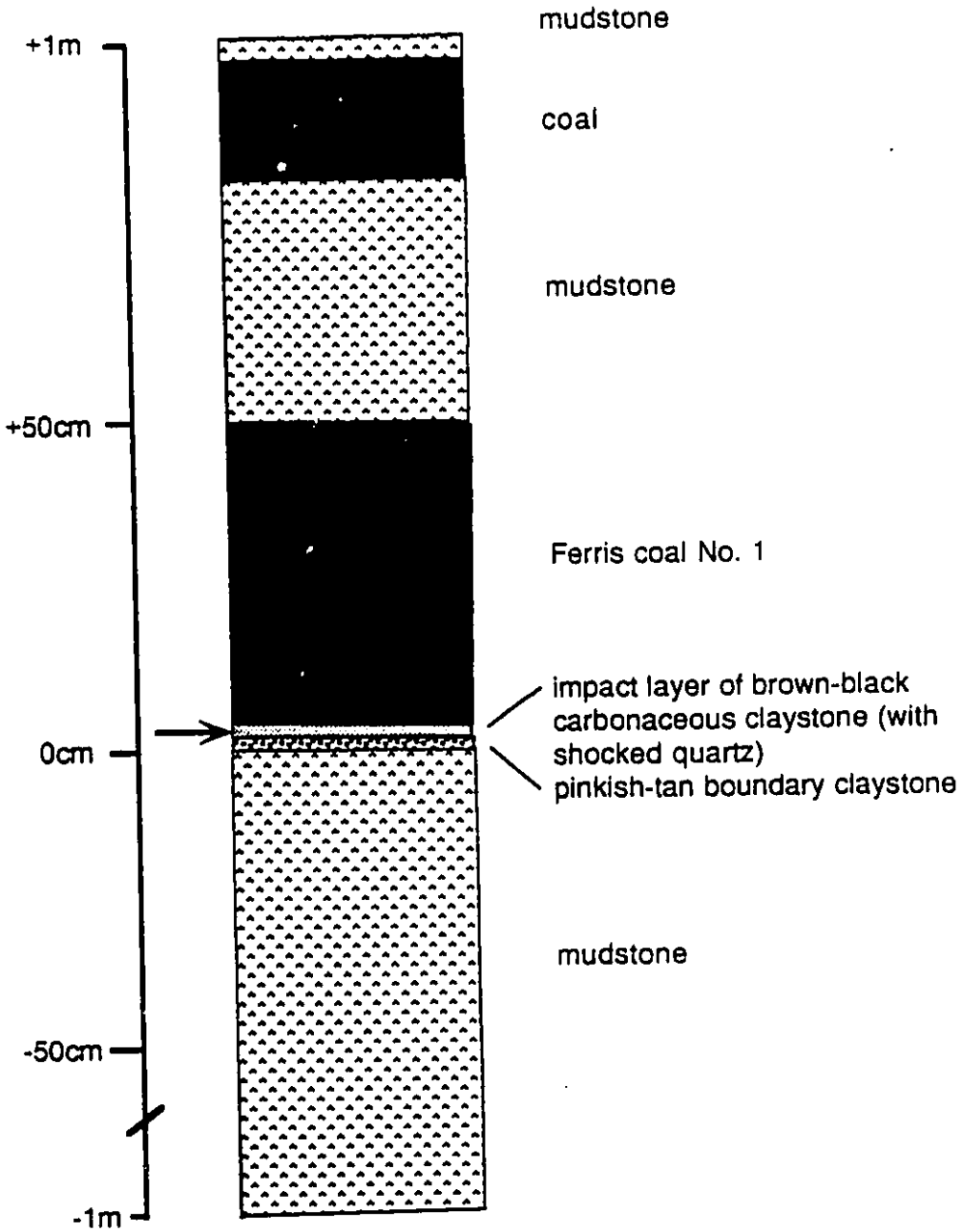

Lance Creek, Wyoming

The boundary interval at the Lance Creek site (Figure 14) occurs within the Lance Formation. The 0-3 cm thick boundary claystone contains goyazite spherules while the overlying 2-3 mm thick claystone contains shocked minerals (Bohor et al., 1987). The lower Tertiary rocks are clay-shale with numerous plant fragment impressions. The upper Cretaceous rocks are > 25 cm of carbonaceous shale. A sample of the impact layer was donated by D.J. Nichols (USGS Paleobotany locality D6888: SE1/4, SW1/4, SE1/4 Sec. 5, T.38N., R.65W., Niobrara County, Wyoming; USGS Dixon Ranch 71/2' quadrangle).

Figure 14. Stratigraphic section of the K-T boundary interval at Lance Creek, Wyoming (after Bohor et al., 1987b).

Lance Creek, Wyoming

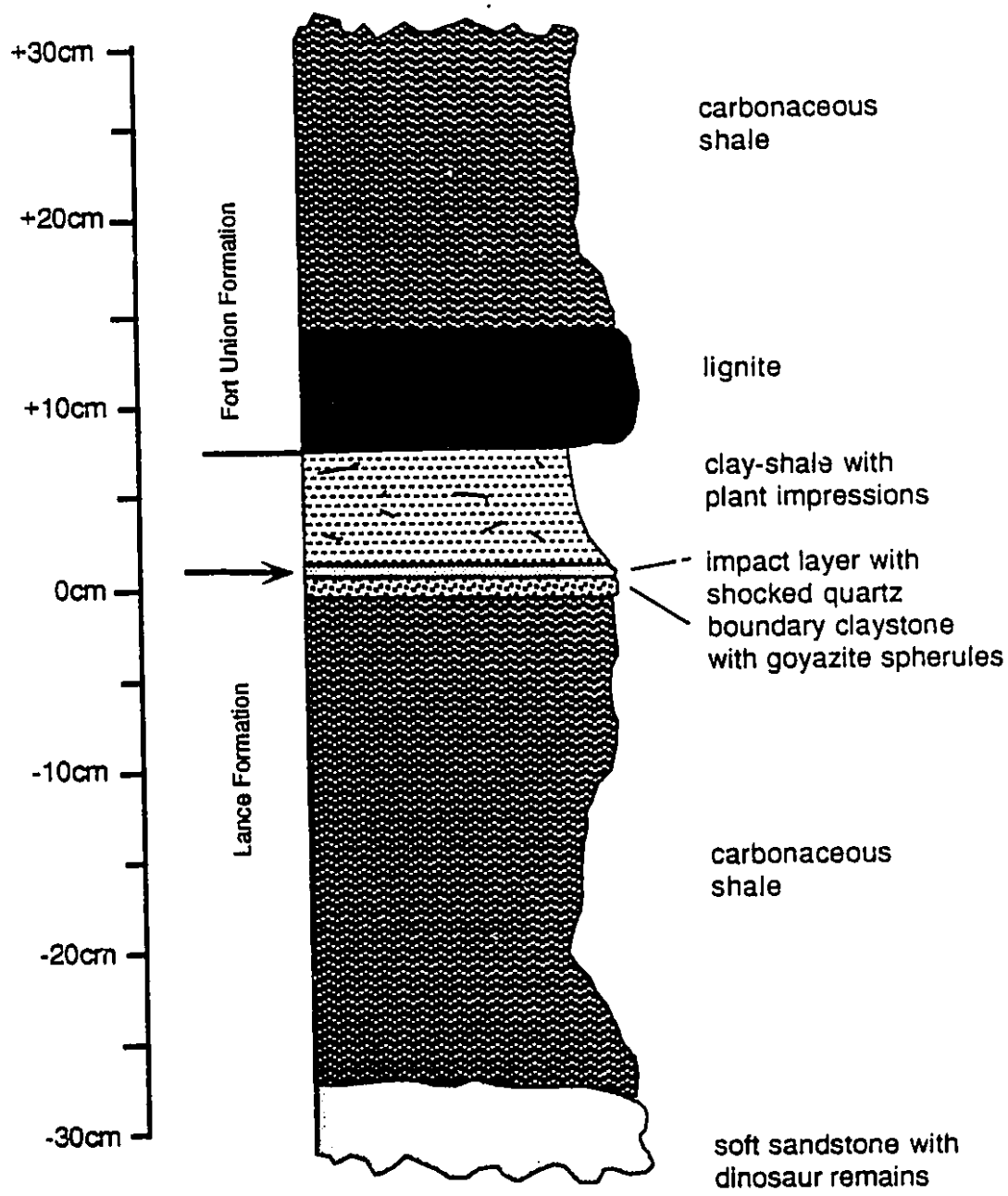

CHAPTER FOUR

GEOCHEMISTRY OF PLATINUM-GROUP ELEMENTS

The most difficult aspect of evaluating the behavior of PGE at the K-T boundary is the dearth of published data for PGE in sediments (Tredoux et al., 1989). A cursory overview of PGE geochemistry follows. The discussion concentrates on the chemical conditions pertinent to the formation of PGE-rich layers in sedimentary environments and presents new background data for crustal PGE abundances.

Geochemical Affinities

The PGE are a group of siderophile (and to a lesser extent chalcophile) elements, thus having a geochemical affinity for metallic iron and sulphide phases (Barnes, 1985). Partition coefficients for PGE between silicate and sulphide liquid are unknown (Barnes, 1985), but $D^{PGE}_{sul/sil}$ estimates range from 10^2 (Ross and Keays, 1979) to 10^5 (Campbell and Barnes, 1984) with a trend of increasing D from Os > Ir > Ru > Rh > Pt > Pd (Barnes, 1985). Gold, not strictly a PGE but a noble metal, will be included in the term PGE, unless otherwise indicated. Within igneous melts, PGE exist in discrete minerals or as intermetallic compounds of < 1 μm-size in oxide or silicate minerals (Cousins and Vermaak, 1976). Common carrier phases (hereafter defined as a phase with which PGE are found to be associated) are olivine, sulphides, chromite and platinum-group minerals (PGM; Barnes et al., 1985). Lattice substitution of PGE for metallic cations, although theoretically possible, is not widely accepted (Cousins and Vermaak, 1976). Based on their geochemical coherence, the PGE can be subdivided into groups, such as Iridium

PGE (IPGE; Ir, Os, Ru) and Platinum PGE (PPGE; Pt, Pd, Rh and Au). This grouping is a result of differences in size (Table 3) and in the chalcophile nature of the PPGE. The PGE content in sulphur-poor silicate rocks increases from felsic to ultramafic types (Crocket, 1981a), a trend that may abruptly change with the appearance of sulphides at sulphur-saturation. Platinum-group elements are more abundant in iron than stony meteorites (see Table 19). They are concentrated in the metallic phases of meteorites (Crocket, 1972; Rambaldi, 1976, 1977a, 1977b) and are purported to be concentrated in the Earth's core and lower mantle (Cousins, 1973). Detailed reviews of PGE geochemistry and partitioning are presented elsewhere (Cousins, 1973; Crocket, 1981a; Barnes et al., 1985).

Table 3. Physical Characteristics of the PGE.

Element	Z	Charge	I.R.[1] (Å)	M.P.[2] (°C)	B.P.[2] (°C)
Ru Ruthenium	44	+2 +3 +4	0.74 0.68 0.62	2310	3900
Rh Rhodium	45	+2 +3 +4	0.72 0.66 0.60	1966	3727
Pd Palladium	46	+2 +3 +4	0.86 0.76 0.615	1552	3140
Os Osmium	76	+2 +4	0.74 0.68	3045	5027
Ir Iridium	77	+2 +3	0.74 0.62	3045	5027
Pt Platinum	78	+2 +4	0.80 0.625	1722	3822
Au Gold	79	+1 +3	1.37 0.85	1064	3080

I.R = ionic radius; M.P. = melting point; B.P. = boiling point.
[1] Shannon (1976)
[2] Weast (1989)

Mobility of PGE

The early work emphasized the resistance of PGE to chemical attack and remobilization, particularly at the K-T boundary, where much of the modelling is based on the assumption that the PGE abundance is primary (e.g., Kyte et al., 1985; Strong et al., 1987). It is now clear that the PGE can be remobilized in most geological environments, when rocks are altered and during sediment diagenesis (Cousins, 1973; Feather, 1976; Westland, 1981; Barnes et al., 1985; Bowles, 1986; Mountain and Wood, 1988; Wallace et al., 1990). Of specific pertinence to the present work is the observation that PPGE can be mobilized in acidic low temperature aqueous solutions and redeposited in carbonaceous-rich sediments during weathering and diagenesis (Bowles, 1986; Izett, 1990).

The susceptibility of PGE (metal) to solubility in aqua regia increases in the order: Pd > Pt > Rh > Ru > Os = Ir (Cousins, 1973). This is considered to represent the general order of PGE mobility during weathering (Westland, 1981). Since aqua regia attack mimics that of prolonged chemical attack in nature (Cousins and Vermaak, 1976), Pt and Pd should mobilize readily in nature in acidic chloride-solutions. This has been substantiated thermodynamically (Mountain and Wood, 1988) and the order of reactivity listed above has been given some support from the study of neutral surface waters in placer deposits (Cousins and Vermaak, 1976). Platinum and palladium are also known to form amine and purine organic complexes and can, therefore, possibly complex with free carboxylic acid and with soil organic matter (Westland, 1981; Bowles, 1986).

The IPGE alloys are less effected by weathering, burial and metamorphism than the PPGE alloys (Feather, 1976) and, unlike Pt (Goldberg et al., 1988), Ir does not form

strong complexes with chloride and bromide in the marine environment. This is not to say that Ir, Ru and Os are not at all susceptible to remobilization and, in fact, low-temperature mobilization of all PGE, including Ir, has been demonstrated in the formation of laterites (Bowles, 1986) and around the Acraman impact structure (Wallace et al., 1990). Acraman is the first documented case of a widespread ejecta blanket (ejecta found up to 450 km from the crater lake; Gostin et al., 1989) with anomalously high cosmogenic siderophile contents, shown to be derived from a known impact structure (Gostin et al., 1986). Low-temperature mobilization of PGE into shale horizons up to 100 cm above and below the Acraman ejecta layer has been documented, however, relative degrees of mobility could not be estimated due to the possibility of terrestrially-derived PGE contamination (Wallace et al., 1990). Micro-organisms can also play a role in PGE redistribution and/or dispersal or may enhance Ir anomalies such as those at the K-T boundary (Dyer et al., 1989). This work will show that Ru and Ir are mobilized and fixed in organic matter, although to a lesser degree than the other PGE. Gold is at least five orders of magnitude more soluble than Pt as a chloride and is frequently mobile under various geological conditions (Seward, 1984; Webster and Mann, 1984; Barnes et al., 1985).

In this study, it was important to assess the degree to which PGE were associated with organic matter, in order to select the elements most valuable for identification of the mineralogical carrier phase(s). The results from the present work are presented in Table 4 and Figure 15. The percentage of organically-associated PGE varies between sites and elements. In general, marine and terrestrial trends (from Table 4 and Figure 15) are as follows: Rh > Au > Pd > Pt > Ru > Ir and Au > Pd > Pt ≈ Rh > Ru > Ir,

Figure 15. Percentage of total PGE abundance associated with the organic fraction in the K-T impact layer. For all elements except Au, marine sites show a higher degree of PGE-organic association. Mean values noted as "+".

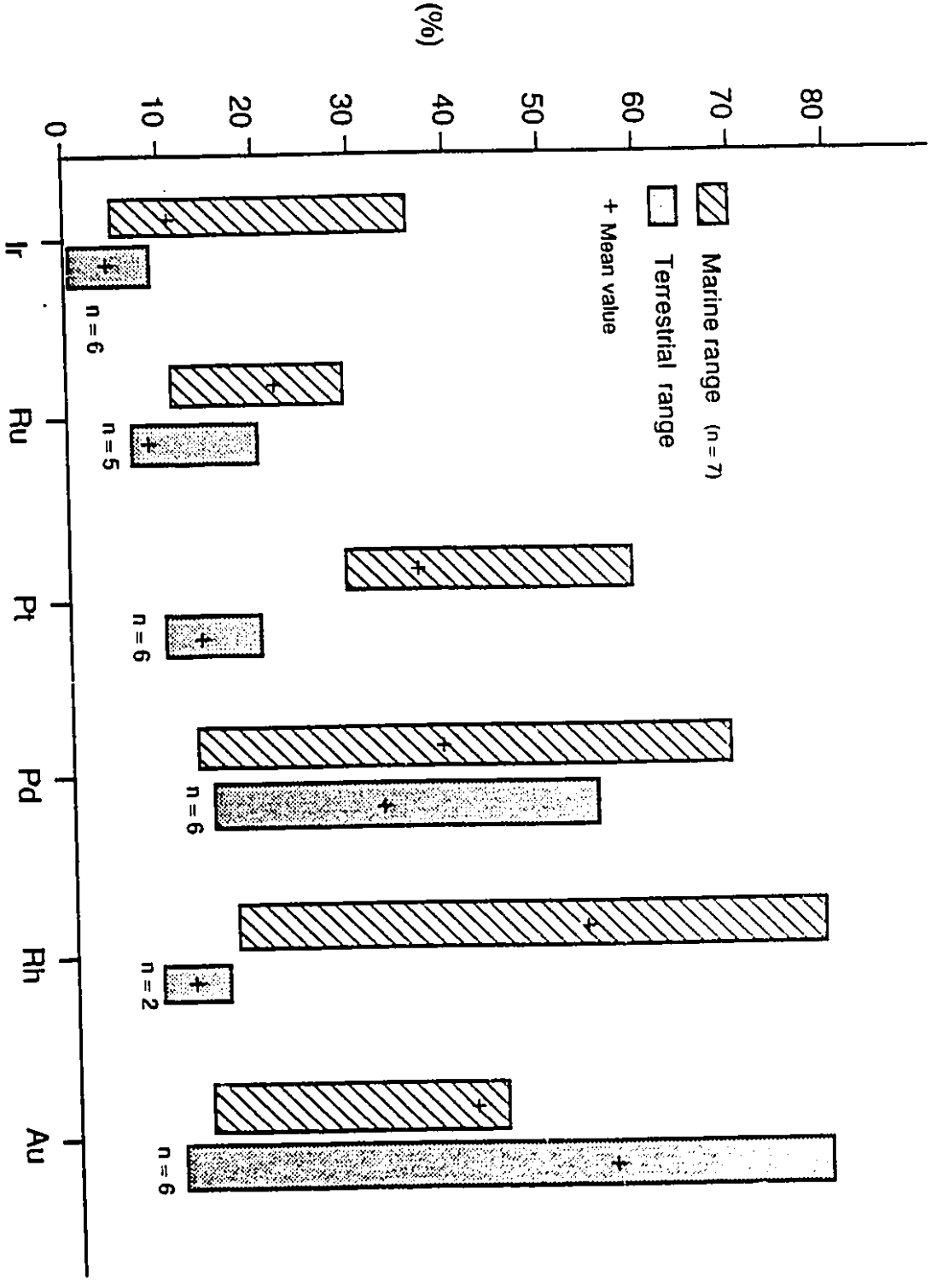
(%)
0
10
20
30
40
50
60
70
80
Marine range (n = 7)
Terrestrial range
+ Mean value
Ir
Ru
Pt
Pd
Rh
Au
n = 6
n = 5
n = 6
n = 6
n = 2
n = 6

respectively. The organic association of Ir has been suggested in the Stevns Klint and Caravaca boundary clay (Schmitz et al., 1988) where 50% of the bulk sample Ir was found to be associated with organic compounds. The discrepancy between that value and the 3% organic association determined here for Stevns Klint may be related to analytical technique (see Chapter 2). It seems likely, however, that the association of PGE with organic matter varies throughout the boundary layer. Much variation is noted within the boundary layer at Petriccio and Starkville South (Table 4). The data indicate that an organic carrier phase is present at all sites. Ruthenium and Ir, in both environments, show the least partitioning into the organic carrier and they are, therefore, more useful for identification of the PGE mineral carrier phase and of the impactor than previously quoted Au/Ir or Pt/Ir ratios (Alvarez et al., 1982; Kastner et al., 1984; Tredoux et al., 1989). The high degree of Pt-organic association in marine sites may explain the previously observed heterogeneous nature of Pt distribution (Tredoux et al., 1989) in the Stevns Klint fish clay.

Except for Au, the terrestrial sites show, on average, a lesser degree of association of PGE with the organic phase than their marine counterparts (Figure 15), but much variation exists even within one site (Table 4). The degree of organic association is taken as an indicator of potential mobility. It is proposed here that the original host of PGE was a mineral or amorphous phase and that its subsequent alteration led to partial remobilization of the PGE into organic complexes, the degree of mobilization varying with the element. Uniess otherwise specified, the term "mobility", therefore, refers to fixing of PGE in organic phases. Once released from the original carrier, it is possible that some PGE were lost from the boundary layer. The degree of loss is site and element

dependent. Since Ru and Ir are the least organically associated and are the most resistant to chemical attack in nature (Cousins, 1976; Barnes, 1985), most of the following discussion will focus on these elements and their ratio.

Table 4. Percent of total PGE associated with the organic fraction in the K-T impact layer.

	Pt	Pd	Ru	Ir	Rh	Au
Marine sites						
Petriccio P1	31	23	22	5	75	24
Petriccio P2	58	54	22	15	32	50
Petriccio P3	30	69	14	7	17	41
Knappengraben K1	50	17	12	16	61	38
Knappengraben K2	49	37	29	36	60	38
Elendgraben	49	22	28	13	61	45
Woodside Creek	29	12	19	9	77	14
Stevns Klint	11	73	19	3	16	73
Terrestrial Sites						
Berwind Canyon 2-5μm	10	27	7	2	9	73
Starkville South <2μm 50μm	20 12	37 55	20 8	8 8	16 -	77 74
Clear Creek North <2μm 5-20μm 50μm	11 10 13	26 25 13	6 6 -	2 2 4	- - -	17 11 16

- denotes values below the limit of detection. Sample ID for Knappengraben and Petriccio are given in Table 9.

Small sample size precluded analysis of organic phases on each size-fraction for marine sites and the organically-bound PGE proportions in bulk clay are given in Table 4. Larger sample size at terrestrial sites has enabled the determination of organically-associated PGE for coarse and fine fractions. No consistent trend of PGE partitioning has been observed for these two fractions.

PGE Background Levels

Table 5 summarizes PGE abundances and their interelement ratios for Cretaceous limestones collected in Spain. PGE values are low and interelement ratios are erratic. Possible reasons for the eratic ratios include: 1) near-detection limit determinations and 2) addition of non-cosmic flux and heterogeneously distributed PGE-rich components. No ready explanation is available for the higher PGE abundances in Limestone-3, except that it was taken at a different location than 1 and 2. All values, however, are within the range of normal sediments (Table 6).

Table 5. PGE content (in ppb) and interelement ratios of Cretaceous limestone samples, remcte from the K-T boundary.

Location	Pt	Pd	Ru	Ir	Au	Rh
Lmst-1						
clay	7.4	1.5	0.02	0.01	0.57	0.04
2-5μm	11	2.1	0.07	0.05	-.-	-.-
5-20μm	13	1.3	0.02	0.02	0.55	0.03
20-50μm	-.-	-.-	-.-	-.-	-.-	-.-
sand	0.72	4.7	0.05	0.03	-.-	0.03
Lmst-2						
clay	1.4	2.0	0.06	0.03	2.3	0.03
2-5μm	0.82	1.2	0.03	0.01	0.87	0.03
5-20μm	0.89	1.2	0.02	0.02	0.46	0.02
20-50μm	-.-	-.-	-.-	-.-	0.08	0.03
sand	0.28	0.61	0.03	0.008	0.13	-.-
Lmst-3						
clay	-.-	2.8	-.-	-.-	3.4	0.21
2-5μm	1.8	2.7	-.-	0.15	3.6	0.52
5-20μm	1.0	1.9	-.-	0.12	9.3	0.39
20-50μm	-.-	-.-	0.06	0.06	-.-	0.11
sand	1 2	1.9	0.13	0.16	11	0.10

Table 5 con't

Location	Pt/Ir	Pd/Ir	Au/Ir	Rh/Ir	Ru/Ir
Lmst-1					
clay	740	150	57	4.0	2.0
2-5μm	220	42	-.-	-.-	1.4
5-20μm	650	65	28	1.5	1.0
20-50μm	-.-	-.-	-.-	-.-	-.-
sand	24	157	-.-	1.0	1.7
Lmst-2					
clay	47	67	77	1.0	2.0
2-5μm	82	120	87	1.0	3.0
5-20μm	45	60	23	1.0	1.0
20-50μm	-.-	-.-	-.-	-.-	-.-
sand	35	76	16	-.-	3.8
Lmst-3					
clay	-.-	-.-	-.-	-.-	-.-
2-5μm	12	18	24	3.5	-.-
5-20μm	8.3	16	78	3.3	-.-
20-50μm	-.-	-.-	-.-	1.8	1.0
sand	7.5	12	69	0.6	1.8

-.- denotes values below limit of detection.
All determinations are on a carbonate-free basis.

Table 6. Background PGE abundance (in ppb) for sediments remote from extinction boundaries (other studies).

	Pt	Pd	Ru	Ir	Rh	Au
Italy[1]				0.09-0.1		
Saskatchewan[2]				0.028		
Colorado[3]				0.022-0.03		
Alberta[4]				0.06-0.11		
France[5]	1.1-3.9	0.99-6.5	0.091-0.89	0.12-<0.05	<0.02	1.0-14.0
Arctic Islands[6]	0.12-4.2	0.23-3.2	<0.05	<0.05	<0.02	

Blank spaces indicate no data for that element. All data from sediments (sandstone, limestone, shale) greater than 10 cm above and 10 cm below extinction horizons. Data from Italy, Saskatchewan, Colorado and Alberta are for sediments above and below the K-T boundary. Range of data from France is for sediments above and below the Frasnian-Famenian boundary. Data from the Arctic Islands is for sediments above and below the Ordovician-Silurian boundary. Sources of data: 1. Montanari et al. (1983); 2. Nichols et al. (1986); 3. Izett (1990); 4. Lerbekmo and St. Louis (1986); 5., 6. Unpublished data from W.D. Goodfellow.

PGE Abundance Above and Below the K-T Boundary Clay

Layers above and below the boundary clay were studied to investigate the PGE mobility and to assess their previously documented enrichments in the adjacent rocks (e.g., Crocket et al., 1988; Rocchia et al., 1990). Figure 16 is a profile of Ir and Ru concentration across the boundary layers at Berwind Canyon, Colorado. Although the peak PGE abundance is found in the impact layer, significant bulk concentrations (e.g., abundance in all size-fractions added) are also seen in the layers above (coal seam) and below (boundary claystone). The concentration of PGE in the terrestrial impact layer is usually higher than that in the coal layer above or kaolinitic boundary claystone below (see Table 13a-c, Figure 17). The Ru/Ir ratio in the terrestrial impact layer is 0.92 ± 0.28[1], whereas it is more variable and slightly higher in the coal layer (1.4 ± 1.1; different to impact layer at 60-80% confidence level; Student's t-test) and boundary claystone (1.6 ± 0.76; different to the impact layer at the 80-90% confidence level) (Figure 17). In the Acraman ejecta horizon, the Ru/Ir ratio has a mean value of 1.3 ± 0.57 (three localities), whereas the green and red shales within 100 cm above and 100 cm below the ejecta have higher and more variable ratios (mean = 4.2 ± 4.5; Wallace et al., 1990). The incorporation of PGE into adjacent layers at the K-T boundary could originate from: 1) organic or inorganic remobilization of elements out of the impact layer, 2) physical redistribution by burrowing organisms or roots, or 3) primary input into the claystone and coal layer as they were deposited. Comparison to the background data presented in Table 5 indicates the bulk PGE abundances in the coal and claystone are too high to be derived solely from cosmic dust. Primary input from another extraterrestrial

[1] X ± Y denotes a mean (X) and an associated 1σ standard deviation (Y).

Figure 16. Iridium and ruthenium abundance profile across the boundary layers at Berwind Canyon, Colorado. All data are bulk abundances, taken from Tables 13a-c.

Berwind Canyon, Colorado

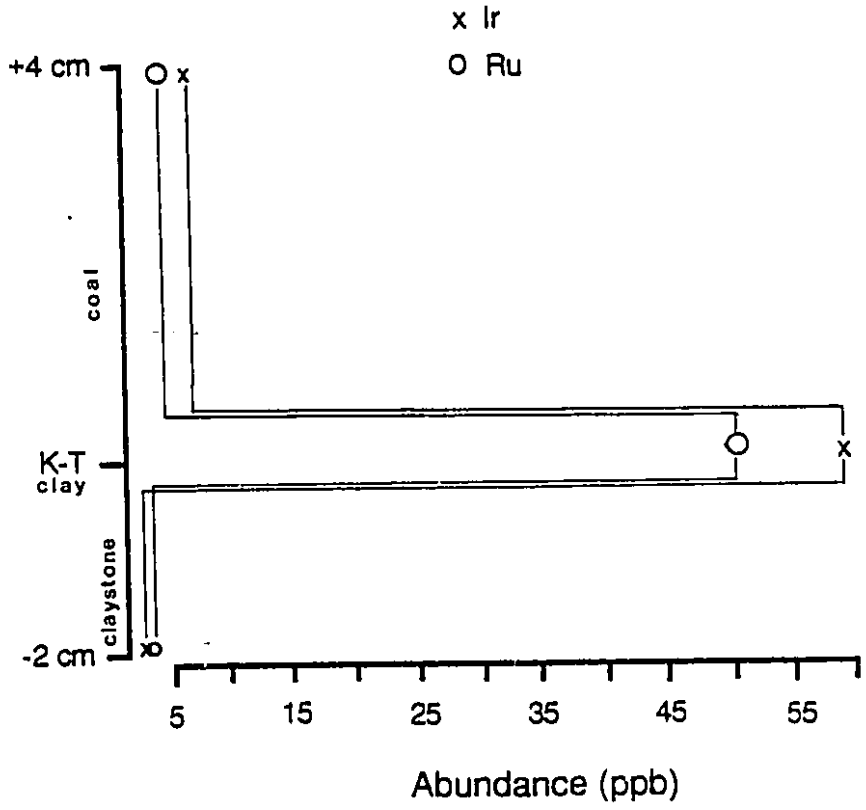

Figure 17. Iridium versus Ru/Ir ratio for terrestrial K-T boundary layers (boundary claystone, impact layer, boundary coal seam). Lower Ir content, more variable and higher Ru/Ir ratios are characteristic of the boundary claystone and coal layers. Where the impact layer was subdivided for analysis, total abundances for that layer are plotted for each site. Where more than one section was sampled at a given location, mean values are plotted for that site.

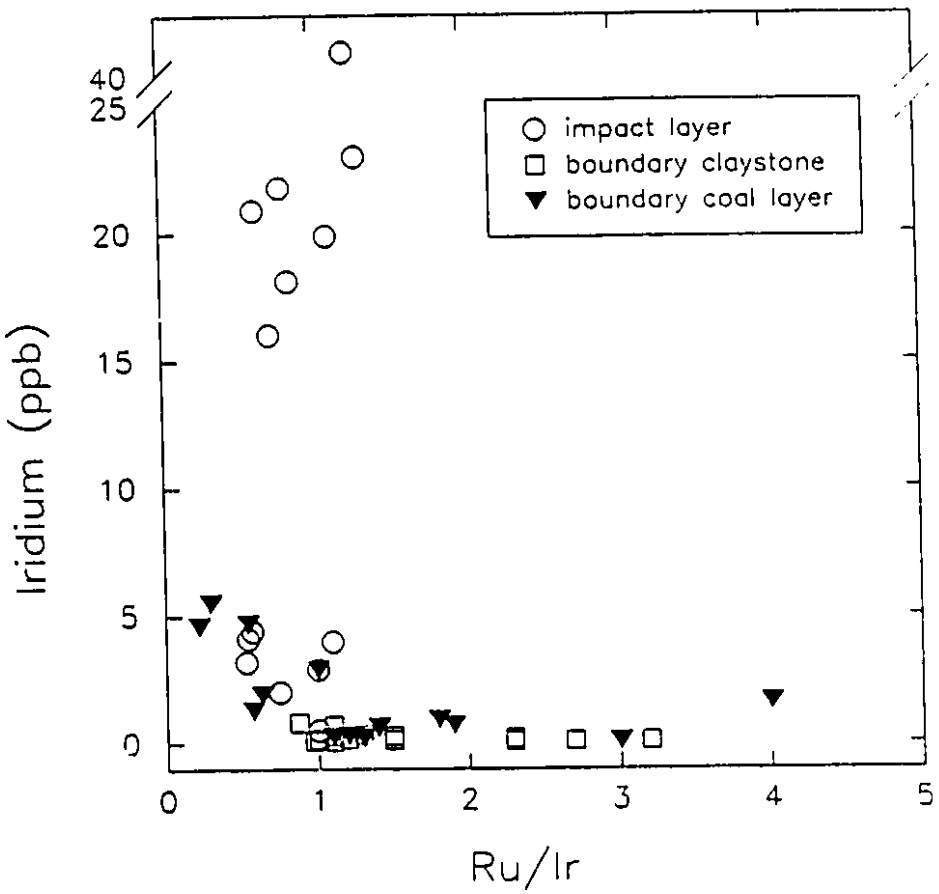
impact layer
boundary claystone
boundary coal layer
Iridium (ppb)
Ru/Ir
40
25
20
15
10
5
0
0
1
2
3
4
5

or terrestrial source is not supported by other evidence (Izett, 1990), nor is physical redistribution of the elements by burrowing organisms (Izett, 1990). The first scenario seem most likely. Indications of remobilization can be deduced from the Ru/Ir ratio. The slightly higher degree of Ru mobility in the terrestrial environment would lead to a higher Ru/Ir ratio in layers where PGE were derived by remobilization. It is interesting to note that integration over the entire sequence (coal, impact layer, boundary claystone) yields a Ru/Ir value close to that of the impact layer alone (Table 7). This implies that despite some migration of Ru and Ir out of the impact layer, the chemical coherence of these elements has left the integrated ratio intact over a 4 cm interval. The enrichment of PGE in coal sequences has been previously documented in non-K-T deposits (Kucha, 1982; Van der Flier-Keller and Fyfe, 1987) and such carbonaceous layers are an effective trap for noble metals (Bowles, 1986).

Table 7. Integrated ruthenium/iridium ratios in samples from terrestrial K-T boundary sections.

	Berwind Canyon	Starkville South	Clearcreek North
Ru/Ir integrated	0.89	0.97	0.71
Ru/Ir of impact layer	0.90	0.98	0.60
Difference (%)	1	1	18
Integrated value calculated as follows: $[\Sigma Ru_{impact\ layer} + \Sigma Ru_{claystone} + \Sigma Ru_{coal}] / [\Sigma Ir_{impact\ layer} + \Sigma Ir_{claystone} + \Sigma Ir_{coal}]$			

In marine sections, samples of limestone were taken from up to 2 m above and 2 m below the K-T clay at Petriccio and Elendgraben (Table 8). Figure 18 is an Ir and Ru profile over this interval. Although the peak concentration of PGE is in the impact layer, the peak is not sharply defined and some PGE are in adjacent sediments. The mean Ru/Ir ratio (0.83 ± 0.1) in the adjacent sediments is lower than that of the marine

Figure 18. Iridium and ruthenium abundance profile across an interval 2 meters above and 2 meters below the impact layer at Petriccio, Italy. All data are bulk abundances, taken from Tables 8 and 9 with integrated values from the Gubbio, Italy site (data for Gubbio taken from Rocchia et al., 1990).

Petriccio, Italy

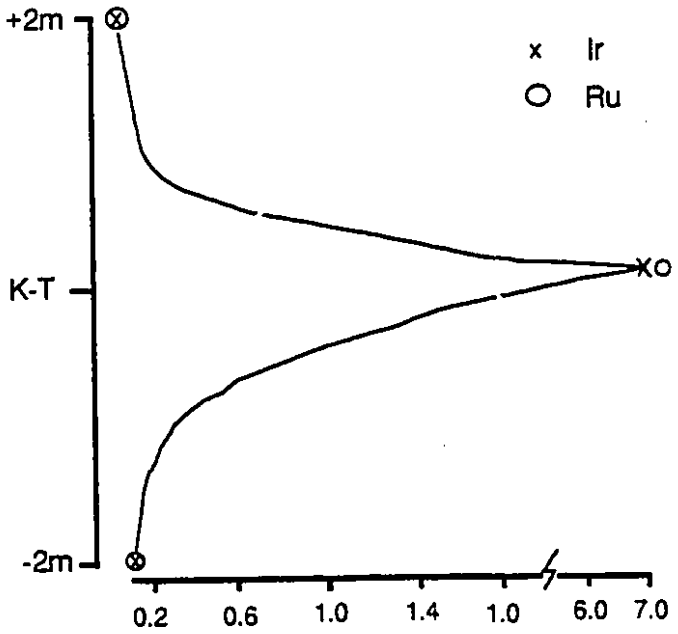

impact layer (1.77 ± 0.53) (different at the 90-95% confidence level). The concentration of Ru and Ir is higher in these Petriccio and Elendgraben samples than in the background limestones (Table 5) and other sediments (Table 6). Samples in Table 8 included sediment 0 to 2 m on either side of the impact layer, and may, therefore include cosmogenic PGE, remobilized out of the impact layer. This may account for abundances above background sediment levels (e.g., Table 5, Table 6). Integration comparable to terrestrial sections was not possible because the samples across the 4 meter interval were not taken on a fine scale.

Table 8. PGE content (in ppb) and interelement ratios of the Tertiary and Cretaceous limestones at Petriccio and Elendgraben.

Location	Pt	Pd	Ru	Ir	Au	Rh
Petriccio-1	2.3	1.8	0.11	0.18	-.-	-.-
Petriccio-2	1.9	2.6	0.39	0.42	-.-	-.-
Elendgraben-1	1.3	3.0	0.14	0.17	-.-	-.-
Elendgraben-2	2.2	1.8	0.23	0.24	-.-	-.-

Location	Pt/Ir	Pd/Ir	Au/Ir	Rh/Ir	Ru/Ir
Petriccio-1	12.8	10.0	-.-	-.-	0.61
Petriccio-2	4.5	6.2	-.-	-.-	0.93
Elendgraben-1	7.6	17.6	-.-	-.-	0.82
Elendgraben-2	9.2	7.5	-.-	-.-	0.96

-.- denotes values below limit of detection.
Petriccio-1 and -2 are limestone samples from a section 0-2 meters above and 2-10 cm below the boundary clay, respectively.
Elendgraben-1 and -2 are marl and limestone from a section 2-8 cm above and 0-2 meters below the boundary clay, respectively.
All determinations are on a carbonate-free basis.

Iridium background levels for limestones and shales, up to 5 m above and 5 m below the boundary clay in the Gubbio section are 0.103 ± 0.028 and 0.133 ± 0.015 ppb, respectively, that is, 1.5 to 2 % of the peak Ir anomaly at the K-T boundary (values on a carbonate-free basis; Rocchia et al., 1990). Since Petriccio and Gubbio are

geographically close and part of the same Scaglia Rossa Formation, they should also contain comparable Ir values. Comparison of the data of Rocchia et al. (1990) with the present data (Table 8) shows the values are similar. The Ir spikes in shale 5 m from the impact layer at Gubbio is attributed to post-depositional enhancement caused by dissolution of carbonates (Rocchia et al., 1990). At Caravaca and Agost, Spain, Ir-enrichments have been found at the base of the carbonate-poor layer, immediately overlying the impact layer (Figure 3a, Figure 10). Since no concurrent enrichment of Co, Ni, As, Sb or Cr were noted, the Ir is thought to have been brought in with hemipelagic detritus, eroded from other K-T ejecta-covered, Ir-rich areas (Smit et al., 1988). This sediment recycling, together with chemical remobilization documented in this work, may explain PGE anomalies on both sides of the boundary clay, thus obviating the need for long-term volcanic events or for multiple impacts as a cause.

CHAPTER FIVE
PLATINUM-GROUP ELEMENTS AT THE CRETACEOUS-TERTIARY BOUNDARY

Marine Sites

The location of the marine K-T sites is given on Figure 2a,b. Platinum-group element determinations for each size-fraction of the impact layer are given in Table 9 and results from other studies are in Table 10. The impact boundary clay mineralogy for each site is given in Table 11. Plots relating the size-fraction, PGE content and smectite content are given in Figure 19a,b.

Petriccio

The thick Petriccio boundary clay (2.6 cm) was subdivided into three layers for analysis. A bulk clay sample (donated by A. Montanari) was also analysed for comparison. The highest PGE concentrations are in the middle of the boundary clay ("red layer"; P3, Table 9), which has been shown to correlate with peak spherule abundances (Montanari et al., 1983). Bulk Ir content in P2 and P3 is a factor of 2 lower than that previously determined (Table 10) and previous analyses were not performed on a carbonate-free basis. Incomplete carbonate dissolution during sample preparation in this work may have depressed the abundance of PGE at this site. The lack of data for the sand fraction of P2 has resulted in a lower bulk value here (Table 9). No explanation is readily available to explain the discrepancy for P3 which may be related to incomplete carbonate dissolution or to inhomogeneous distribution of Ir throughout the boundary clay. The total value for PGE in the subdivided Petriccio sample (P1+P2+P3) is a factor of 4 higher than the bulk values for the donated Petriccio sample, except for Ru and Ir which are only slightly higher. This may also indicate heterogeneous distribution

of PPGE throughout the boundary clay in different areas sampled.

Figure 19a,b shows an enrichment of Ir and Ru in the finer fractions of the boundary clay (clay, fine silt, medium silt) and smectite is present in these size-fractions. Iridium and Ru show similar trends of enrichment with size-fraction. X-ray diffractometry indicated the presence of smectite $(X_{0.8}(Si_{7.7}Al_{0.3})(Al_{2.6}Fe_{0.9}{}^{+3}Mg_{0.5})O_{20}(OH)_4 \cdot nH_2O)$, kaolinite $(Al_4[Si_4O_{10}](OH)_8)$, mica and quartz within the clay as indicated in Table 11. The enrichment of smectite in the red layer of the Italian K-T boundary sites has been related to a slight climatic warming at that time (Robert and Chamley, 1990).

Knappengraben and Elendgraben

The boundary clay at Knappengraben was sampled at two locations (Knappengraben-1 and Knappengraben-2), approximately 20 meters apart. Bulk PGE abundances at the two locations compare within a factor of 2 for all elements (Table 9). Iridium contents in the samples are identical, although, there is no data for the coarse silt size-fraction of Knappengraben-2. This fraction is usually low in PGE and gave values below the limits of detection for Knappengraben-1. The similarity of Ir contents between the two locations implies lateral continuity of Ir distribution throughout the section of boundary clay sampled. PGE abundances are higher in the Elendgraben section ($\approx$ 110 km away) (Table 9). Comparison to previous analyses (Table 10) shows Ir is approximately a factor of 2 lower in this work, possibly due to incomplete carbonate dissolution during sample preparation. As at Petriccio, the Austrian sites have Ir and Ru enrichments in the fine size-fractions where clay minerals dominate (Figure 19a,b, Table

Figure 19a,b. Plots of PGE content in size-fractions separated from the impact layer sampled at marine K-T sites; Ir (a) and Ru (b). Note the very general trend of decreasing PGE content in coarse silt and sand fractions, particularly at Petriccio, Elendgraben and Knappengraben. Stars represent corresponding smectite content (Table 11) for each size-fraction.

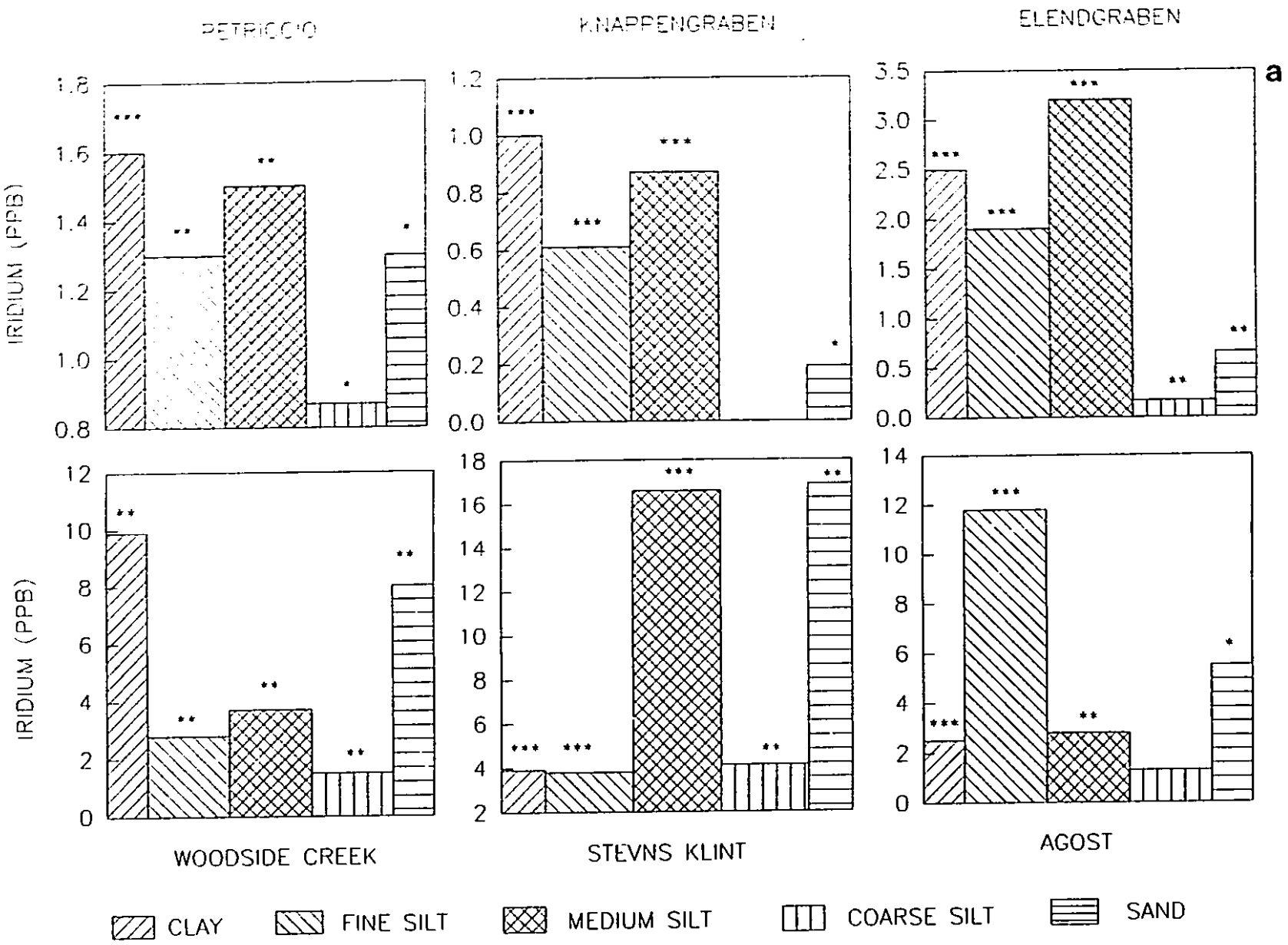
PETRICCIO
KNAPPENGRABEN
ELENDGRABEN
a
IRIDIUM (PPB)
IRIDIUM (PPB)
WOODSIDE CREEK
STEVNS KLINT
AGOST
CLAY
FINE SILT
MEDIUM SILT
COARSE SILT
SAND

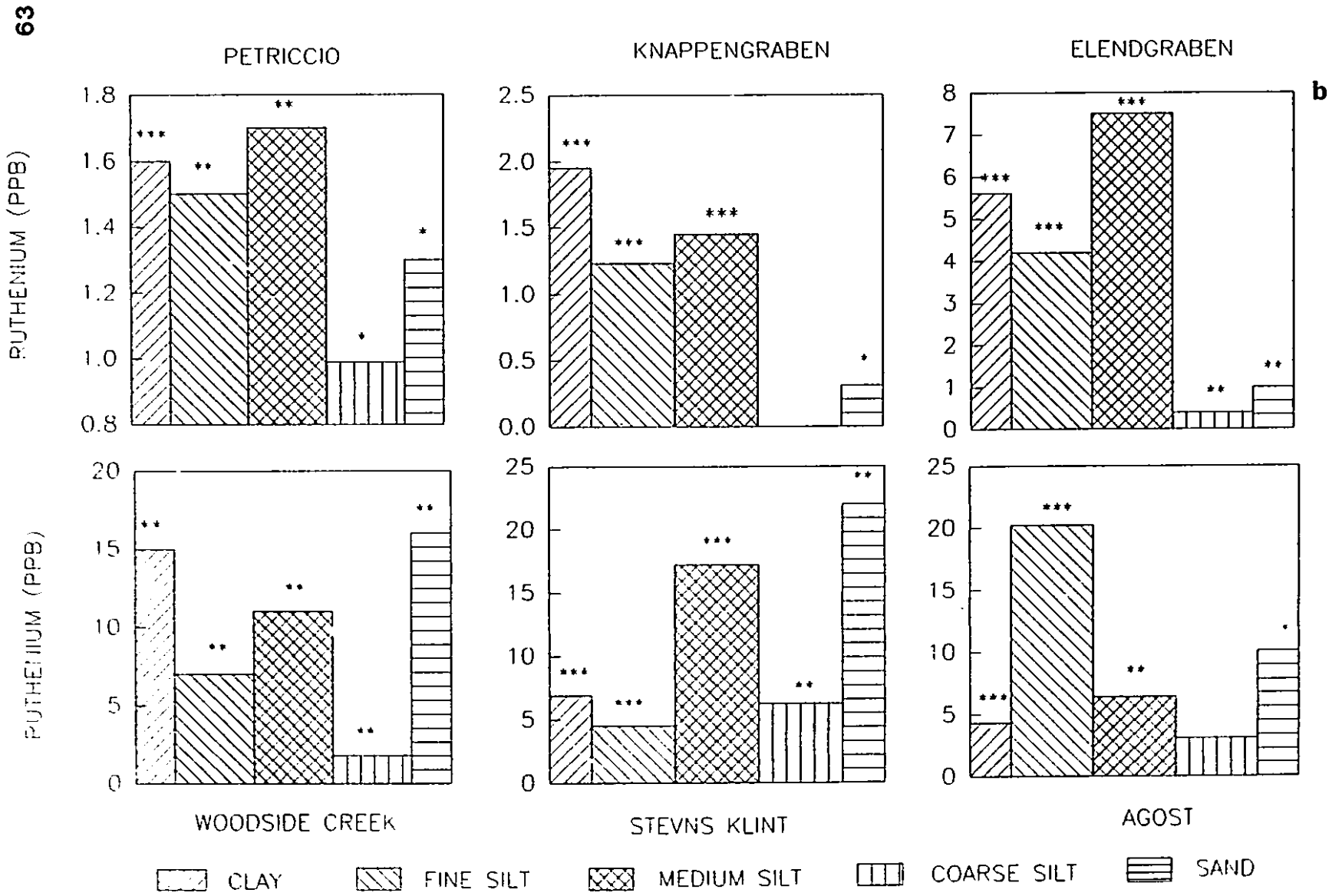
PETRICCIO
KNAPPENGRABEN
ELENDGRABEN
b
RUTHENIUM (PPB)
RUTHENIUM (PPB)
WOODSIDE CREEk
STEVNS KLINT
AGOST
CLAY
FINE SILT
MEDIUM SILT
COARSE SILT
SAND

11). The mineralogy of the boundary layer is similar at each site (Table 11) but Ca-smectite (Preisinger et al., 1986) and kaolinite persist into the coarse fractions to a higher degree at Elendgraben. Figure 20a,b shows the SEM image for an Al-Si-Mg-Fe-spherule, identified in the 5-20 μm size-fraction and a grain of ilmenite found in the 20-50 μm size-fraction.

Woodside Creek

This New Zealand site is one of the most PGE-enriched of all K-T sites studied (Table 9). Previous analysis of the Woodside Creek boundary clay determined 70 ppb Ir whereas the bulk Ir content from this study is 26 ppb. Heterogeneity of PGE distribution between different sample locations at this site is indicated. Figure 19a,b shows the PGE are concentrated in the clay and sand size-fractions of the boundary clay and that smectite is present throughout all size-fractions. Enrichment trends for Ru and Ir in each size-fraction are very similar (Figure 19a,b). The mineralogy is simple (Table 11) with only Ca-smectite, quartz and minor barite detected. Figure 21a,b shows SEM images of a clay aggregate with barite, separated from the 20-50 μm size-fraction and an overall image of the sand size-fraction from Woodside Creek.

Stevns Klint

Stevns Klint is the most PGE-rich site studied (Table 9). The fish clay was subdivided for analysis based on the lithology of Schmitz (1985)(Figure 9b). The highest PGE content is in the black marl (SK 2) and red layer (SK 3) in all studies (c.f., Table 9 and Table 10). Detailed analysis of the subdivided fish clay by Tredoux et al. (1989) are

Figure 20a,b. SEM image of an Al-Si-Mg-Fe spherule (a) from the 5-20 μm size-fraction of the Elendgraben impact layer and an ilmenite grain (b) from the 20-50 μm size-fraction (b) of the same layer.

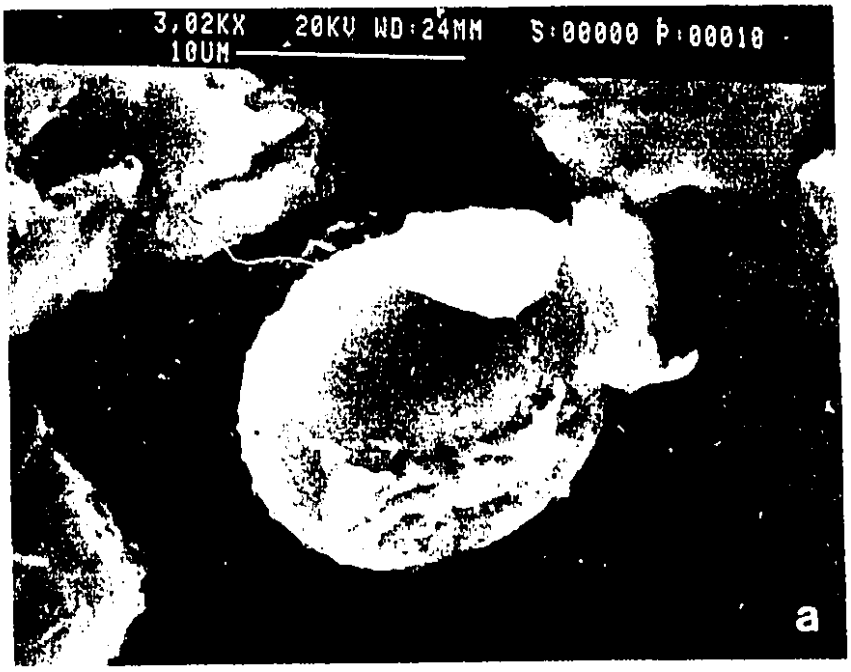
3,02KX 20KV WD:24MM S:00000 P:00010
10UM
a

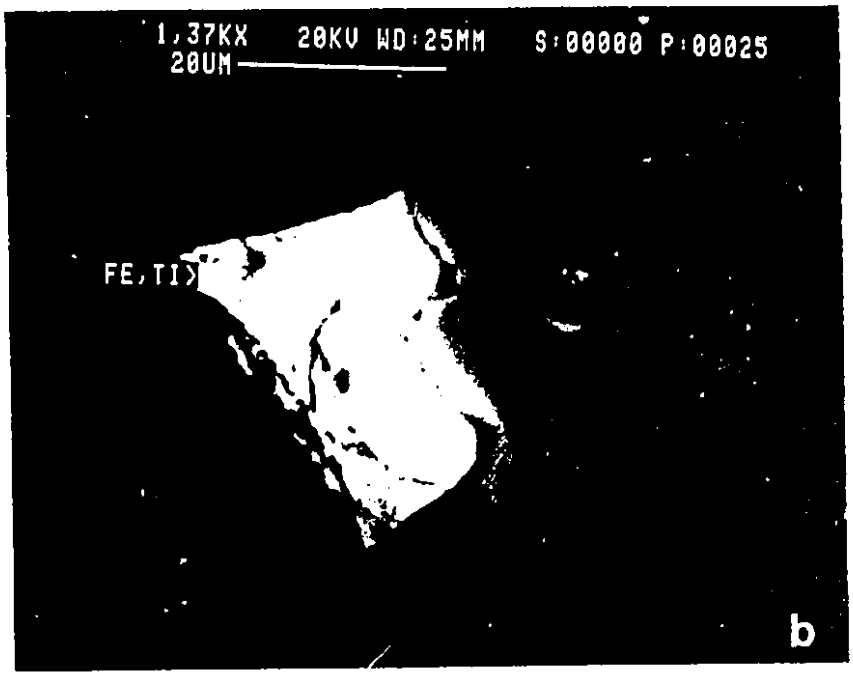
1,37KX 20KV WD:25MM S:00000 P:00025
20UM
FE,TI)
b

Figure 21a,b. SEM image of a Fe-Si-Al agglomerate with ≈5% barite from the 20-50 μm size-fraction of the impact layer at Woodside Creek (a) and an overall image of the sand size-fraction (b) of the impact layer at Woodside Creek with barite.

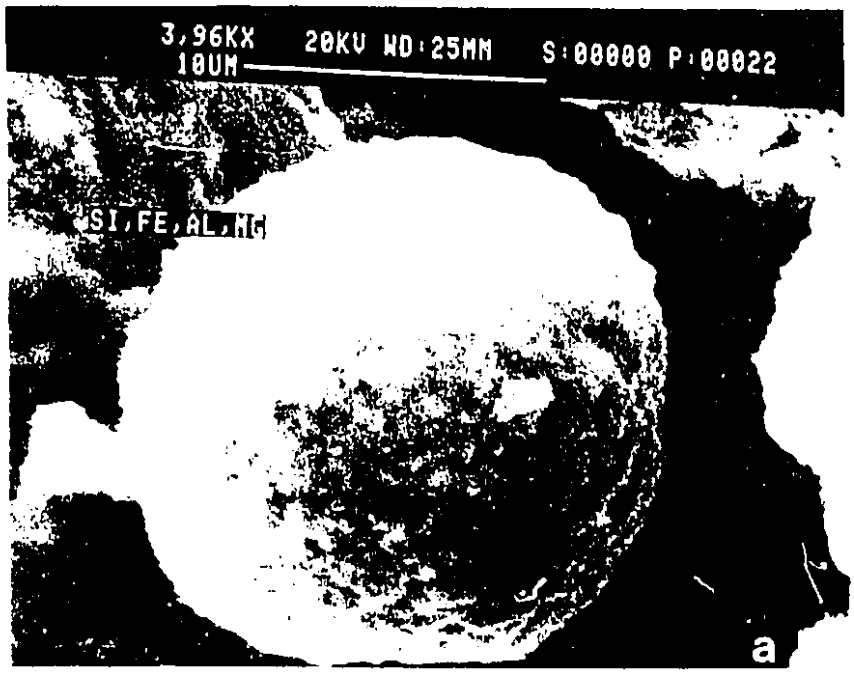
3,96KX 20KV WD:25MM S:00000 P:00022
10UM
SI,FE,AL,MG
a

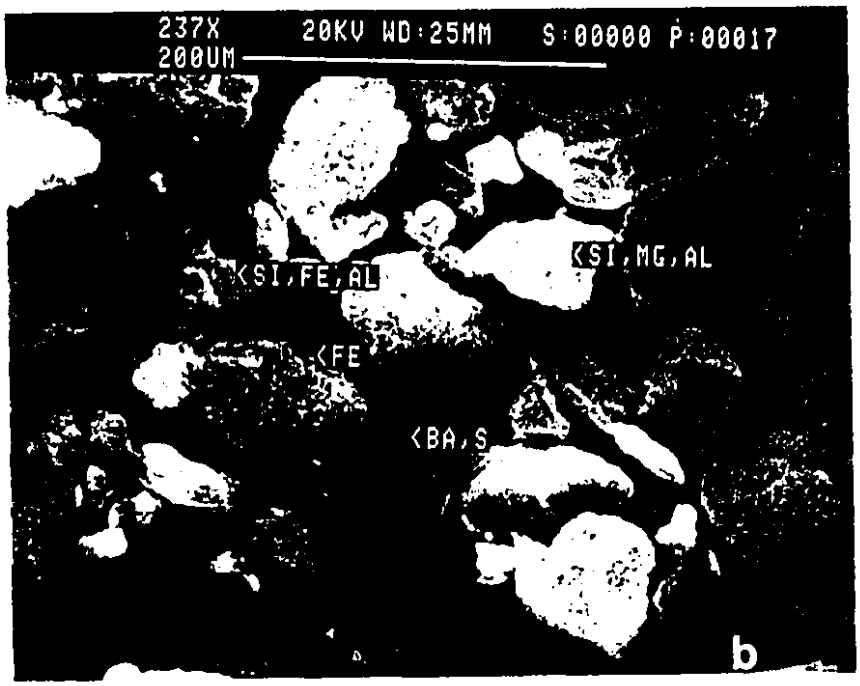
237X 20KV WD:25MM S:00000 P:00017
200UM
KSI,FE,AL
KSI,MG,AL
KFE
KBA,S
b

given in duplicate (Table 10). Not only is there poor agreement between the three studies (this work, Schmitz, 1985 and Tredoux et al., 1989), but duplicates from the later work can be variable (e.g., Ir abundance in SK3). Bulk fish clay Ir abundance in this work (136 ppb) are higher than those determined by Schmitz (1985) (Table 10), however Schmitz (1985) did not analyse the grey marl (SK 1). The overall discrepancy between studies is not surprising since the boundary clay at Stevns Klint varies in thickness and composition depending on the locality sampled (J. Smit, pers. comm., 1988). The pyrite-rich red layer pinches out laterally up the flanks of chalk mounds (Ekdale and Bromley, 1984) and anoxic conditions in the troughs may have altered the form and distribution of PGE. Figure 19a,b shows similar enrichment trends of Ru and Ir in size-fractions and that most of the PGE content is concentrated in the medium silt- and sand-sized portions of the layer. The same pattern is shown for all sublayers of the fish clay (Table 9). Mg-Smectite (Kastner et al., 1984; Elliot et al., 1989) is present in all size-fractions (Figure 19a,b) and the only other mineral detected was quartz (Table 11). The unusual smectitic composition has previously been related to alteration of impact ejecta (Kastner et al., 1984).

Agost

The Ir abundance determined in this work for the boundary clay at Agost (24 ppb) compares well to that found previously (25 ppb; Smit et al., 1988). These values compare well to other Spanish sections with high sedimentation rates such as Zumaya (26 ppb) and Caravaca (27 ppb) (Smit et al., 1988; Smit, 1990). The highest PGE contents are in the fine silt and, to a lesser degree, the sand size-fractions (Figure 19a,b, Table 9).

Ruthenium and Ir correlate well as seen by the size-fraction-PGE enrichment trends on Figure 19a,b. Ca-Smectite dominates in the fine silt size-fraction and is a minor component of the sand. Other minerals detected include kaolinite, mica and quartz.

Table 9. PGE content (in ppb) and Ru/Ir ratios of the K-T boundary impact layer from Petriccio, Knappengraben, Elendgraben, Woodside Creek, Stevns Klint and Agost.

WEIGHTED ABUNDANCE							
Sample	Pt	Pd	Ru	Ir	Au	Rh	Ru/Ir
Petriccio (P1-top 0.5cm)							
clay	7.4	1.5	1.58	1.4	0.85	0.7	1.1
2-5μm	10.6	2.1	0.92	0.64	-.-	0.26	1.4
5-20μm	12.8	1.3	1.0	0.67	0.23	0.85	1.5
20-50μm	-.-	-.-	-.-	-.-	0.12	-.-	-.-
sand	0.72	4.7	0.17	0.11	-.-	0.11	1.6
BULK	**31.5**	**9.6**	**3.7**	**2.8**	**1.2**	**1.9**	
Petriccio (P2-bottom 0.5cm)							
clay	4.0	7.6	0.99	0.74	0.67	0.20	1.4
2-5μm	2.8	3.7	0.60	0.30	-.-	0.24	2.0
5-20μm	2.4	5.0	0.82	0.61	0.78	0.33	1.4
20-50μm	-.-	-.-	-.-	-.-	0.60	0.11	-.-
sand	nd	nd	nd	nd	nd	nd	nd
BULK	**9.2**	**16.3**	**2.4**	**1.7**	**2.1**	**0.88**	
Petriccio (P3-red layer, middle 0.5cm)							
clay	2.9	5.7	1.7	1.4	0.35	0.38	1.2
2-5μm	1.6	2.5	1.0	0.68	0.31	0.25	1.5
5-20μm	-.-	4.9	0.92	1.1	-.-	0.73	0.81
20-50μm	2.1	-.-	0.34	0.14	-.-	-.-	2.4
sand	0.97	1.6	0.67	0.37	-.-	0.38	1.8
BULK	**7.8**	**14.7**	**4.6**	**3.7**	**0.66**	**1.7**	
TOTAL (P1+P2+P3)	**48.5**	**40.6**	**10.7**	**8.2**	**4.0**	**4.5**	**1.3**
Petriccio							
clay	3.7	3.6	1.6	1.6	0.03	0.03	0.98
2-5μm	2.4	2.5	1.5	1.3	-.-	0.04	1.1
5-20μm	3.0	2.4	1.7	1.5	0.07	0.06	1.1
20-50μm	1.2	1.5	0.99	0.87	0.04	0.05	1.1
sand	-.-	3.9	1.3	1.3	-.-	0.08	1.0
BULK	**10.3**	**9.1**	**7.1**	**6.6**	**0.14**	**0.26**	**1.08**

Table 9 con't

WEIGHTED ABUNDANCE							
Sample	Pt	Pd	Ru	Ir	Au	Rh	Ru/Ir
Knappengraben (K1)							
clay	1.6	4.0	1.4	1.0	-.-	0.19	1.3
2-5μm	1.2	2.0	0.86	0.51	0.37	0.30	1.7
5-20μm	1.6	2.7	1.2	0.82	0.38	0.6	1.5
20-50μm	0.43	-.-	-.-	-.-	-.-	-.-	-.-
sand	0.43	0.77	0.31	0.19	-.-	-.-	1.6
BULK	5.3	9.5	3.8	2.5	0.75	1.1	1.5
Knappengraben (K2)							
clay	5.7	8.0	2.5	0.95	-.-	0.73	2.6
2-5μm	2.7	4.7	1.6	0.71	-.-	0.58	2.1
5-20μm	3.8	4.5	1.7	0.90	0.38	0.42	1.9
20-50μm	nd	nd	nd	nd	nd	nd	nd
sand	0.15	0.54	-.-	-.-	-.-	-.-	-.-
BULK	12.4	17.7	5.8	2.5	0.38	1.7	
ΣBULK*	9.0	13.6	4.9	2.5	0.75	1.4	2.0
Elendgraben							
clay	8.5	17	5.6	2.5	-.-	3.2	2.2
2-5μm	5.9	8.1	4.2	1.9	-.-	2.8	2.2
5-20μm	9.4	12	7.5	3.2	-.-	3.9	2.3
20-50μm	1.0	-.-	0.39	0.17	-.-	0.54	2.2
sand	2.6	1.7	1.0	0.66	0.35	0.4	1.5
BULK	27.4	38.8	18.7	8.4	0.35	10.4	2.2
Woodside Creek							
clay	33.0	69.0	15.0	9.9	0.52	1.7	1.5
2-5μm	12.0	13.0	7.0	2.8	0.18	0.98	2.4
5-20μm	13.0	20.0	11.0	3.7	0.16	1.3	2.9
20-50μm	1.2	2.5	1.8	1.5	-.-	0.34	1.2
sand	17.0	67.0	16.0	8.0	1.3	5.1	2.0
BULK	76.2	172	36.8	25.9	2.2	9.4	1.4
Stevns Klint (SK-1)**							
clay	10.8	5.9	4.3	3.4	0.48	0.08	1.2
2-5μm	11.2	8.1	4.4	2.8	0.55	0.08	1.6
5-20μm	18.1	26.0	15.4	19.8	2.5	0.25	0.78
20-50μm	6.8	5.6	4.3	2.4	0.41	0.07	1.8
sand	22.9	29.0	19.3	10.0	2.3	0.31	1.9
BULK	69.8	74.6	47.7	38.4	6.2	0.79	

Table 9 con't

WEIGHTED ABUNDANCE							
Sample	Pt	Pd	Ru	Ir	Au	Rh	Ru/Ir
Stevns Klint (SK-2)**							
clay	14.4	8.9	7.9	4.9	1.4	0.12	1.6
2-5μm	15.2	9.9	8.7	5.7	1.0	0.13	1.5
5-20μm	27.3	29.0	16.8	16.6	2.6	0.36	1.0
20-50μm	16.8	13.7	8.9	6.6	1.1	0.18	1.3
sand	49	-.-	16.6	21.2	0.02	0.4	0.78
BULK	123	61.5	58.9	55.0	6.1	1.2	
Stevns Klint (SK-3)**							
clay	14.4	6.8	8.4	3.3	1.1	0.13	2.5
2-5μm	21.0	5.3	5.3	3.0	1.1	0.11	1.7
5-20μm	26.0	15.6	19.5	13.3	1.1	0.32	1.5
20-50μm	10.8	5.3	5.5	3.4	0.65	0.12	1.6
sand	37.3	42.0	30.7	19.6	3.2	0.63	1.6
BULK	110	75.0	69.4	42.9	7.2	1.3	
TOTAL SK (1+2+3)	302	211	176	136	19.5	3.3	1.3
Agost							
clay	6.1	2.6	4.3	2.5	-.-	0.03	1.7
2-5μm	21.4	20.2	20.2	11.8	5.0	0.38	1.7
5-20μm	7.0	4.8	6.4	2.8	1.2	0.2	2.3
20-50μm	2.9	1.3	3.1	1.3	0.75	0.08	2.3
sand	9.3	5.5	10.1	5.5	0.73	0.2	1.8
BULK	46.7	34.4	44.1	23.9	7.7	0.89	1.9
Marine mean Ru/Ir = 1.77 ± 0.53; Bulk Ru/Ir = 1.6 ± 0.34							

Concentrations are normalized to the total weight of all size-fractions for a given site.

-.- = denotes values below limit of detection (3 times the standard deviation for 10 reagent blanks, treated as samples).

nd = no data

BULK value is the total PGE abundance for all size-fractions at that site.

* ΣBULK per element for Knappengraben is calculated as $\Sigma[(x_1 + x_2)/2]$ where x_1 and x_2 are the PGE content in each size-fraction at site K1 and K2, respectively.

**SK-1 = Layer IV of Schmitz (1985); Grey marl, +3 to +4 cm above the top of Maastrichtian

**SK-2 = Layer III of Schmitz (1985); Reduced black marl, +1 to +3 cm above the top of Maastrichtian

**SK-3 = lower Layer III of Schmitz (1985); Spheroid-rich red clay, 0 to +1 cm above the top of Maastrichtian

Sample size limitations precluded organic separations for each size-fraction and concentration, therefore, represents both inorganic and organic PGE.

The non-subdivided Petriccio sample was provided by A. Montanari.

Several general observations can be made for the marine K-T sites studied. 1) The PGE abundances determined in this work seldom replicate those determined previously. This implies that PGE are not homogeneously distributed throughout the

Table 10. PGE Abundance (in ppb) in the K-T boundary clay at various sites (other studies).

		Pt	Pd	Ru	Ir	Au	Rh
Marine K-T Sites							
Petriccio[1]	P1				2.0		
	P2				3.5		
	P3				8.4		
Elendgraben[2]					14.5		
Woodside Creek[3]					70		
Stevns Klint	SK1	56/26[5]	44/26[5]	57/61[5]	nd[4],36[5]	nd[4],16/3[5]	
	SK2	210/201[5]	105/56[5]	nd[5]	39[4],82/47[5]	17[4],57/14[5]	
	SK3	119[5]	47[5]	56[5]	28[4],34/14[5]	<3[4],30[5]	
Stevns Klint[6]	bulk fish clay	<80			51	31	
Agost[7]					24.5		
Terrestrial K-T Sites							
Starkville South[8]	coal				0.4	nd	
	impact layer				1.21	1.7	
	claystone				0.27	1.1	
Clear Creek North[8]	coal				9.5	nd	
	impact layer				14.6	7.3	
	claystone				0.22	2.0	
Red Deer Valley[9]		11.9			3.36	0.51	0.58
Morgan Creek[10]					3.0		
Lance Creek[11]	lignite	<2.6			1.1	3.8	
	clay-shale	<3.1			2.1	4.7	
	impact layer	47			21	7.5	
	claystone	<1.9			1.6	4.4	

Sources of data: 1. Montanari et al. (1983); 2. Preisinger et al. (1986); 3. Brooks et al. (1986); 4. Schmitz (1985); 5. Tredoux et al., 1989 (duplicates given); 6. Elliot et al. (1989); 7. Smit et al. (1988); 8. Izett (1990); 9. Lerbekmo and St. Louis (1986); 10. Nichols et al. (1986); 11. Bohor et al. (1987b). Note that none of the terrestrial sites were analysed on a carbonate-free basis in these studies. Methods of analysis for PGE: 1. NAA; 2. NAA; 3. Not given; 4.INAA, ICP-Optical Emission Spectrometry; 5. NiS preconcentration, NAA; 6. RNAA; 7. Not given; 8. RNAA; 9. NAA; 10. RNAA; 11. NAA.

Table 11. Mineralogy of the marine K-T boundary clay (sites as in Table 9).

Site	Smectite	Kaolinite	Mica	Quartz	Other
Petriccio					
clay	***	*	*	**	carbonate
2-5μm	**	**	*	**	throughout
5-20μm	**	*	*	**	
20-50μm	*	*	*	***	
sand	*	–	–	***	
Knappengraben					
clay	***	*	*	*	carbonate
2-5μm	***	*	*	**	
5-20μm	***	*	*	**	
20-50μm	*	*	*	***	
sand	*	*	*	***	
Elendgraben					
clay	***	*	*	*	
2-5μm	***	*	*	*	
5-20μm	***	*	*	*	
20-50μm	**	**	*	**	
sand	**	**	*	**	
Woodside Creek					minor
clay	**	–	–	***	barite
2-5μm	**	–	–	***	throughout
5-20μm	**	–	–	***	
20-50μm	**	–	–	***	
sand	**	–	–	***	
Stevns Klint					
clay	***	–	–	*	
2-5μm	***	–	–	*	
5-20μm	***	–	–	*	
20-50μm	**	–	–	**	
sand	**	–	–	***	
Agost					
clay	***	**	**	*	
2-5μm	***	**	*	*	
5-20μm	**	**	*	**	
20-50μm	–	–	–	**	
sand	*	*	*	***	

Estimation of mineral abundance was made on the main line for each trace and recalculated to 100%.
>50% = ***; 10-50% = **; <10% = *; – = not detected.

boundary layer. 2) The covariance of Ru and Ir is consistent (Figure 19a and 19b; Figure 22a). The Pd-Ir correlation (Figure 22b) is not as perfect as that for Ru-Ir (Figure 22a), perhaps due fixing of Pd by organic matter. 3) Smectite is present at all sites and varies in composition from Mg- to Ca-smectite. 4) Smectite is present, in varying amounts, in all size-fractions of each site.

Previous studies of marine sites did not yield conclusive identification of the carrier phase(s). Possible hosts for PGE that have been proposed include ilmenite (Preisinger et al., 1986), submicron-size smectitic clay particles (Kastner et al., 1984; Elliot et al., 1989), Pt-micronuggets (Margolis and Doehne, 1988), magnesioferrite (Bohor et al., 1986), magnetic spheroids (Smit and Kyte, 1984) and carbonaceous material (Schmitz, 1985; Hansen et al., 1987). Rocchia et al. (1990) suggest that Ir is in a dispersed state, not attached to a particular mineral phase. These studies were limited to only a few sites and no consensus has been reached as to how the PGE came to be incorporated into the suggested carrier(s). In this work, detailed correlation between mineral abundances and PGE content is limited by the low purity of some physical separates and by the semi-quantitative abundances estimated by XRD. For Petriccio, Knappengraben and Elendgraben, a correlation exists between fine size-fractions and high PGE abundances, indicating a fine-grained carrier phase (Table 9, Figure 19a,b). At Stevns Klint, Agost and Woodside Creek the situation is more complex, as both coarse and fine size-fractions contain the highest PGE contents. It is therefore possible that either a single mineral carrier exists as small and larger grains, or two host minerals of naturally different grain sizes or densities are the carriers.

Based on the mineralogy (Table 11), three mineral phases within the clay may be

Figure 22a,b. Iridium versus Ru (a) and Ir versus Pd (b) for marine sites (same symbols apply to both). The excellent correlation of iridium and ruthenium ($r = 0.94$) is not seen for medium silt and sand samples from Stevns Klint where Ir "excess" emphasizes the anomalous nature of this site. The lower correlation coefficient for Ir versus Pd ($r = 0.67$) results from the more mobile nature of Pd. Error bars for Ru (3%) fall within the bounds of the symbol outline. Error bars for Ir (13%) are within the symbol bounds for abundances < 10 ppb and are marked by a line for higher abundances. Error bars for Pd (10%) are within the symbol bounds for abundances < 35 ppb and are marked by a line for higher abundances.

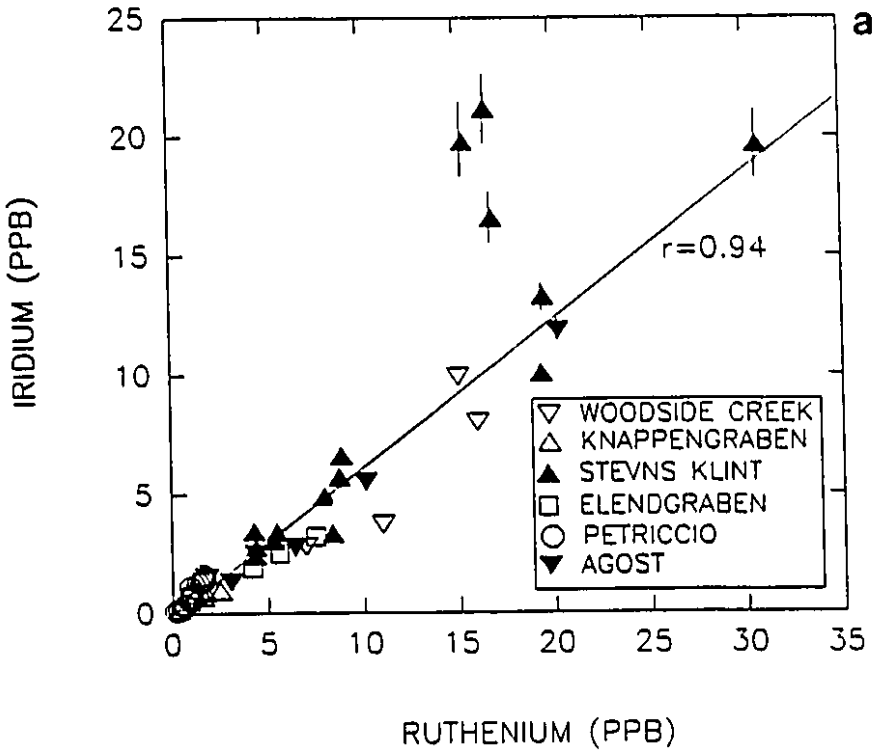
a
IRIDIUM (PPB)
RUTHENIUM (PPB)
r=0.94
WOODSIDE CREEK
KNAPPENGRABEN
STEVNS KLINT
ELENDGRABEN
PETRICCIO
AGOST
0
5
10
15
20
25
30
35

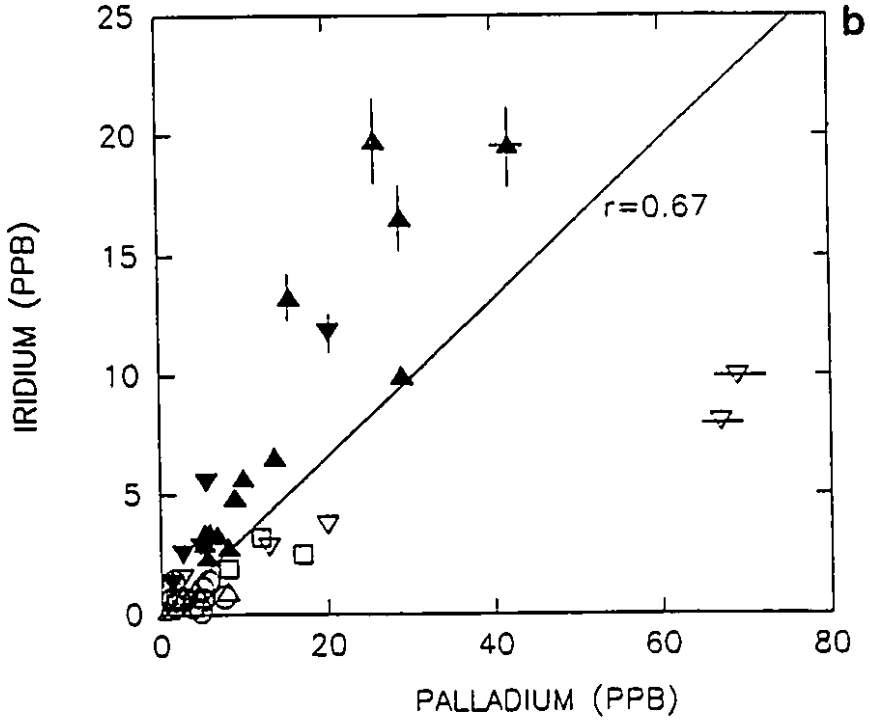
b
IRIDIUM (PPB)
PALLADIUM (PPB)
r=0.67
0
5
10
15
20
25
40
60
80

rich in PGE: mica, clay minerals or a PGE-rich alloy (not identified on XRD traces). No correlation exists between mica abundance and PGE content at any site (c.f., Table 9 and Table 11). Scanning electron microscopy on size-fractions with the highest PGE contents revealed no discrete grains or alloys that could contain PGE. This does not necessarily preclude the existence of this type of carrier. If all the Ir in the clay fraction (<2 μm) from Woodside Creek were concentrated in one single particle, it would have the dimensions of 13 μm^3 (see Appendix I) and could easily go undetected, particularly with the small size of SEM samples and the few number of samples analysed by SEM (2-3 per site). Such a carrier has only been observed in one study (Pt-micronugget at Zumaya, Spain; Margolis and Doehne, 1988) and could have resulted from contamination in that case (Rocchia et al., 1990).

Smectite is the dominant phase in the boundary clay and the only one which shows a good correlation with PGE concentrations in some samples (Figure 19a,b). Due to the large surface area of the smectitic swelling clay (800-600m^2/g; Grim, 1968) and its relatively high cation exchange capacity (100meq/100g; van Ophlen and Fripat, 1979), it is possible that an element the size of Ir (Table 3) could reside in available exchangeable interlayer cation sites of smectite[1]. Kaolinite is a less feasible PGE carrier due to the physical limitations on substitution in this mineral (Grim, 1968; van Ophlen and Fripat, 1979). At Knappengraben, the clay minerals are smectite and kaolinite (Table 11). Kaolinite persists into coarser fractions, whereas PGE concentrations and smectite decrease markedly in the coarse silt and sand (Figure 19a,b). At Woodside Creek,

[1] The form of the PGE in the clay is unknown. They may exist in micro-alloys in/on the clay minerals or in a dispersed metallic form (Rocchia et al., 1990).

kaolinite was not detected yet this site has the highest abundance of PGE. Elliot et al. (1989) also concluded that Ir, Ag, Au and Pt are concentrated in submicron grains in fractions composed dominantly of smectite, and PGE-clay mineral associations have been noted in sedimentary rocks other than those from the K-T boundary (Van der Flier-Keller and Fyfe, 1987).

If smectite is the primary mineral host to PGE, some explanation must be given for the high PGE abundances in the coarser fractions at Woodside Creek, Stevns Klint and Agost (Figure 19a,b). Not only are the PGE distributions anomalous, but relative PGE concentrations are highest at these sites (Table 9). Aggregates of clay minerals (200-500 μm) cemented by silicate and/or barite were identified by SEM in the sand-size-fraction at Woodside Creek (Figure 21a,b). This New Zealand site is highly silicified (Kyte, 1990; Brooks et al., 1986b), an anomalous feature among the K-T sites studied. Winnowing and redeposition of the boundary material into shallow depressions in the Maastrichtian limestone (Bohor, 1990b) may have obscured the original patterns of grain-size-PGE concentration correlations (see Chapter 4). Smectite may still be the dominant carrier, but present as both coarse, diagenetically-formed agglomerates and fine grains. Neither the Stevns Klint nor Agost sites are silicified. At Stevns Klint, pronounced biohermal development in the late Maastrichtian provided an uneven platform for boundary clay deposition. Anoxic conditions in the troughs (Bohor, 1990b; Zhou et al., 1991) may have altered the form and distribution of PGE. This may explain the "excess" Ir present in the medium silt and sand fractions in samples from Stevns Klint (Figure 19a). The very simple mineralogy (smectite + quartz) of the Stevns Klint site (Table 11) indicates that either the moderate amount of smectite in the sand fraction is agglomerated,

or that an undetected alloy is the dominant PGE carrier. At Agost, a weak correlation exists between smectite content and PGE concentration. In this case, perhaps a dense PGE-rich alloy is also present.

The Ir in the boundary clay from Elendgraben, Austria was thought to be hosted in ilmenite exsolved from magnetite (Preisinger et al., 1986). Ilmenite was discovered here in the 20-50 μm size-fraction (Figure 20b). This fraction, however, contained the lowest Ir abundances ($\leq$1 ppb) for this site.

Interelement PGE ratios, with Ir as the denominator are given in Table 12. Ir is used as the reference since it is the least mobile. For the marine sites, all ratios are higher than those of a C1 chondrite meteorite (Table 20). The Pd/Ir and Pt/Ir ratios at the K-T are higher than most chondrite types, whereas the Au/Ir ratio is within the range of most types. The Ru/Ir ratio corresponds closely to most chondrite types. The high degree of association of Rh and Pt with organic matter in the marine environment, and hence the higher mobility, is reflected in the large standard deviation on the Pt/Ir and Rh/Ir ratios. The only ratio which is chondritic[2] within error, has a small range of values and is comprised of the least organically-associated in marine sites is Ru/Ir. Of all the PGE, therefore, only Ru and Ir and their ratio are useful for modelling or mineral carrier phase identification. The site-dependant variation in Ru/Ir ratios is illustrated in Figure 23. Iridium enrichment or Ru depletion in the medium silt and sand size-fractions for Stevns Klint and Ru enrichment or Ir depletion in the medium silt size-fraction from Woodside Creek are the major deviations from the mean Ru/Ir value (1.77 $\pm$ 0.53).

[2]Hereafter "chondrite" refers to C1 chondrite unless otherwise indicated.

Figure 23. Iridium versus Ru/Ir ratio for the marine K-T impact layer. Mean Ru/Ir for all marine sites is 1.77 ± 0.53. Deviation from correlation is limited to the medium silt and sand fractions for Stevns Klint and Woodside Creek, the two most PGE-enriched sites. Error bars for Ir (13%) are within the symbol bounds for abundances < 10 ppb and are marked by a line for higher abundances. Where the impact layer was subdivided for analysis, total abundance for that layer is plotted for each site. Where more than one section was sampled at a given location, mean Ru and Ir contents are plotted for that site.

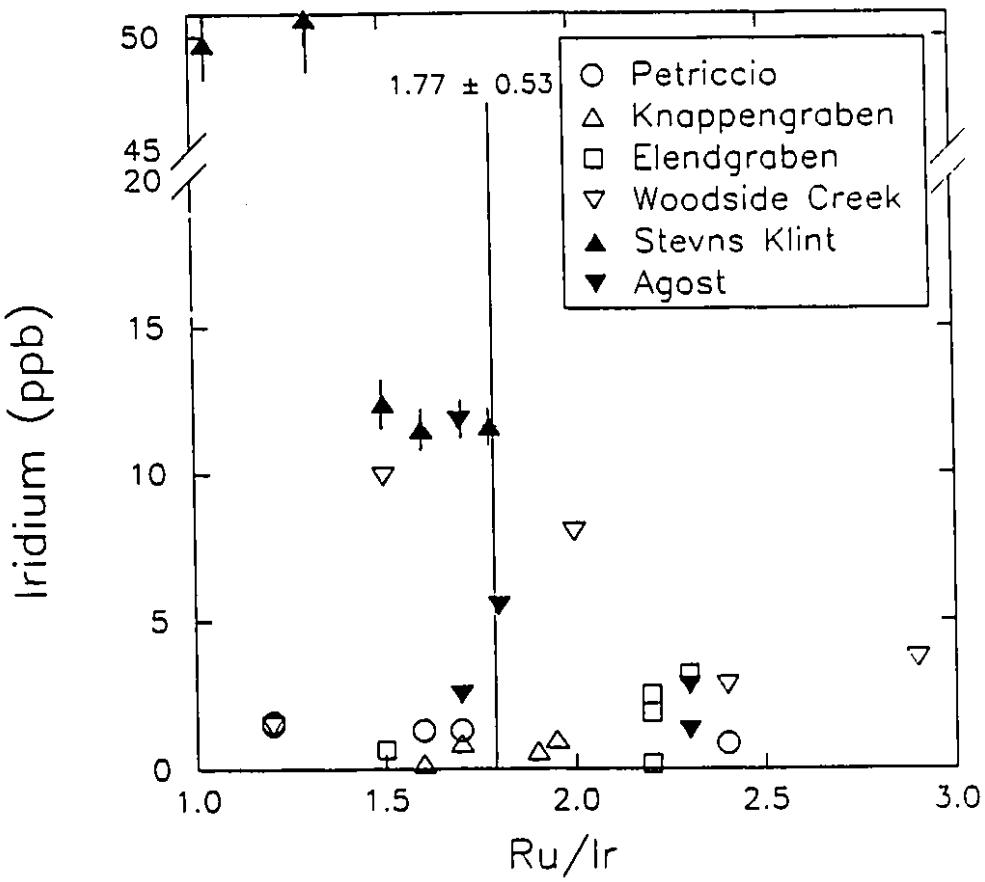
50
45
20
15
10
5
0
1.0
1.5
2.0
2.5
3.0
Iridium (ppb)
Ru/Ir
1.77 ± 0.53
Petriccio
Knappengraben
Elendgraben
Woodside Creek
Stevns Klint
Agost

Table 12. Interelement PGE ratios for all marine and terrestrial K-T sites.

	Pt/Ir	Pd/Ir	Au/Ir	Rh/Ir	Ru/Ir
Marine Sites					
Mean (SD)	3.8 (4.6)	4.1 (2.3)	0.37 (0.24)	0.53 (0.66)	1.77 (0.53)
Range	0.8-27	1.0-8.4	0.05-0.8	0.01-3.1	1.1-2.9
n	29	27	20	28	30
Terrestrial Sites					
Mean (SD)	8.7 (12)	2.7 (3.5)	3.3 (4.1)	0.03 (0.04)	0.92 (0.28)
Range	1.2-36	0.6-15	0.002-13	0.007-0.18	0.53-1.6
n	29	29	27	21	29
C1 Chondrite	2.06	1.16	0.29	0.30	1.48

Chondrite values from Anders and Grevesse (1989). Values for other chondrite types given in Table 20. Where the boundary clay was subdivided for analysis (e.g., Petriccio, Stevns Klint) or more than one site was sampled (e.g., Knappengraben), an average value for each size-fraction was used to prevent skewing the overall mean.

Terrestrial Sites

The location of the terrestrial K-T sites studied is shown on Figure 2a,b. Platinum-group element determinations for each size-fraction are given in Table 13a-c and results from other studies are in Table 10. The impact layer, boundary claystone and coal layer mineralogy for each site is given in Table 14. Plots relating the size-fraction, PGE content and clay content are given in Figure 24a,b. In the Raton Basin, samples span the boundary and include both the overlying coal layer and underlying kaolinitic boundary claystone.

At the Raton Basin sites, bulk PGE content at Berwind Canyon and Starkville South are similar and much higher than those at Clear Creek North (Table 13a). The reason for this is unclear as Starkville South and Clear Creek North are only 1.7 km apart. Higher PGE abundances are found in the Clear Creek North boundary claystone (Table 13b), except for Pd and Rh. All sites show significant PGE contents in the coal seam overlying the impact layer (Table 13c). Iridium and Au abundances in the impact layer at Starkville South are a factor of 50 and 12, respectively, higher than those determined by Izett (1990), however, his analysis were not performed on a carbonate-free basis. Figure 24a,b shows that the PGE are distributed in both coarse and fine size-fractions of the impact layer for all Raton Basin sites. Ruthenium and Ir correlate well in the impact layer (c.f., Figure 24a and 24b). Illite/smectite irregular interstratified mixed layer (I/S) clay (>50% illite; Izett, 1990) was detected in all size-fractions, and is more abundant in finer fractions (Figure 22a,b, Table 14a). Other minerals present include kaolinite, jarosite ($KFe_3(SO_4)_2(OH)_6$) and quartz. Jarosite laminations are common in the Clear Creek North impact layer and at Starkville South (Table 14a). Izett (1990) describes the impact layer clay as having an open wavy framework, similar to smectite and I/S clay. The mineralogy of the claystone (Table 14b) is dominantly kaolinite, with less I/S mixed layer clay than in the impact layer, some quartz and minor goethite. Izett (1990) noted that the polygonal framework of kaolinite, filled with micrometer-size kaolinite spherules, was distinct from the texture of the overlying impact layer. The coal layer (Table 14c) contains kaolinite, jarosite and quartz and amorphous inorganic material.

Figure 24a,b. Plots showing the PGE content of size-fractions, separated from the impact layer sampled at the terrestrial sites; Ir (a) and Ru (b). Correlation of PGE content with grain size is not as good as for the impact layer from marine sites. Stars represent corresponding I/S mixed layer clay content of each size-fraction (Table 14a) and stars beside (s) represent smectite content (Table 14a).

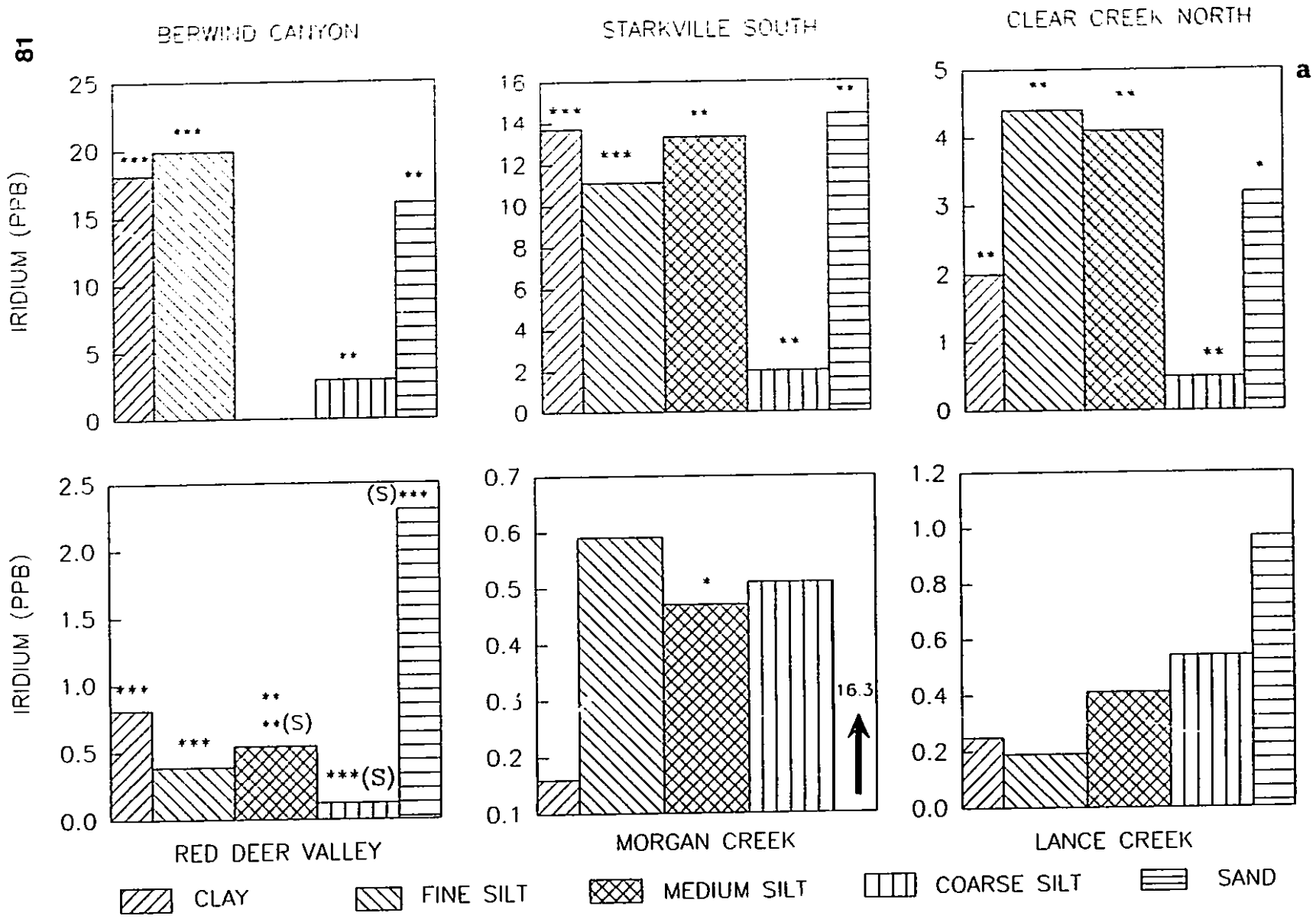
BERWIND CANYON
STARKVILLE SOUTH
CLEAR CREEK NORTH
a
IRIDIUM (PPB)
IRIDIUM (PPB)
RED DEER VALLEY
MORGAN CREEK
LANCE CREEK
16.3
CLAY
FINE SILT
MEDIUM SILT
COARSE SILT
SAND

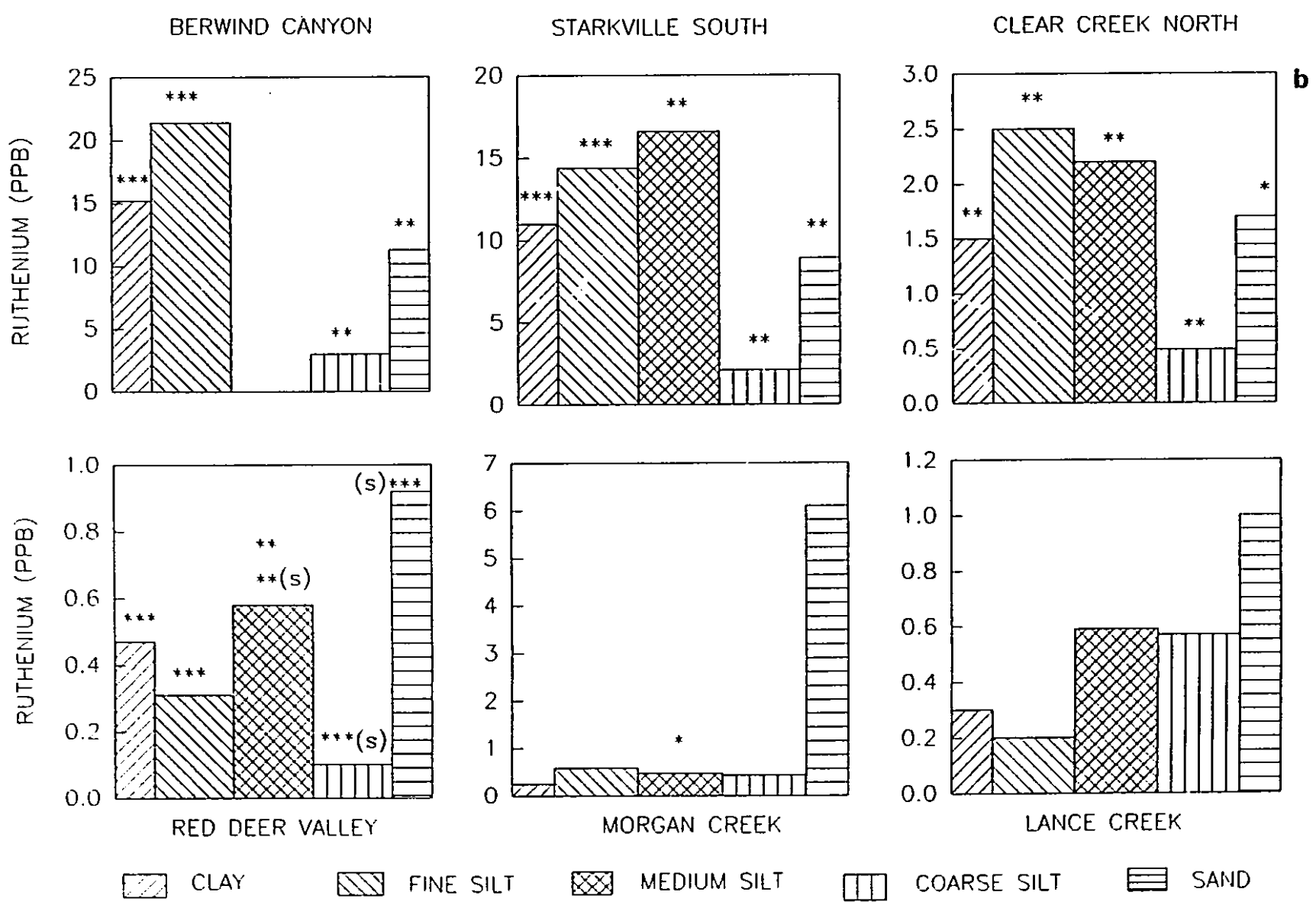
BERWIND CANYON
STARKVILLE SOUTH
CLEAR CREEK NORTH
b
RUTHENIUM (PPB)
RUTHENIUM (PPB)
RED DEER VALLEY
MORGAN CREEK
LANCE CREEK
CLAY
FINE SILT
MEDIUM SILT
COARSE SILT
SAND

Red Deer Valley

Red Deer Valley -1 and -2 are splits taken from one sample of the impact layer. Taking into consideration the lack of data for the clay fraction of Red Deer Valley-1, the bulk values from each split are comparable (Table 13a). A high Pt content is found in the sand fraction of Red Deer Valley-1, although other PGE are also enriched in that fraction (Table 13a). The Ir and Rh bulk abundance determined in this work compare within 1 ppb and 0.38, respectively to those determined by Lerbekmo and St. Louis (1986), however, their determinations were not done on a carbonate-free basis. This is more evident when Pt and Au values are compared since those of this work are a factor of 11 and 35 higher, respectively. Iridium and Ru are distributed throughout all size-fractions of the impact layer with the highest content being in the sand size-fraction (Figure 24a). Ruthenium and Ir show the same PGE content-size-fraction trends (c.f., Figure 24a and Figure 24b). The impact layer of the Red Deer Valley site (Table 14a) is constituted of kaolinite, I/S clay, smectite, quartz and minor jarosite. I/S clay dominates in fine size-fractions whereas smectite is most prevalent in coarse size-fractions of the impact layer (Figure 24a,b, Table 14a).

Morgan Creek

The bulk Ir content of the impact layer at Morgan Creek determined in this work (Table 13a) is a factor of 6 higher than that of the non-carbonate-free analysis of Nichols et al. (1986)(Table 10). Platinum-group elements are concentrated in all size-fractions of the impact layer, particularly in the sand fraction. Ruthenium and Ir show similar trends of enrichment with grain size. The presence of amorphous material made interpretation

Table 13a. PGE contents (in ppb) and Ru/Ir ratios in terrestrial K-T boundary impact layer from Berwind Canyon, Starkville South, Clear Creek North, Red Deer Valley, Morgan Creek and Lance Creek.

WEIGHTED ABUNDANCE							
Sample	Pt	Pd	Ru	Ir	Au	Rh	Ru/Ir
Berwind Canyon							
clay	41.3	51.4	15.2	18.1	0.09	0.22	0.84
2-5μm	32.1	37.8	21.4	19.9	3.5	0.09	1.1
5-20μm	nd	nd	nd	nd	nd	nd	nd
20-50μm	5.7	3.4	3.0	2.9	9.2	0.03	1.1
sand	25.9	21.5	11.3	16.0	-.-	0.12	0.7
BULK	**105**	**114**	**50.9**	**56.9**	**12.8**	**0.46**	**0.89**
Starkville South-1							
clay	12.9	9.2	7.4	9.8	0.34	-.-	0.8
2-5μm	14.9	11.0	9.5	8.5	9.8	0.11	1.1
5-20μm	27.3	38.9	10.9	8.7	0.01	0.13	1.3
20-50μm	4.0	2.4	2.1	2.0	6.4	0.02	1.0
sand	15.1	7.4	6.9	12.2	0.32	-.-	0.57
Starkville South-2							
clay	8.9	5.3	3.6	3.9	0.09	-.-	0.92
2-5μm	8.1	5.4	4.9	2.6	3.5	0.03	1.9
5-20μm	13.1	24.5	5.7	4.6	0.03	0.06	1.2
20-50μm	nd	nd	nd	nd	nd	nd	nd
sand	5.8	1.4	2.0	2.2	0.35	-.-	0.91
BULK	**110**	**106**	**53.0**	**54.5**	**20.8**	**0.35**	**0.97**
Cleer Creek North							
clay	4.8	2.8	1.5	2.0	0.02	-.-	0.75
2-5μm	11.4	10.3	2.5	4.4	0.01	0.04	0.57
5-20μm	4.8	3.4	2.2	4.1	0.02	-.-	0.54
20-50μm	1.1	1.1	0.49	0.49	0.74	-.-	1.0
sand	4.3	1.9	1.7	3.2	0.21	-.-	0.53
BULK	**26.4**	**19.5**	**8.4**	**14.2**	**1.0**	**0.04**	**0.59**
Red Deer Valley-1							
clay	nd	nd	nd	nd	nd	nd	nd
2-5μm	14.8	0.68	0.42	0.57	0.14	0.01	0.75
5-20μm	15.6	0.67	0.70	0.55	0.85	0.01	1.3
20-50μm	0.82	0.67	0.08	0.14	0.28	-.-	0.57
sand	183	3.2	1.3	4.1	13.4	0.32	0.32
BULK	**214**	**5.2**	**2.5**	**5.4**	**14.6**	**0.34**	**0.46**

Table 13a con't

WEIGHTED ABUNDANCE							
Sample	Pt	Pd	Ru	Ir	Au	Rh	Ru/Ir
Red Deer Valley-2							
clay	3.5	1.3	0.47	0.81	9.5	-.-	0.58
2-5μm	9.7	0.55	0.2	0.22	0.11	0.01	0.91
5-20μm	16.0	0.74	0.45	0.53	1.0	0.01	0.85
20-50μm	6.0	0.12	0.12	0.1	0.17	-.-	1.2
sand	7.8	0.86	0.54	0.48	1.0	0.02	1.1
BULK	43.0	3.6	6.9	2.1	11.8	0.04	
ΣBULK*	130	5.1	2.4	4.2	18.0	0.20	0.57
Morgan Creek							
clay	1.0	0.59	0.25	0.16	0.83	-.-	1.6
2-5μm	3.4	1.2	0.58	0.59	5.4	-.-	0.98
5-20μm	2.6	0.78	0.47	0.47	4.6	0.01	1.0
20-50μm	2.2	1.6	0.43	0.51	1.9	-.-	0.84
sand	21.0	10.9	6.1	16.3	17.9	0.12	0.37
BULK	30.2	15.1	7.8	18.0	30.6	0.13	0.43
Lance Creek							
clay	2.0	3.9	0.3	0.25	-.-	-.-	1.2
2-5μm	1.3	2.8	0.2	0.19	2.3	-.-	1.1
5-20μm	4.5	2.8	0.59	0.41	2.4	-.-	1.4
20-50μm	9.6	0.69	0.57	0.54	0.86	0.02	1.1
sand	11.4	1.8	1.0	0.97	3.4	0.17	1.0
BULK	28.8	12.0	2.7	2.4	9.0	0.19	1.1
Terrestrial Mean Ru/Ir = 0.92 ± 0.28; Bulk mean Ru/Ir = 0.86 ± 0.28							

Concentration normalized to total weight of all size fractions for a given site.

-.- = values below limit of detection (3 times the standard deviation for 10 reagent blanks, treated as samples).

nd = no data

BULK value is the total PGE abundance for all size fractions at that site.

*ΣBULK for Red Deer Valley calculated as: $\Sigma[(x_1 + x_2)/2]$ where x_1 and x_2 are the PGE content in each size fraction at site Red Deer Valley-1 and Red Deer Valley-2, respectively.

Sample size limitations prelude organic separation on each size fraction and therefore concentration represents both inorganic and organic PGE. All determination are on a carbonate free basis.

Red Deer Valley-1 and Red Deer Valley-2 are split from one boundary clay sample (41C) taken 0 to 1 cm below the base of the Nevis Coal seam, donated by J. Lerbekmo (Lerbekmo and St. Louis, 1986).

Starkville South-2 is the red layer lying directly on top of the boundary claystone. Starkville South-1 is the yellow layer overlying the red layer, making up the remainder of the impact clay.

Table 13b. PGE contents (in ppb) and Ru/Ir ratios in terrestrial K-T boundary claystone from Berwind Canyon, Starkville South and Clear Creek North.

WEIGHTED ABUNDANCE							
Sample	Pt	Pd	Ru	Ir	Au	Rh	Ru/Ir
Berwind Canyon-1							
clay	2.2	6.3	1.0	1.0	0.05	-.-	0.97
2-5μm	3.5	3.8	2.4	1.9	2.0	0.03	1.3
5-20μm	3.2	3.2	2.0	1.3	0.05	-.-	1.5
20-50μm	1.2	1.1	0.59	0.37	0.64	-.-	1.6
sand	7.1	2.1	1.0	1.2	0.02	0.02	0.83
Berwind Canyon-2							
clay	nd	nd	nd	nd	nd	nd	nd
2-5μm	1.7	0.85	0.25	0.13	-.-	0.01	1.9
5-20μm	1.7	3.3	0.38	0.27	-.-	0.01	1.4
20-50μm	2.7	0.57	0.32	0.09	0.17	-.-	3.7
sand	nd	nd	nd	nd	nd	nd	
BULK	6.1	4.7	0.95	0.83	0.17	0.02	1.1
Starkville South							
clay	1.8	-.-	0.69	0.79	0.03	-.-	0.87
2-5μm	0.50	0.26	0.29	0.09	0.17	-.-	3.2
5-20μm	1.2	1.5	0.45	0.2	-.-	-.-	2.3
20-50μm	0.69	0.13	0.09	0.08	0.19	-.-	1.1
sand	1.4	0.81	0.15	0.15	-.-	0.01	1.0
BULK	5.6	2.7	1.7	1.3	0.39	0.01	1.3
Clear Creek North-1							
clay	1.4	-.-	0.36	0.36	0.13	-.-	1.0
2-5μm	-.-	-.-	-.-	-.-	-.-	-.-	-.-
5-20μm	0.47	-.-	0.18	0.36	-.-	-.-	0.50
20-50μm	0.48	0.24	0.21	0.07	-.-	-.-	2.9
sand	2.5	1.0	0.16	0.09	-.-	-.-	1.7
Clear Creek North-2							
clay	0.52	-.-	0.50	0.30	0.11	-.-	1.6
2-5μm	1.9	0.54	0.21	0.17	-.-	-.-	1.2
5-20μm	1.4	1.9	0.25	0.15	-.-	-.-	1.7
20-50μm	0.28	0.24	0.14	0.09	0.46	-.-	1.6
sand	0.24	-.-	0.21	0.50	-.-	-.-	0.42
BULK	9.2	3.9	2.2	2.1	0.7		1.1

Concentration normalized to total weight of all size fractions for a given site.

-.- = values below limit of detection (3 times the standard deviation for 10 reagent blanks, treated as samples) for that sample size.

nd = no data

BULK value is the total PGE abundance for all size-fractions at that site

Berwind Canyon-1 is the top of the boundary claystone, 0 to -0.5 cm below the impact layer. Berwind Canyon-2 is the boundary claystone -0.5 to -2 cm below the impact layer. Berwind Canyon-1 may include some impact layer material, elevating the PGE concentrations. For this reason, only Berwind Canyon-2 is included in the bulk calculation. The bulk value is therefore a minimum for this site.

Clear Creek North-1 is the top of the boundary claystone from 0 to -2 cm below the impact layer. Clear Creek North-2 is the base of the boundary claystone from -2 to -2.5 cm below the impact layer.

Table 13c. PGE contents (in ppb) and Ru/Ir ratios in terrestrial K-T boundary coal seam at Berwind Canyon, Starkville South and Clear Creek North.

WEIGHTED ABUNDANCE							
Sample	Pt	Pd	Ru	Ir	Au	Rh	Ru/Ir
Berwind Canyon							
clay	4.4	-.-	1.7	5.5	0.17	-.-	0.30
2-5μm	1.4	1.0	0.85	0.63	0.56	-.-	1.4
5-20μm	5.5	18.7	1.7	0.93	0.02	0.02	1.8
20-50μm	-.-	-.-	-.-	-.-	-.-	-.-	-.-
sand	4.4	7.5	0.72	1.3	-.-	-.-	0.57
BULK	15.7	27.2	5.0	8.4	0.75	0.02	0.59
Starkville South							
clay	11.5	6.9	2.9	2.9	0.09	0.04	1.0
2-5μm	4.7	2.3	6.3	1.6	1.3	0.16	4.0
5-20μm	5.6	0.38	2.6	4.7	0.29	-.-	0.54
20-50μm	1.6	0.22	0.37	0.31	1.4	-.-	1.2
sand	3.4	0.71	1.1	4.6	0.03	-.-	0.22
BULK	26.8	10.5	13.3	14.1	3.1	0.20	0.94
Clear Creek North							
clay	3.2	0.44	0.29	0.26	0.32	-.-	1.1
2-5μm	1.4	0.29	0.29	0.23	4.2	-.-	1.3
5-20μm	3.1	1.3	1.4	0.71	2.9	-.-	1.9
20-50μm	0.94	0.50	0.26	0.08	0.20	-.-	3.0
sand	21.7	7.5	1.2	1.9	0.03	-.-	0.63
BULK	30.3	10.0	3.4	3.2	7.7	-.-	1.1

Concentration normalized to weight of all size fractions for a given site.

-.- = values below limit of detection (3 times the standard deviation for 10 reagent blanks, treated as samples) for that sample size.

BULK value is the total PGE abundance for all size-fractions at that site.

of the XRD trace difficult. Some I/S clay and smectite were detected, but the proportion could not confidently be established (Table 14a). The remainder of the impact layer is kaolinite and quartz.

Lance Creek

The bulk Ir and Pt content of the impact layer at Lance Creek determined in this work is a factor of 9 and 2 lower than that determined by Bohor et al. (1987b), even though their analysis was not done on a carbonate-free basis (c.f., Table 13a and Table 10). This implies some heterogeneity in the distribution of PGE within the impact layer. There is a marked trend of increased PGE abundance with increasing size-fraction at Lance Creek (Figure 24a) and no I/S clay or smectite is present (Table 14a). Ruthenium and Ir show the same enrichment toward coarse fractions in this impact layer. The data of Bohor et al. (1987b) suggest some remobilization of PGE into layers above and below the boundary clay at Lance Creek (Table 10).

Table 14a. Mineralogy of terrestrial K-T impact layer (sites in Table 13).

Site	Kaolinite	I/S	Smectite	Jarosite	Quartz	Other
Berwind Canyon						
clay	**	***	--	*	--	minor goethite in
2-5μm	**	***	--	*	--	sand
5-20μm	**	**	--	*	**	
20-50μm	**	**	--	--	**	
sand	**	**	--	--	***	
Starkville South						
clay	**	***	--	**	--	minor chlorite in
2-5μm	**	***	--	**	--	med. silt
5-20μm	**	**	--	**	*	
20-50μm	**	**	--	*	***	
sand	**	**	--	*	***	

TABLE 14a CON'T

Site	Kaolinite	I/S	Smectite	Jarosite	Quartz	Other
Clear Creek North						
clay	**	**	--	**	--	minor chlorite in
2-5μm	**	**	--	**	--	med. silt
5-20μm	**	**	--	**	--	
20-50μm	**	**	--	*	*	
sand	**	*	--	**	**	
Red Deer Valley						
clay	**	***	--	*	--	
2-5μm	**	***	--	--	--	
5-20μm	**	**	**	--	*	
20-50μm	*	--	***	--	**	
sand	**	--	***	--	**	
Morgan Creek						
clay	*	--	--	--	--	all traces contained
2-5μm	**	--	--	--	**	amorphous material
5-20μm	*	*	--	--	*	
20-50μm	**	--	*	--	**	
sand	**	--	*	--	**	
Lance Creek						goethite in silt
clay	***	--	--	--	*	fractions
2-5μm	***	--	--	--	*	
5-20μm	***	--	--	--	**	
20-50μm	***	--	--	--	**	
sand	**	--	--	--	***	

Table 14b. Mineralogy of the terrestrial boundary claystone (Raton Basin sites).

Site	Kaolinite	I/S	Smectite	Jarosite	Quartz	Other
Berwind Canyon						
clay	***	**	--	--	--	minor goethite in
2-5μm	***	**	--	--	--	fine silt and sand
5-20μm	***	*	--	--	--	
20-50μm	***	*	--	--	*	
sand	***	*	--	--	**	
Starkville South						
clay	***	**	--	*	--	minor goethite in
2-5μm	***	*	--	--	*	sand
5-20μm	nd	nd	nd	nd	nd	
20-50μm	***	*	--	--	*	
sand	***	*	--	--	*	

TABLE 14b CON'T

Site	Kaolinite	I/S	Smectite	Jarosite	Quartz	Other
Clear Creek North						
clay	***	**	--	*	--	minor chlorite in
2-5μm	***	*	--	*	**	med. silt
5-20μm	nd	nd	nd	nd	nd	
20-50μm	**	*	--	*	***	
sand	**	*	--	*	***	

Table 14c. Mineralogy of the terrestrial K-T boundary coal seam (Raton Basin sites).

Site	Kaolinite	I/S	Smectite	Jarosite	Quartz	Other
Berwind Canyon						
clay	***	--	--	--	--	minor chlorite in
2-5μm	***	--	--	**	*	fine and med. silt.
5-20μm	**	--	--	*	--	
20-50μm	nd	nd	nd	nd	nd	
sand	**	--	--	*	**	
Starkville South						minor goethite in
clay	***	--	--	**	--	med. silt and sand.
2-5μm	***	--	--	**	--	
5-20μm	**	--	--	--	*	
20-50μm	*	--	--	*	**	
sand	*	--	--	*	***	
Clear Creek North	Poor orientation of sample or abundant amorphous inorganic material made interpretation of trace impossible.					

For the Red Deer Valley impact layer, XRD results from the two sites were combined to conserve space.
Estimation of mineral abundance was made on the main line for each trace and recalculated to 100%.
>50% = ***; 10-50% = **; <10% = *; -- = not detected; nd = no data
I/S = irregular interstratified illite/smectite mixed layer clay.

General observations on the terrestrial boundary clay layers are as follows. 1) the clay mineralogy (kaolinite, I/S clay, smectite) and associated minerals suggest that there were local variations in the conditions under which the K-T boundary layers were deposited, and subsequently altered, throughout the Western Interior of North America and 2) the covariance of Ru and Ir is good in the terrestrial impact layer, demonstrating

the geochemical coherence of these two elements (Figure 24a,b, Figure 25a). As at the marine sites, the correlation of Ir with Pd is weak (Figure 25b). The correlation between Ru and Ir is less good in the boundary claystone (Raton Basin only) (Figure 26) due to differential mobility of the two elements.

The correlation of PGE concentration and mineralogy in each size-fraction for the terrestrial sections (impact layer) is not as simple as for the marine sites. Of all the minerals present in detectable amounts in the impact layer, only the I/S clay or smectite seem likely hosts for PGE. An irregular interstratified mixed layer clay is as feasible a structural host for PGE as is pure smectite, since the interlayer space in smectite layers is still present. In the Berwind Canyon site, there is a general correlation of PGE concentration and I/S mixed layer clay content, except in the sand size-fraction that has a high PGE content but only a moderate I/S clay content (c.f., Table 13a and Table 14a). The I/S clay-PGE relationship holds for the Starkville South site where the correlation is moderately high (c.f., Tables 13a and 14a). At Clear Creek North, the abundance of PGE is less than at the other Raton sites, and the correlation with I/S clay is generally weak (c.f., Tables 13a and 14a).

At Red Deer Valley, both smectite and I/S clay are present and may be hosts to PGE. The highest PGE contents are found in the sand size-fraction of the Red Deer Valley-1 site (Table 13a, Figure 24a,b), which contains abundant smectitic clay (c.f., Tables 13a and 14a). In the Morgan Creek boundary clay, PGE are concentrated in the coarse size-fraction (Figure 24a,b), where smectite was detected, but the presence of abundant unidentifiable amorphous material obscured the traces at this site (c.f., Tables 13a and 14a). Only kaolinite and quartz were detected at Lance Creek. At this site,

Figure 25a,b. Iridium versus Ru (a) and Ir versus Pd (b) for the terrestrial impact layer. Correlation coefficients high ($r = 0.92$). The lower correlation coefficient for Ir versus Pd ($r = 0.77$) results from the more mobile nature of Pd. Note that Ir is enriched in the sand fraction for Morgan Creek. Error bars for Ru (3%) fall within the bounds of the symbol outline. Error bars for Ir (13%) are within the symbol bounds for abundances < 10 ppb and are marked by a line for higher abundances. Error bars for Pd (10%) are within the symbol bounds for abundances < 35 ppb and are marked by a line for higher abundances.

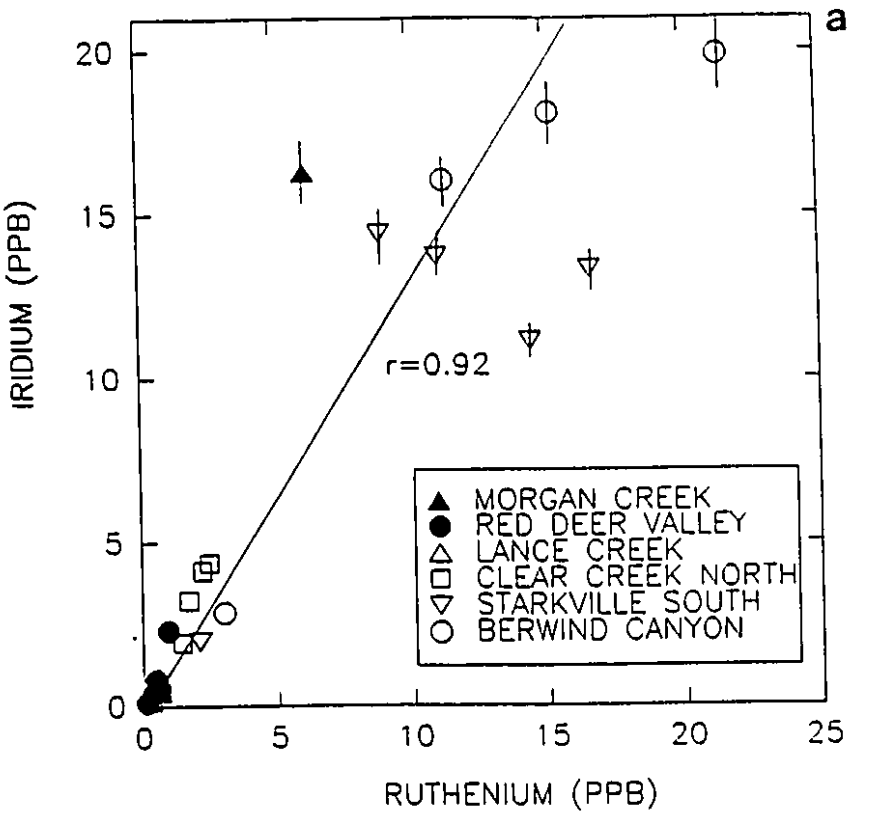
a
IRIDIUM (PPB)
RUTHENIUM (PPB)
r=0.92
MORGAN CREEK
RED DEER VALLEY
LANCE CREEK
CLEAR CREEK NORTH
STARKVILLE SOUTH
BERWIND CANYON
0
5
10
15
20
25

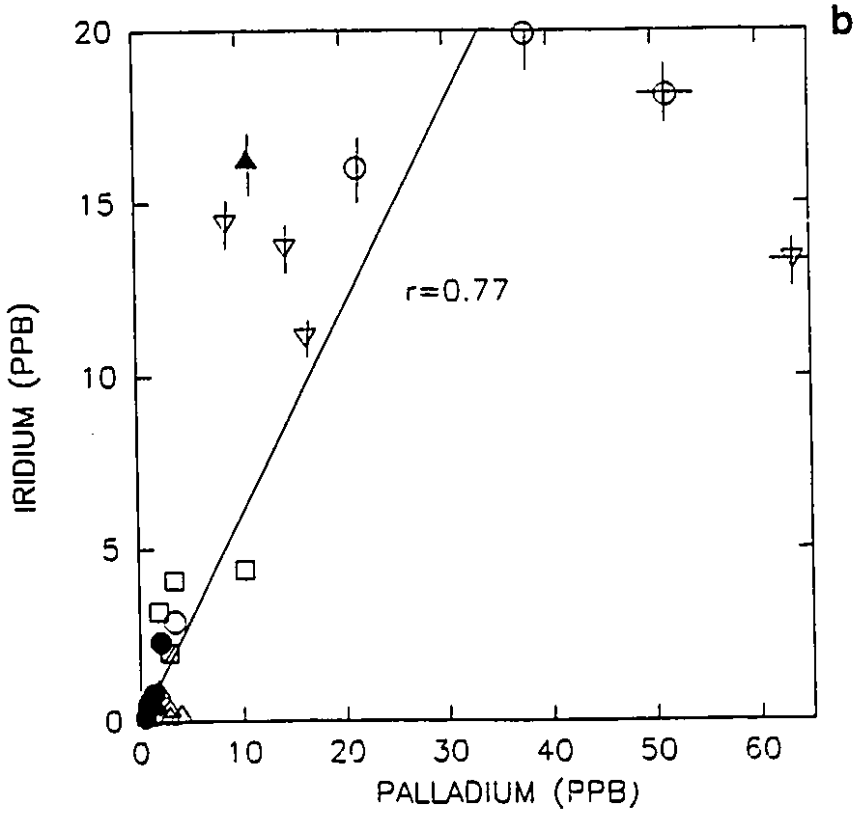
b
IRIDIUM (PPB)
PALLADIUM (PPB)
r=0.77
0
5
10
15
20
30
40
50
60

Figure 26. Iridium versus Ru for the boundary claystone for all terrestrial sites ($r = 0.84$ with the point at 0.69,0.79; $r = 0.61$ without the extreme point). The correlation between Ru and Ir is lower than in the impact layer (Figure 23a) due to differential element mobility. Data for Berwind Canyon is sample Berwind Canyon-2.

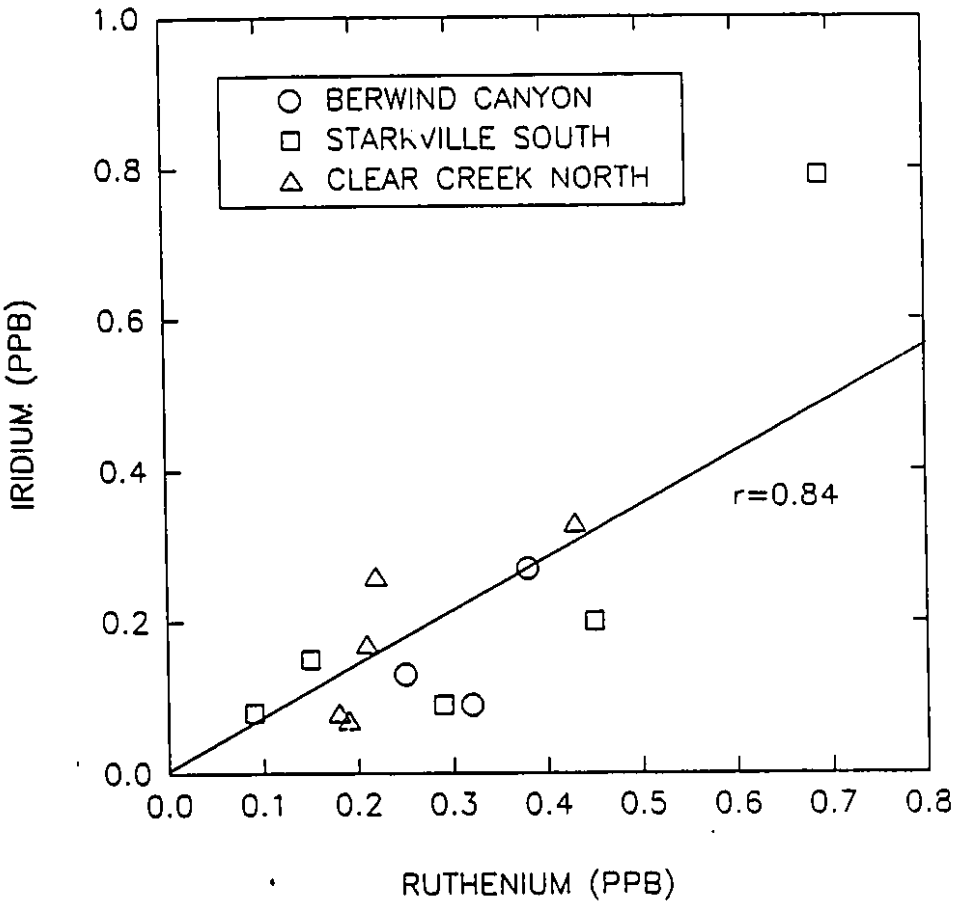
BERWIND CANYON
STARKVILLE SOUTH
CLEAR CREEK NORTH
r=0.84
IRIDIUM (PPB)
RUTHENIUM (PPB)
1.0
0.8
0.6
0.4
0.2
0.0
0.0
0.1
0.2
0.3
0.4
0.5
0.6
0.7
0.8

perhaps a small, undetectable amount of smectite or I/S clay is present or there is another undetected carrier.

Terrestrial interelement PGE ratios are given in Table 12. As with the marine sites, the only ratio which can be considered useful statistically is the Ru/Ir (0.92 ± 0.28), as the others have all been affected to varying degrees by the mobility of the numerator element. All ratios except the Ru/Ir are higher than in any type of chondrite (Table 20). The standard deviation exceeds the mean for all but the Ru/Ir ratio (Table 12). This again reflects the geochemical coherence of these elements and their low mobility. The site-dependant variation in Ru/Ir ratios is illustrated in Figure 27. The Ru/Ir ratio is, nevertheless, lower than all chondrite ratios (Table 21) and the average Ru/Ir ratio for all marine K-T sites (1.77 ± 0.53). The boundary claystone and coal layers in the Raton Basin generally have higher Ru/Ir ratios (Table 13a,b,c and Figure 17) than the impact layer, a result of the higher propensity for Ru mobilization over Ir and the greater degree of mixing with terrestrial sediments which typically have higher ratios (Table 5).

Implications for Global Dispersal of PGE

The question remains as to how PGE came to be associated with the smectite or I/S mixed layer clay. One possible explanation is that a precursor, condensed glass phase was the original carrier for the PGE. In the Acraman impact ejecta, the highest Ir and Cr abundances are in coarse-grained ejecta material, indicating that most of the Ir was carried by ejecta glass or clasts of devitrified glass (Gostin et al., 1989). The PGE-bearing ejecta from the K-T impact likely originated as glass (hereafter referred to as

Figure 27. Iridium versus Ru/Ir ratio for the impact layer from all terrestrial sites. Mean Ru/Ir is 0.92 ± 0.28. Error bars for Ir (13%) are within the bounds of the symbol for abundances < 10 ppb and are marked by a line for higher abundances. Where the boundary impact layer was subdivided for analysis, total abundance for the layer is plotted for each site. Where more than one section was sampled at a given location, means are plotted for that site.

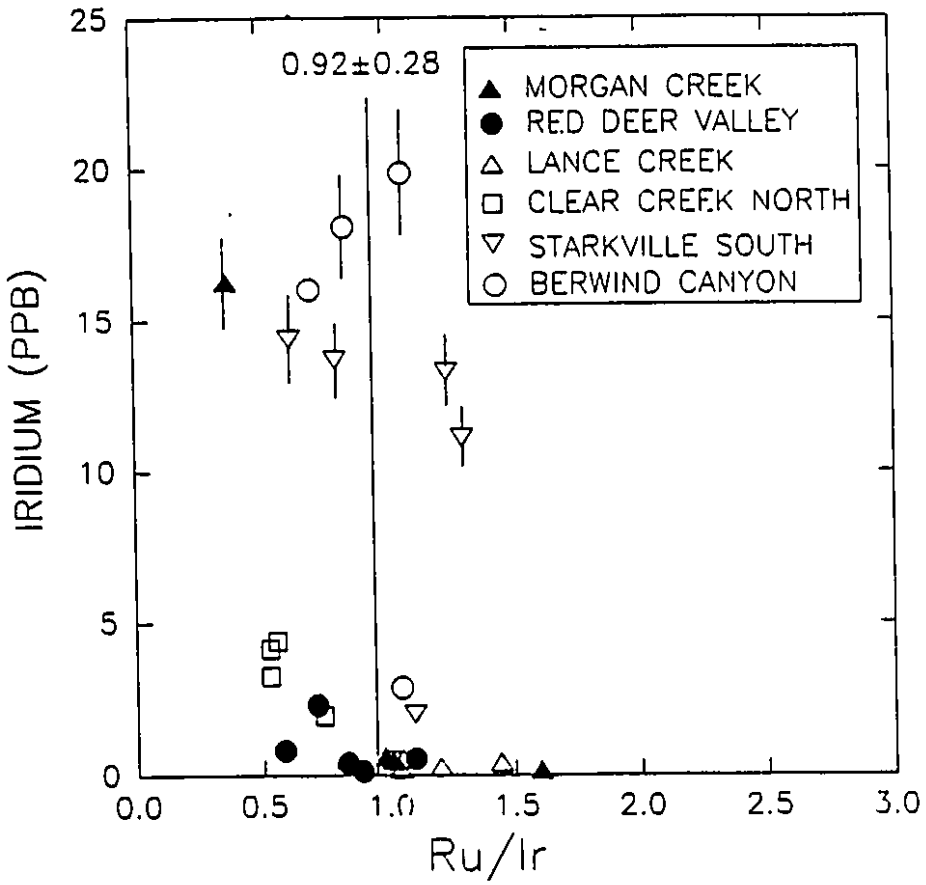
25
20
15
10
5
0
0.0
0.5
1.0
1.5
2.0
2.5
3.0
IRIDIUM (PPB)
Ru/Ir
0.92±0.28
MORGAN CREEK
RED DEER VALLEY
LANCE CREEK
CLEAR CREEK NORTH
STARKVILLE SOUTH
BERWIND CANYON

SCEG; stratospheric condensed ejecta glass), condensed from high-energy ejecta melt and vapour (O'Keefe and Ahrens, 1982; Smit, 1991). Particles larger than 0.5 μm are removed from the stratosphere and lower atmosphere in about 1 week, whereas smaller particles can remain in the stratosphere for 3-6 months (Toon et al., 1982). After fallout, the SCEG alter to smectite (Rampino, 1982; Kastner, 1984; Sigurdsson et al., 1991), freeing the PGE to be adsorbed to the clays or remobilized in organic matter. The strong refractory nature of Ir and Ru (Crocket, 1981b) renders them less mobile and they, therefore, retain original signatures better than the other PGE. The stratigraphic correlation of peak PGE concentration and highest spherule abundance (altered impact droplets, Montanari et al., 1983) at Petriccio may lend support to SCEG being the original PGE host. Millimeter-sized smectite-coated tektite-like glass spherules have been identified in the thick K-T ejecta deposit at the Beloc site, Haiti (Smit, 1991; Sigurdsson et al., 1991). Laser ablation inductively coupled mass spectrometry was applied to individual smectite coatings and enclosed tektite glass in a search for PGE enrichments (Izett et al., 1990). None were found, but the detection limits of the laser ablation method of 5-10 ppb PGE (Izett et al., 1990) are too high for the present purpose.

Only a small portion of the smectite in the boundary clay would be derived from SCEG alteration. The extraterrestrial component of the K-T boundary clay is small and most of the clay minerals in the layer are detrital products of local sedimentation (Rampino and Reynolds, 1983; Izett, 1990). This accounts for the variation in boundary clay smectite composition from site to site (e.g., Mg-smectite at Stevns Klint and Ca-smectite at Elendgraben). It has been calculated (O'Keefe and Ahrens, 1982) that glassy

particles would make up only 15% of the globally dispersed ejecta. The alteration of this material would contribute, therefore, only a minor amount of smectitic material to the boundary clay at any given location. Dominant clay mineral associations depend mainly on latitudinal climatic zonation and, to a lesser degree, on continental erosion related to tectonic uplift (Robert and Chamley, 1990). At the boundary, increased erosion and the predominance of locally-derived detritus are responsible for the character of clay associations. Widespread smectite occurrences in open marine sediments likely represent erosion of proximally exposed volcanic terrain plus some authigenic formation (sedimentary precipitation, hydrothermal alteration of volcanic material or recrystallization of detrital smectite; Robert and Chamley, 1990). The clay assemblages in marine sections mask the small contribution from the impact by responding with extreme sensitivity to other long-term global instabilities, such as tectonic uplift or sea-level fall (Robert and Chamley, 1990). The differences in dominant clay mineralogy between marine and terrestrial sites (marine sites smectite-dominated and terrestrial kaolinite-dominated) are, therefore, due to local effects and are not related directly to the event.

Since only a small portion of the smectite in the boundary clay can be related to SCEG alteration, it is this small portion that may host PGE. Imperfect correlation of PGE content with smectite abundance at some sites may therefore reflect variation in the PGE-bearing /non-PGE smectite ratio.

If the global carrier of the PGE was SCEG, which altered to smectite in the marine environment, possible consequences for the terrestrial impact layer may be the following: 1) the small amount of smectite originating from SCEG alteration was

transformed to I/S clay, or 2) the amount of smectite from SCEG alteration was so small that it is not detectable in some of the terrestrial sites, or 3) the microtektite altered directly to I/S clay at some terrestrial sites and to smectite at others. The latter suggestion seems unlikely since smectite is the natural alteration product of impact glass documented in the literature (Kastner et al., 1984; Gostin et al., 1989). The second interpretation is contradicted by the detailed XRD analysis. This leaves the first scenario as the most likely one.

The process of smectite to illite transformation through intermediate steps of mixed-layer illite-smectite is well known as "illitization" (Fanning et al., 1989). It has been reported to occur noticeably at temperatures >50°C, well within the possible range of temperatures measured in sedimentary basins (Blatt et al., 1980) such as the Raton Basin. The conditions suitable for illite formation include high pH and high K^+ activity (Fanning et al., 1989). The proposed massive influx of decaying organic matter and soot at the K-T boundary (Wolbach et al., 1986) may have generated conditions that are conducive to the illitization of altered SCEG.

As at the marine sites, an imperfect correlation of clay abundance with PGE does not necessarily negate a clay mineral being the PGE host since only a small amount of the I/S clay in the layer would be related to the PGE. High PGE contents in sand size-fractions of the Raton Basin sites may be a reflection of proximity to the impact site (Izett, 1990; Hildebrand and Boynton, 1990) as will be discussed in Chapter 8. A different and unknown carrier may still be required for Lance Creek, where no I/S clay was detected (Table 14a). The effect of illitization on PGE ratios will be discussed in Chapter 8.

The mean PGE abundances for marine and terrestrial sites are given in Table 15. The large standard deviations reflect site-dependent variations in elemental deposition, concentration and remobilization. Both Ru and Rh are depleted in the terrestrial environment, as is Ir, although to a lesser degree.

Table 15. Comparison of mean PGE abundance (in ppb) in the marine and terrestrial K-T impact layer.

	Pt	Pd	Ru	Ir	Au	Rh
Marine Sites	6.2 (4.4)	7.6 (3.7)	4.9 (3.6)	2.9 (3.6)	0.63 (4.9)	0.35 (4.2)
Terrestrial Sites	7.7 (3.2)	3.4 (4.0)	1.5 (4.6)	1.7 (5.0)	0.89 (8.2)	0.05 (3.1)

All means and standard deviations (bracketed) are geometric since all arithmetic distributions were lognormal. Means calculated on bulk PGE abundance for each site. Where more than one site was sampled per location, overall mean values were used. For sites which were subdivided for analysis, total PGE abundance for the impact layer was used.

Origin of the Boundary Claystone

There are two possible interpretations for the origin of the boundary claystone layer: 1) it is an ejecta horizon that is comprised of early fallout from the impact event, or 2) it is a terrestrially-derived clay bed, unrelated to impact. The supporting evidence for the first interpretation includes: 1) a regular spatial association of the boundary claystone and impact layer over large distances across North America and now in Haiti (Hildebrand and Boynton, 1990), 2) the similarity between the porosity and major element composition of the impact layer and claystone (Fastovsky et al., 1989), 3) the chemical similarity between the Beloc tektite-like glass in Haiti and the boundary claystone (Sigurdsson et al., 1991) implying that the boundary claystone may be an impact ejecta horizon, and 4) the spherulitic texture of kaolinite in the claystone that has been interpreted as having formed from the alteration of original tektite glass (Pollastro

and Pillmore, 1987).

Arguments that favour a terrestrial origin for the claystone are the following (Izett, 1990): 1) the concentration of shocked minerals is not in the boundary claystone but in the overlying impact layer, 2) the common fossil plant material within the claystone layer suggests slow accumulation in a normal fluvial or lacustrine environment, 3) a gradational contact is seen between the claystone and underlying carbonaceous shale or mudstone, 4) there evidence for plant growth on the paleosurface of the claystone, prior to deposition of the impact layer and this suggests at least a year of growing time between deposition of the two layers, 5) there is evidence that the claystone underwent pedogenic processes prior to the deposition of the overlying impact layer, 6) there is usually a sharp contact between the impact layer and boundary claystone which might not be expected if both are fallout layers, 7) the microspherulitic texture of kaolinite is not seen at all terrestrial K-T sites, and 8) the boundary claystone has not been found at any of the marine K-T sites (Izett, 1990 and references therein). This last observation may argue against its ejecta origin or support the contention that the impact site was close to North America, thereby limiting ejecta to more local sites. It has been suggested that the boundary claystone layer component was mixed in with impact layer material during passage through the water column in the marine environment, thus forming one composite layer (Bohor, 1990c).

Both the PGE abundances and interelement ratios are distinctly different for the impact layer and the underlying claystone (Table 13a,b). The claystone PGE abundances are often a factor of 10 or more depleted relative to the overlying impact layer, and their PGE ratios do not resemble any for the known meteorite-types. Izett (1990) has

suggested that the PGE in the Raton Basin have been mobilized in acidic, low temperature fluids (Bowles, 1986) during diagenetic alteration of the K-T boundary sediments, and consequently "fixed" in adjacent carbonaceous sediments and coal. There is little doubt that an episode of widespread coal formation (New Mexico to southern Canada) followed deposition of the impact layer, and that it was not related to the event which deposited the PGE. The higher boundary claystone Ru/Ir ratios (Figure 17) are likely the result of differential PGE mobility, with Ru being more mobile (Chapter 4). This elemental redistribution most likely resulted from chemical processes since there is no evidence for reworking by physical or biological processes.

In summary, there is evidence in support of both an impact-related and purely terrestrial origin for the K-T boundary claystone. The PGE abundances and their ratios do not provide conclusive support to either model, although, the depletion in PGE and the distinct Ru/Ir ratios are consistent with a non-impact origin for the claystone layer.

CHAPTER SIX
SOURCE OF THE PLATINUM-GROUP ELEMENTS AT THE CRETACEOUS-TERTIARY BOUNDARY: TERRESTRIAL OR EXTRATERRESTRIAL

Varied, and often contradictory causes that have been proposed for the mass extinction at the end of the Cretaceous include; gradual or rapid changes in oceanographic, atmospheric, or climatic conditions in response to a random or cyclical coincidence of ultimate causative factors (e.g., magnetic reversal, or nearby supernova, or the flooding of the ocean surface by a postulated arctic lake) (Alvarez et al., 1980 and references therein). The extremely abrupt extinction of major groups at the K-T boundary (Birkelund and Bromley, 1979; Smit and Hertogen, 1980) has encouraged scientists to propose a more catastrophic extinction mechanism and two theories prevail; volcanic eruption or meteorite impact. Due to the controversy over the cause of the K-T extinctions, the source of the PGE in the boundary clay is also being actively debated. The geochemical nature of the PGE necessitates that any terrestrial source must involve tapping mantle regions. Analysis and discussion of PGE in mantle-derived rocks (including the Deccan Trap basalt) is, therefore, warranted and is presented in this chapter.

Arguments given in support of a volcanic origin for the PGE include the following: 1) shock mosaicism was identified in plagioclase from the Toba volcanic crater, Sumatra (Carter et al., 1986), implying that this texture is not solely a product of impact, 2) an episode of major flood basalt volcanism ($> 10^6$ km^3 of material) spans the K-T boundary (Deccan Trap basalt; 69-65 Ma, Courtillot et al., 1988) as well as the largest Phanerozoic extinction event at the Permo-Triassic boundary (Siberian Flood

Basalt, 2 x 10^6 km^3 of material; Huffman, 1990) implying that major volcanic events may have caused mass extinction, 3) iridium concentrations (0.17 pg/m^3) 55 times the normal values ($\approx$ 0.003 pg/m^3) were measured in volatiles from Kilauea volcano, Hawaii (Zoller et al., 1983), which indicates that hot spot volcanoes can tap PGE-rich mantle regions, and 4) anomalously high Ir abundances are spread over a 4 meter section across the K-T boundary at Gubbio, Italy (Crocket et al., 1988), suggesting a long-term, rather than instantaneous event. It should also be noted that $^{187}Os/^{186}Os$ ratios in the boundary clay layer cannot distinguish between a meteoritic or mantle source for the K-T boundary PGE (Luck and Turekian, 1983).

Many convincing arguments have been advanced to negate the above evidence. Sharpton and Schuraytz (1989) provide evidence that the mosiac extinction patterns in the Toba feldspars are related to distinct compositional zoning, not shock deformation of the crystal lattice. The single set of lamellae in the Toba feldspar bears little resemblance to the many rational orientations found in K-T shocked feldspar (Izett, 1990) and no shocked quartz was identified at Toba (Bohor et al., 1987a; Sharpton and Schuraytz, 1989; Bohor, 1990a). Alexopoulos et al. (1988) show that shock features in quartz, such as those at the K-T boundary, are distinct from lamellar deformation features in quartz from tectonic or explosive volcanic environments. It is even more difficult to imagine how effusive volcanism, such as that of the Deccan Trap flood basalt, could produce the pressures necessary to create shocked minerals and to distribute them globally. Deccan Trap volcanism began well before, and persisted after the boundary extinction event. If the PGE at the K-T boundary originated from volatiles effused during the flood volcanism, several peaks in PGE concentration or one extended enrichment would be

expected over the 69-65 Ma time span. Only one large PGE peak is found, localized in a thin layer, directly at the paleontological K-T boundary. Where extended Ir anomalies have been identified, contamination, bioturbation, reworking and redeposition, chemical diffusion or mixing during coring have all been evoked as possible causes (J.H. Crocket, pers. comm., 1991; McLaren and Goodfellow, 1990; Rocchia et al., 1990). Iridium enrichment in volatiles, likely as IrF_6, has been identified at two hot spot volcanoes: Kilauea and Piton de la Founaise (Toutain and Meyer, 1989), in sublimates and incrustations formed upon gas cooling. No other PGE have been studied. These volcanoes are characterized by highly fluorinated and chlorinated, high temperature gasses (Olmez et al., 1986). Iridium condenses to particulate form very soon after its release (Finnegan et al., 1990) and this may make it unable to reach the stratospheric altitudes necessary for global dispersion.

Recent detailed re-sampling and re-analysis of Ir in the Gubbio section (Rocchia et al., 1990) has substantiated a spread in the anomaly over a period stratigraphically equivalent to a maximum of 500-600 Ka, considerably less than estimated duration of 1-4 Ma for the Deccan Trap eruption. Also, the peak Ir anomaly is 7 ppb (in the boundary clay) while the highest anomalous value found within 3.5 meters above and below the boundary was 0.8 ppb. It is hard to imagine a series of long-term, effusive volcanic eruptions suddenly producing such a large, globally distributed concentration of Ir. Rocchia et al. (1990) were not able to eliminate redeposition or chemical diffusion as possible mechanisms to account for the vertical spread of the anomaly at the Gubbio site.

Recently it has been shown that the composition of tektites from the K-T ejecta deposit in Haiti are inconsistent with a volcanic origin. The tektites, dated by $^{40}Ar/^{39}Ar$

as 64.5 ± 0.5 Ma, contain no small crystals (like obsidian) and are virtually free of gas and water, unlike any kind of volcanic glass (Sigurdsson et al., 1991).

It seems unlikely, therefore, that the Deccan Trap eruption was responsible for the formation of the shocked minerals or tektites at the K-T boundary. However, the detection of Ir in volatiles from hot spot volcanoes and the inability to distinguish geochemically between a mantle and meteoritic source for the K-T PGE means the possibility that there was some PGE input from the Deccan Trap basalt to the K-T boundary clay, cannot be ignored. PGE abundances and Ru/Ir ratios determined here for the largest suite of Deccan Trap samples ever analysed for PGE, and for pristine Tertiary mantle representatives, afford the first opportunity to make such a distinction.

Deccan Trap basalt and Other Volcanic and Mantle-Derived Rocks

Twenty six samples of Deccan Trap basalt (Figure 2) from various localities and stratigraphic horizons were analyzed for PGE (Table 16) along with several other volcanic and mantle-derived rocks (Table 17). The mantle-derived xenoliths and picrites were analyzed to establish mantle PGE abundances and ratios and because the available database (for Ru and Rh in particular) is not satisfactory. Note that the only aspect of these rocks investigated here is their PGE geochemistry and its relation to the origin of PGE in the K-T boundary clay. References cited in the text and in Table 17 provide all other relevant geological information.

The Alligator Lake (southern Yukon) lherzolite xenoliths (mid Tertiary) have been used to indicate the geochemistry of the source region for melts extracted from the upper mantle (30-60 km depth) and are considered to represent metamorphic rocks, equilibrated

at sub-solidus temperatures (Francis, 1987). Likewise, the Tertiary Baffin Bay picrites (northeastern tip of Padloping Island) are compositional analogues of primary magmas (Francis, 1985) and, together with the xenoliths, provide an indication of upper mantle PGE compositions almost contemporaneous with the K-T boundary. The picrites are from one of the most primitive recent volcanic suites in the world (Robillard et al., 1991). Olivine spinifex-textured komatiite samples, dominantly Archean in age, represent primitive magmas (Barnes et al., 1988). Due to the high temperature of their eruption, sulphur solubility remains high and komatiites, therefore, retain the noble metal budget of their mantle source. They are the best available analogues for Archean mantle PGE compositions (Campbell et al., 1989). The Munro Township komatiite sequences are complete and relatively pristine, having only been metamorphosed to prehnite-pumpellyite facies (Arndt et al., 1977). The Ottawa Island komatiites (Perlay Islands, eastern Hudson Bay) are younger (1800-1700 Ma), and significantly altered (4.5% H_2O; Baragar and Lamontagne, 1980). The Galapagos andesite and n-MORB are fractionated rocks from the East Pacific Rise. The 675 Ma old Natkusiac flood basalt sample (northeast Minto Arch, Victoria Island) is relatively uncontaminated by the crust and therefore provides a good estimate of PGE in the Late Proterozoic upper mantle source regions (Dostal et al., 1986).

Table 16. PGE abundance (in ppb) in the Deccan Trap basalt.

ID	Location	Pt	Pd	Ru	Ir	Au	Rh	Ru/Ir
DT-1	Pangidi	16±2.5	18±1.1	0.5±0.13	0.18±0.13	10±4.1	0.04±0.36	5
DT-2	Igatpuri	89	0.17	-.-	-.-	26	1.9	-.-
DT-31	Ambadungar	26	1	0.35	0.098	7.4	0.01	3.6
DT-32	Ambadungar	17	23	0.33	-.-	14	0.076	-.-
DT-33	Ambadungar	40±2.5	17±1.1	0.13±0.13	0.28±0.13	15±4.1	0.11±0.36	0.46

TABLE 16 CON'T

ID	Location	Pt	Pd	Ru	Ir	Au	Rh	Ru/Ir
DT-34	Ambadungar	15	0.68	0.199	-.-	13	-.-	-.-
DT-35	Ambadungar	9.8±2.5	17±1.1	0.43±0.13	0.06±0.13	11±4.1	0.07±0.36	6.5
DT-36	Nagpur	17	21	0.18	-.-	3.6	0.084	-.-
DT-37	Nagpur	18	21	0.14	0.045	15	0.095	3.1
DT-38	Pavagarh	4.9±2.5	2.7±1.1	0.07±0.13	0.05±0.13	6.8±4.1	0.02±0.36	1.4
DT-39	Pavagarh	1.7	0.93	0.087	-.-	4.5	-.-	-.-
DT-40	Mundwara	8.5	4.7	0.2	0.7	4.7	0.042	2.9
DT-41	Mundwara	6.8	7.4	0.19	-.-	5.1	0.055	-.-
DT-42	Mundwara	9.8±2.5	5.4±1.1	0.11±0.13	0.1±0.13	14±4.1	0.02±0.36	1.1
DT-43	Mundwara	0.5±2.5	0.73±1.1	0.07±0.13	0.05±0.13	2.5±4.1	-.-	1.6
DT-44	Kala Doongar	0.83	1.1	0.079	-.-	2.9	-.-	-.-
DT-45	Kala Doongar	4.3±2.5	4.6±1.1	0.07±0.13	0.17±0.13	5.2±4.1	0.02±0.36	0.53
DT-46	Nara Dome	7.1±2.5	21±1.1	0.26±0.13	0.06±0.13	11.5±4.1	0.07±0.36	4.3
DT-47	Nara Dome	31	20	0.24	0.048	9.6	0.067	5.0
DT-48	Phenai Mata	6.3	6.4	0.12	-.-	9.2	0.024	-.-
DT-49	Phenai Mata	1.5	0.9	-.-	-.-	4.4	-.-	-.-
DT-50	Girnar	9±2.5	6.1±1.1	0.99±0.13	0.16±0.13	6±4.1	0.03±0.36	5.3
DT-51	Girnar	8	7.8	0.23	-.-	6.3	0.02	-.-
DT-52	Khopoli	118	-.-	0.9	0.17	44	-.-	5.3
DT-53	Akot-Harisal	8	9.1	0.77	0.21	10	0.032	3.7
DT-54	Behramghat	6.2	5.4	0.66	0.21	6.4	0.22	3.1
Range		0.5-118	0.1-23	0.05-1.0	0.05-0.7	2.5-44	0.01-1.9	0.29-6.5

-.- denotes values below the limit of detection. Confidence limits (95%) for duplicate analysis is x±1.4SD where SD is given in Table 1.
Values with standard deviations are means of multiple measurements. Actual data is given in Table 1.
Samples from the same location are from the same stratigraphic horizon. Sample locations given in; Raju et al. (1965), Karkare (1985) and Sethna and Sethna (1990).

Table 17. Abundance of PGE (in ppb) in volcanic and other mantle-derived rocks.

Sample	Pt	Pd	Ru	Ir	Au	Rh	Ru/Ir
Alligator Lake Xenoliths[1]							
AL-72	171	4.2	5.8	1.8	47	0.22	3.3
AL-74	55	3.3	4.9	2.1	30	-.-	2.4
AL-75	86	9.7	4.7	2.1	3.4	-.-	2.2
AL-79	324	15	6.5	2.2	9.4	0.031	2.9

TABLE 17 CON'T

Sample	Pt	Pd	Ru	Ir	Au	Rh	Ru/Ir
AL-85	79	2.3	2.0	0.93	-.-	0.034	2.2
Mean							2.6 ±0.48
Baffin Bay Picrites[2]							
Pd-10	25	8.2	3.2	1.1	4.4	0.69	2.8
Pd-13	59	11	3.0	0.98	4.5	0.049	3.1
Pd-15	32	8.2	2.0	0.55	13	0.072	3.6
Pd-19	195	8.5	2.3	0.31	31	0.124	7.3
Pd-21	56	16	3.2	0.84	7.4	0.059	3.8
Mean *							4.1 ±1.8
Munro Township Komatiites[3]							
SA1	28	15	5.1	1.3	9.2	-.-	4.0
SA2	36	11	6.2	1.5	6.5	0.034	4.1
SA2-c	45	16	4.1	2.0	4.3	0.096	4.0
NA2	32	15	7.2	1.5	3.8	0.065	4.8
NB2	37	25	7.0	0.82	2.3	0.145	8.6
Mean							5.1 ±2.0
Ottawa Island Komatiites[4]							
BLS-60-79	9.5	7.7	0.92	0.09	4.2	0.51	10.2
BLS-73-79	10	8.5	0.87	0.21	2.2	0.46	4.1
Sleeper Island Tholeiitic Basalt[5]							
BLS-33-79	1.5	1.2	-.-	-.-	3.1	0.49	-.-
Natkusiac Flood Basalt[6]							
BLS-35-75	8.1	17	0.25	0.1	6.4	0.72	2.5

Sample	Pt	Pd	Ru	Ir	Au	Rh	Ru/Ir
Galapagos Islands							
GR-1645-3E andesite	2.0±1.5	0.59 ±0.11	0.09 ±0.08	0.07 ±0.06	1.6±0.56	0.011	1.5
GR-D5 basalt	1.2±1.5	0.19 ±0.11	0.13 ±0.08	0.07 ±0.06	0.98 ±0.56	-.-	2.0

1. Francis (1987); 2. Francis (1985); 3. Crocket and MacRae (1986); 4. Baragar and Lamontagne (1980); 5. Baragar and Scoates (1987); 6. Dostal et al. (1986).
-.- denotes values below the limit of detection.
Mean values for miltiple analyses of Galapagos rocks are given with associated confidence limits (95%) calculated from multiple analyses in Table 1. Individual values are given in Table 1.

Discussion

The Alligator Lake Xenoliths, Baffin Bay picrites and Munro Township komatiites are a factor of 10 more enriched in PGE than the Deccan Trap basalt. The Ottawa Island komatiites have lower PGE abundances. Most results for the Sleeper Island tholeiites (1960 Ma old; eastern Hudson Bay) are below detection limits. The Natkusiac flood basalt has lower PGE values than the mantle-derived rocks, and one more comparable to the Deccan Trap values. The fractionated (Mg # = 51.3 and 24.2 for GR-D5 and GR-1645-3E, respectively; I. Jonasson, pers. comm., 1990) Galapagos n-MORB and andesite are depleted in PGE (Table 17). The PGE may have been partitioned into immiscible sulphide phases and retained in the mantle (Mitchell and Keays, 1981; Hamlyn et al., 1985).

The abundances of Ru and Ir in the Deccan Trap basalt are 0.3-0.5 ppb and 0.5-0.7 ppb, respectively. Rocchia et al. (1988) previously noted that Ir in the Deccan Trap basalt was depleted and they suggested that massive outgassing from the magma was responsible. As already pointed out, such interpretation is not supported by the sharp PGE concentration spike at the boundary. It should also be noted that when Ir escapes

from outgassing magma, it does so in fluoride complexes (Zoller et al., 1983; Olmez et al., 1986). If the relative degree of Ir and Ru fluoride complexing was comparable to their respective tendency for chloride complexing (Goldberg et al., 1988), the vent gasses and the Deccan Trap volatiles should have high Ru/Ir ratios. Yet, the K-T boundary Ru/Ir ratio (1.77 $\pm$ 0.53, 0.92 $\pm$ 0.28) is less than that of the "residual" Deccan Trap basalt (3.42 $\pm$ 1.96). Nevertheless, since Ir has been found in anomalously high amounts in hot spot volatiles, the possibility of some PGE input to K-T sites proximal to the Deccan Trap basalt cannot be entirely dismissed. This will be discussed further in Chapter 8.

The mean Ru/Ir ratio of the Deccan Trap basalt (3.42 $\pm$ 1.96) is statistically different from marine (1.77 $\pm$ 0.53; 95% confidence level; Student's t-test) as well as from terrestrial K-T sites (0.92 $\pm$ 0.28; 99.9% confidence level). It also differs at the 99.9% confidence level from the chondrite meteorite Ru/Ir value (1.48 $\pm$ 0.09). It should be kept in mind, however, that the degree of PGE outgassed from the basalt is not well constrained and that remobilization of PGE may have altered Ru/Ir ratios in each environment.

A difference between the Ru/Ir ratio of the Alligator Lake xenoliths, Baffin Bay picrites and the Deccan Trap basalts cannot be detected with confidence (statistically different only at the 60% confidence level). Assuming that the mantle chemistry, as represented by the xenoliths and picrites, is close to that of the Deccan Trap source region, the PGE depletion in the Deccan Trap basalt implies that the PGE were either lost to volatiles upon eruption, or that PGE-bearing phases were retained in the mantle. The Ru/Ir ratio allows differentiation between these possibilities. If the PGE were

removed from the Traps into volatile phases, the present Deccan Trap Ru/Ir ratio should be increased relative to the mantle by a degree complimentary to that accumulated in the K-T boundary clays. Since the mantle and the Deccan Trap basalt have the same Ru/Ir ratio, the PGE depletion in the Deccan Trap basalt is not due to their global dispersal in volatile phases and deposition in the boundary clay, but rather to the retention of PGE-bearing phases in the mantle. Little fractionation of Ru from Ir occurred during eruption and emplacement of the Deccan Trap basalt, again emphasizing the geochemical coherence of these elements.

CHAPTER SEVEN
IMPACTOR IDENTIFICATION

Impact melt rocks from several Canadian craters (Figure 28, Table 18) were analyzed to explore the general usefulness of specific PGE ratios as tools for impactor identification. If it is possible to use PGE ratios to corroborate suggested impactor types at known impact craters, application of PGE elemental ratios to identify impactors at the K-T boundary may be possible. All major classes of meteorites are represented among the projectile types for terrestrial impact craters (Grieve, 1980).

Table 18. Location, size and age of terrestrial impact craters studied.

Crater	Latitude	Longitude	Diameter (km)	Age (Ma)
East Clearwater	56°5'N	74°7'W	22	290 ± 20
Brent	46°5'N	78°29'W	3.8	450 ± 30
New Quebec	61°17'N	73°40'W	3.4	1.4 ± 0.1
Wanapitei	46°44'N	80°44'W	8.5	37 ± 24

All data from Grieve and Robertson (1987).

Limitations on Projectile Identification

Several factors complicate the use of PGE and siderophile element abundances in melt rocks to identify projectile types: 1) Early-time high speed ejecta (O'Keefe and Ahrens, 1982) usually removes the bulk of the projectile mass from the immediate region of the crater (Grieve, 1982). This material disperses regionally, or globally in the case of large impacts. Thus, the projectile "signature" is generally weak. 2) Corrections must be made for the terrestrial component in the melt rocks. An ultramafic target rock, for example, may add PGE and siderophile elements to the melt rocks of a small crater,

Figure 28. Map showing the location of Canadian impact craters from which samples were studied. 1 = East Clearwater crater, Quebec; 2 = Brent crater, Ontario; 3 = New Quebec crater, Quebec; 4 = Wanapitei Lake, Ontario.

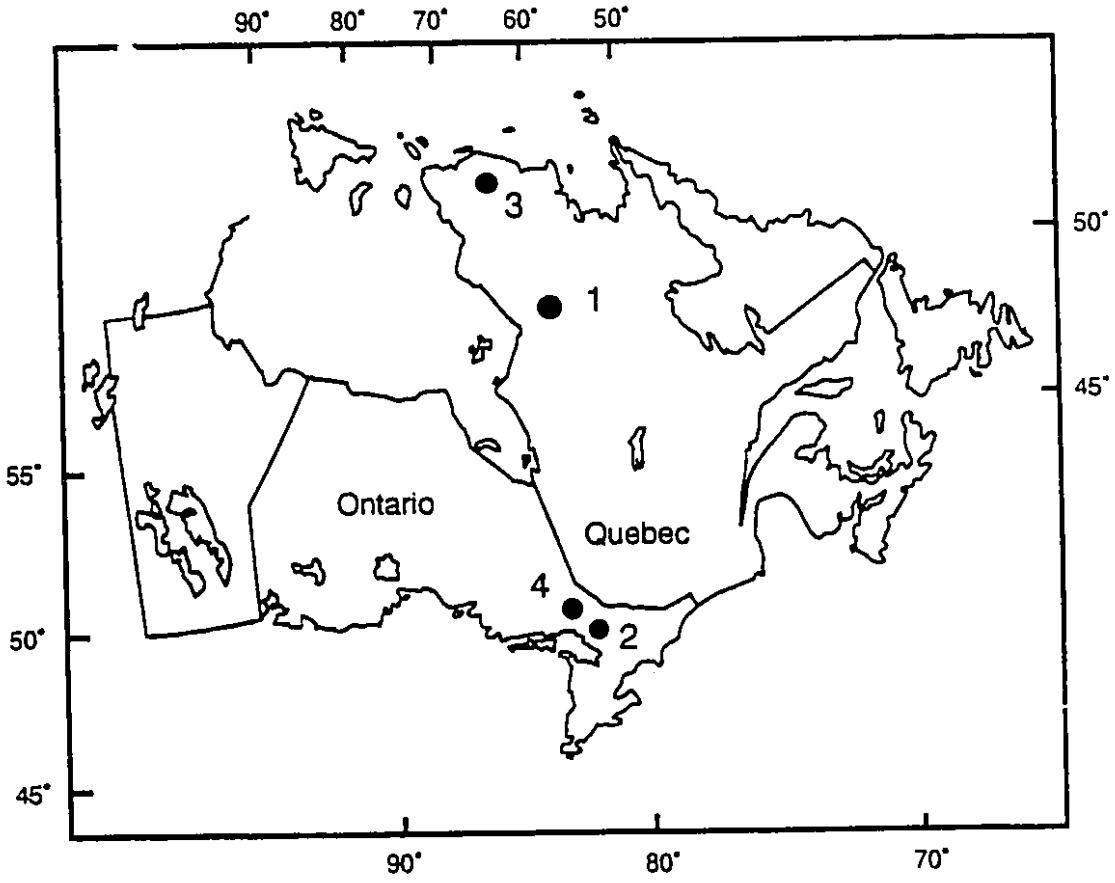
90°
80°
70°
60°
50°
50°
45°
55°
50°
45°
90°
80°
70°
Ontario
Quebec
1
2
3
4

thereby adding terrestrial "noise" to the siderophile data and obscuring meteoritic signatures. 3. Elemental fractionation during impact melting and vaporization, and during crystallization of the melt sheet may alter or mask specific signatures. 4. Subsequent hydrothermal and metamorphic alteration processes may remove elements from the system (Palme et al., 1979; Wallace et al., 1990), or contaminate the system with endogenic PGE and siderophile elements. 5. If the depositional environment is marine, further complications result from the lack of knowledge of geochemical behavior in this environment (Grieve, 1988). It should also be noted that, in some cases, interelement ratios and abundances give ambiguous interpretations. For example, the Rochechouart crater has been interpreted as being formed by an iron and a chondrite projectile (Grieve, 1980 and references therein).

Siderophile Elements in Melt Rocks

The major element chemical homogeneity of impact melts is well established for large craters (Dence, 1971; Grieve and Floran, 1978), but meteoritic component indicator elements, like Ir, may be heterogeneously distributed in the melt sheet. Upon cooling of the melt sheet, fractionation of such elements into minor, heterogeneously distributed carrier phases (e.g., sulphide) may occur (Palme et al., 1979). Meteoritic elements (PGE, Ni, Co, Cr) may be mutually fractionated during this cooling but within the PGE group, Ru and Ir, in particular, should remain chemically coherent (this work), concentrating in metallic iron phases according to their strong siderophile character. The Ru/Ir ratio, taken in conjunction with other indicators (e.g., Cr content) should give an indication of the impactor's composition. Gold is not a suitable element to use for

identification of the impactor since it can be volatilized during terrestrial impact (Morgan, 1978) and is easily mobilized during terrestrial processes. As a result, the content of Au in melt sheets may not be representative of the original meteoritic composition.

A strong enrichment of PGE and siderophile elements in melt rocks indicates either a chondritic or iron impactor. In addition, chondrites are high in Cr (2660 $\pm$ 202 ppm; Anders and Grevesse, 1989) while irons have low Cr contents (122$\pm$171 ppm; Bunch and Olsen, 1975). The combination of Cr-enrichment with chondritic refractory metal ratios (e.g., Ni/Cr, Ni/Co, Co/Cr) is sufficient for identification of the impactor as a chondrite (Palme et al., 1979). All impact craters studied here are believed to have been formed by chondritic impactors (Palme et al., 1979; Wolf et al., 1980; Palme et al., 1981; Grieve et al., 1991) but the type of chondrite is more difficult to ascertain. The absolute abundance of PGE in the melt rock is often not a good indicator of projectile composition due to factors discussed above. The geochemical coherence of PGE, at least within subgroups (PPGE, IPGE), suggests that the ratios might be more useful as indicators of impactor type. Unfortunately, despite an order of magnitude difference in PGE abundance (Table 19), the interelement ratios in various chondrite groups are comparable (Table 20). In addition, the literature data for some elements in specific chondrite groups are sparse. Figure 29 is a chondrite normalized plot for all meteorites for which there is adequate data (from Table 19). All chondrite meteorite traces are flat within an order of magnitude, but the iron meteorites generally show enriched Rh, Ir and Au (IIIAB iron). Comparison of chondrite normalized traces for melt rocks with those for chondrite meteorites (Figure 29) distinguishes between the major meteorite groups (e.g., iron vs. chondrite), but is unable to subdivide projectiles further within a group.

Figure 29. Chondrite normalized PGE plot for different types of meteorites (Table 19). Insufficient data have precluded a plot for LL-chondrites. The range of published Pt data for L-chondrites is represented by open circles. Two points for each type of iron meteorite indicates the ranges of values for PGE in Table 19. IIIAB Pt = Pernicka and Wasson (1987); IIIAB Au = Esbensen et al. (1982). Note that the pattern for all chondrite-types are flat, thereby limiting the use of PGE for fine classification within the group. Pronounced Rh enrichment with a corresponding minor enrichment of Ir and Au characterize iron meteorites and distinguish them from chondrites.

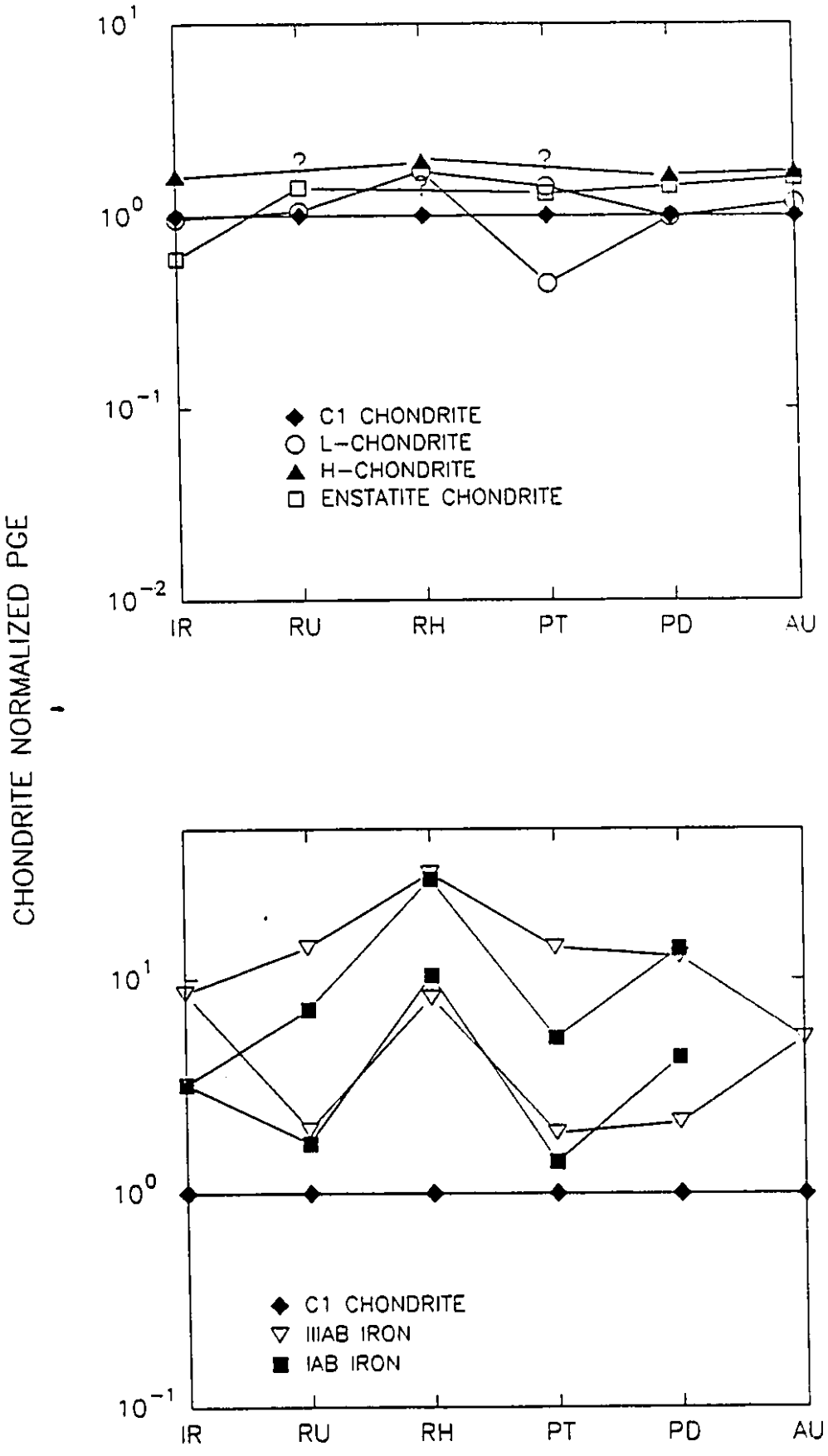
CHONDRITE NORMALIZED PGE
10^1
10^0
10^{-1}
10^{-2}
IR
RU
RH
PT
PD
AU
C1 CHONDRITE
L-CHONDRITE
H-CHONDRITE
ENSTATITE CHONDRITE
C1 CHONDRITE
IIIAB IRON
IAB IRON

Where data sets permit direct comparison (same samples analysed), the literature data agrees to within a factor of 2 with analytical data determined in this work, except some Ir and Au analyses for Wanapitei Lake where the agreement is within a factor of 10. When considering agreement between the published values and this work it should be noted that often the published database is limited, has been obtained by different analytical techniques and that the samples are commonly heterogeneous, with respect to PGE carrier phases. These combined databases will be reviewed for each impact site.

Table 19. PGE and other siderophile element contents (in ppb, unless otherwise noted) in chondrites and iron meteorites.

Type	Pt	Pd	Ru	Ir	Au	Rh	Ni (%)	Co (ppm)	Cr (ppm)
Chondrites									
C-1[1]	990 ±73	560 ±36	712 ±38	481 ±29	140 ±21	134 ±11	1.10 ±0.06	502 ±33	2660 ±202
L-[2]	440-1400	550	750	620 ±8[15]	193 ±3[15]	220	nd	440-780	3400->4000[3]
L-Metal[**]	12900 -1400[4]	nd	12100 ± 5500[6]	5400 ±130[5]	1750 ±230[4]	nd	1.47 ±0.03[4]	7208± 1213[4]	nd
LL-[7]	nd	nd	nd	383 ±130	nd	nd	nd	350-550[3]	3300-3950[3]
LL-[8] Metal	20300 ± 3800	nd	nd	8800± 2100	31500± 350	11700± 850	25.5 ±0.1	11600± 1532	nd
H-[7]	nd	910[2]	nd	779± 67	236± 23	250[2]	nd	700-980[3]	3000-4000[3]
H-[9] Metal	10800 ± 2700	nd	6000 ± 500	4100± 500	1190± 90	nd	9.3± 0.11	4800± 552	nd
Enstatite	1275 ± 35[9]	795± 7[9]	990± 28[9]	290± 29[9]	220[9]	nd	1.59± 0.13[10]	808± 23[10]	3070± 491[10]
			1090 ± 274[10]	617± 59[7]	286± 82[7]				
				552± 63[10]	312± 14[10]				

TABLE 19 CON'T

Type	Pt	Pd	Ru	Ir	Au	Rh	Ni (%)	Co (ppm)	Cr (ppm)
Irons									
IIIAB	5000-23500[2]	1200-7100[2]	5700 ± 4300[14]	4120 ± 60[12]	740 ± 20[12]	1100-4100[2]	7.85 ± 0.23[12]	5030 ± 70[12]	115 ± 43[11]
	7900 ± 6000[14]				1160 ± 750[14]		8.66 ± 1.1[14]		16 ± 8.5[13]
IAB[14]	3320 ± 1900	2400-7700[2]	3130 ± 1970	1530 ± 830	1460 ± 1700	1400-3900[2]	12 ± 6.9	nd	nd

** Metal = metal phase of meteorite only analyzed.
*** note the large error on values.
Reference listed in column 1 apply to all elements for that meteorite type, exceptions noted in table.
1. Anders and Grevesse (1989); 2. Mason (1971); 3. Palme et al. (1979); 4. Rambaldi (1976); 5. Tandon and Wasson (1968), corrected for 10% error as per Kimberlin et al. (1968); 6. Rambaldi (1977b); 7. Ehmann et al. (1970); 8. Rambaldi (1977a); 9. Crocket et al. (1967); 10. Sears et al. (1982); 11. Smales et al. (1967); 12. Esbensen et al. (1982); 13. Malvin et al. (1984); 14. Pernicka and Wasson (1987)***; 15. Haas and Haskin, 1991.

Table 20. Interelement ratios for chondrite and iron meteorites.

Type	Ru/Ir	Pt/Ir	Pd/Ir	Au/Ir	Pt/Au	Pd/Au	Pt/Ru	Pd/Ru	Ni/Ir
Chondrites									
C-1[1]	1.48 ± 0.09	2.05 ± 0.13	1.16 ± 0.07	0.29 ± 0.01	7.07 ± 0.98	4.0 ± 0.50	1.39 ± 0.09	0.79 ± 0.05	2.3 E4 ±5 E3
L-[2]	1.57-1.63	0.92-3.0	1.15-1.2	0.35 ± 0.01[1]	2.3-10	2.9-3.9	0.58-2.5	0.73	nd
LL-	nd	nd	nd	nd	nd	nd	nd	nd	nd
H-	nd	nd	1.08-1.3	0.30 ± 0.03[1]	nd	3.5-4.2	nd	nd	nd
Enstatite[1]	3.4 ± 0.41 (9-9)	4.4 ± 0.54 (9-9)	2.74 ± 0.33 (9-9)	0.65-0.91[2] (9-9)	5.9-5.6[2] (9-9)	3.6 (9-9)	1.3 ± 0.04 (9-9)	0.8 ± 0.02 (9-9)	5.5 E4 ± 1.4 E4 (10-9)
	1.77 ± 0.28 (10-7)	2.06 ± 0.19 (9-7)	1.3 ± 0.11 (9-7)	0.46 ± 1.2 (7-7)	4.5 ± 1.2 (9-7)	2.8 ± 0.75 (9-7)	1.2 ± 0.26 (9-10)	0.73 ± 0.16 (9-10)	2.6 E4 ± 1.4 E4 (10-7)
	1.97 ± 0.38 (10-10)	2.3 ± 0.23 (9-10)	1.4 ± 0.14 (9-10)	0.57 ± 0.05 (10-10)	4.1 ± 0.17 (9-10)	2.54 ± 0.1 (9-10)			2.9 E4 ± 1.3 E4 (10-10)
Irons									
IIIAB[1]	1.38 ± 0.8	1.9 ± 1.1 (14-12)	0.29-1.8[2]	0.18 ± 0.02 (12-14)	10.7 ± 6.1 (14-12)	6.6-33[2]	1.4 ± 1.1 (14-14)	0.12-5.0[2]	1.9 E3 ± 219 (12-12)

TABLE 20 CON'T

Type	Ru/Ir	Pt/Ir	Pd/Ir	Au/Ir	Pt/Au	Pd/Au	Pt/Ru	Pd/Ru	Ni/Ir
				0.28± 0.14 (14-14)	6.8± 5.1 (14-14)				2.1 E3± 714 (14-12)
IAB[1]	2.04± 1.2	2.2± 1.2	1.01-11[2]	0.95± 0.86	2.3± 2.1	>0 - 2.4[2]	1.1± 0.63	0.5-6.6[2]	7.8 E3± 4.4 E3

[1] Values calculated by pooled estimate of variance from the data in Table 19.
[2] Ranges correspond to those of Table 19.
nd = no data for that element.
Numbers in parentheses refer to reference sources for values used in ratio calculation: (numerator-denominator).

Table 21. Abundance of PGE (in ppb) in melt rocks from East Clearwater crater, Brent crater, New Quebec crater and Wanapitei Lake (this work).

Location	Sample	Pt	Pd	Ru	Ir	Au	Rh
East Clearwater[1]	DWC-263-1045	153	124	47	29	35	14
		39	96	50	29	13	0.71
	DWC-263-1022	2.4	0.56	0.17	0.12	1.6	-.-
Brent[2]	BI-59-2778-9	11	12	5.9	1.8	6.7	2.0
	BI-59-2781-0	15	8.8	7.8	3.0	11	2.2
		21	8.9	7.8	2.5	3.2	0.095
New Quebec[3]	RANQ-3a-88	17	5.4	3.9	1.5	3.8	0.069
		17	6.7	4.0	1.9	5.8	0.057
	RANQ-3b-88	16	4.3	3.3	1.7	4.8	1.0
		13	5.4	3.5	2.0	2.4	0.029
	RANQ-3c-88	28	7.9	5.5	2.3	1.8	0.11
Wanapitei[4]	MSWX-154-70	3.5	2.5	0.91	0.29	3.7	0.74
	MSWX-200-70	4.1	4.3	4.3	1.6	15	1.0
		7.5	4.7	4.5	1.9	5.3	0.094
	MSWX-137-79	4.2	2.6	3.7	1.1	4.3	0.96

Sample identification given in the following references; 1. Palme et al. (1979); 2. Palme et al. (1981); 3. Grieve et al. (1991); 4. Wolf et al. (1980).
-.- denotes values below the limit of detection.
Replicate values given where available.

Table 22. PGE and siderophile element abundances (in ppb, unless otherwise noted) for melt rocks (sites in Table 21) (other studies).

Location	Sample	Pt	Pd	Ir	Au	Ni (ppm)	Co (ppm)	Cr (ppm)
East Clearwater[1]	DWC-263-1045	nd	nd	35.8	6.7	845	42.5	269
Brent[2]	BI-59-2773-3	nd	7.8	2.7	0.15	320	21.1	73
	BI-59-2800-2	nd	18.1	9.57	0.93	327	88.1	103
New Quebec[3]	RANQ-3a-88	8.1	nd	1.4	2.3	220	27	100
	RANQ-3b-88	nd	nd	1.7	nd	140	19	72
	RANQ-3c-88	nd	nd	1.3	nd	330	28	120
Wanapitei[4]	MSWX-154-70	nd	4.4	3.03	1.86	103	10.4	45
	MSWX-200-70	nd	4.1	3.8	1.05	85.7	10.6	58
	MSWX-137-79	nd	4.9	4.12	2.03	136	13.2	65

Sample identification and values given in the following references; 1. Palme et al. (1979); 2. Palme et al. (1981); 3. Grieve et al. (1991); 4. Wolf et al. (1980).
nd = no data given for that element.

Table 23. Interelement ratios for melt rocks (sites in Table 21) (this work).

Location	Sample	Ru/Ir	Pt/Ir	Pd/Ir	Au/Ir	Pt/Au	Pd/Au	Pt/Ru	Pd/Ru	Au/Ru
East Clearwater[1]	DWC-263-1045	1.6	3.2	4.2	1.2	4.4	3.6	3.2	2.6	1.2
		1.7	0.77	3.4	0.45	3.0	7.4	0.77	1.9	0.26
	DWC-263-1022	1.4	14	4.7	13	1.5	0.35	14	3.3	9.4
Brent[2]	BI-59-2778-9	3.3	1.9	6.8	3.7	1.7	1.8	1.9	2.1	1.1
	BI-59-2781-0	2.6	2.0	2.9	3.7	1.4	0.8	2.0	1.1	1.4
		3.1	2.7	3.6	1.3	6.7	2.8	2.7	1.1	0.41
New Quebec[3]	RANQ-3a-88	2.6	4.4	3.6	2.5	4.4	1.4	4.4	1.4	0.97
		2.1	4.2	3.5	3.1	2.9	1.2	4.2	1.7	1.5
	RANQ-3b-88	1.9	4.9	2.5	2.8	3.4	0.9	4.9	1.3	1.5
		1.8	3.7	2.7	1.2	5.3	2.3	3.7	1.5	0.69
	RANQ-3c-88	2.4	5.1	3.4	0.78	16	4.4	5.1	1.4	0.33
Wanapitei[4]	MSWX-154-70	3.1	2.8	8.6	13	0.95	0.68	3.9	2.8	4.1
	MSWX-200-70	2.7	2.6	2.7	9.1	0.28	0.29	0.95	1.0	3.4
		2.4	3.9	2.5	2.8	1.4	0.89	1.7	1.0	1.8
	MSWX-137-79	3.4	3.8	2.4	3.9	0.98	0.60	1.1	0.70	1.2

Sample identification given in the following references; 1. Palme et al. (1979); 2. Palme et al. (1981); 3. Grieve et al. (1991); 4. Wolf et al. (1980).

Table 24. Interelement ratios for melt rocks (sites in Table 21) (other studies).

Location	Sample	Pt/Ir	Pd/Ir	Au/Ir	Pt/Au	Pd/Au	Ni/Ir
East Clearwater[1]	DWC-263 -1045	nd	nd	0.187	nd	nd	23.6
Brent[2]	BI-59-2773-3	nd	2.9	0.06	nd	52	119
	BI-59-2800-2	nd	1.89	0.1	nd	19.5	34
New Quebec[3]	RANQ-3a -88	5.8	nd	1.64	3.5	nd	157
	RANQ-3b -88	nd	nd	nd	nd	nd	82
	RANQ-3c -88	nd	nd	nd	nd	nd	253
Wanapitei[4]	MSWX-154-70	nd	1.45	0.61	nd	2.4	34
	MSWX-200-70	nd	1.08	0.28	nd	3.9	23
	MSWX-137-79	nd	1.19	0.49	nd	2.4	33

Sample identification and values given in the following references: 1. Palme et al. (1979); 2. Palme et al. (1981); 3. Grieve et al. (1991); 4. Wolf et al. (1980).
Experimental methods are INAA (Palme et al., 1979), RNAA (Grieve et al., 1991), or both (Palme et al., 1981; Wolf et al., 1980).
nd = no data given for that element.

East Clearwater Lake Crater

The East Clearwater impact structure was, by interpretation, formed by a carbonaceous chondrite meteorite (Palme et al., 1979; Grieve et al., 1980) impacting into granitic gneiss of the Precambrian Shield. Analyzed here were two core samples of melt rock from drill hole DWC-2-63 (Table 21). There is a strong enrichment of PGE in the melt rocks, more so than in any of the other craters studied. This may be due to a low velocity impact which produced relatively less melt and left a higher meteoritic signature (Grieve, 1982). The Ir values determined in this work compare well with those of Palme et al. (1979) (Tables 21, 22), but Au contents determined in this study are higher, possibly due to differences in analytical techniques (NAA vs. ICP-MS) or, more likely, to heterogeneity of Au distribution. Of the interelement PGE ratios (Table 23), Ru/Ir is the most consistent and compares well with the C1-chondrite values (Table 20). This is not surprising considering the relatively low mobilization potential and geochemical coherence of these elements The Ru/Ir ratio also compares well with an H-chondrite and an enstatite chondrite, but these have been dismissed as possible projectile types because of their high Cr content (Palme et al., 1979). The melt rock Cr-content is too high (Table 22) for the impactor to have been an iron meteorite (Palme et al., 1979). The chondrite normalized plot for East Clearwater (elements for all chondrite normalized plots are in order of decreasing melting point according to convention; Naldrett et al., 1979; Figure 30) has a relatively flat pattern ("flat" defined as varying within an order of magnitude), also suggesting a chondritic impactor. Ruthenium and Ir compare well for duplicate analyses of the 291 m sample (Table 21), however, the deviation of Pt analyses may indicate heterogeneous distribution of the Pt carrier phase(s). The depletion of Rh

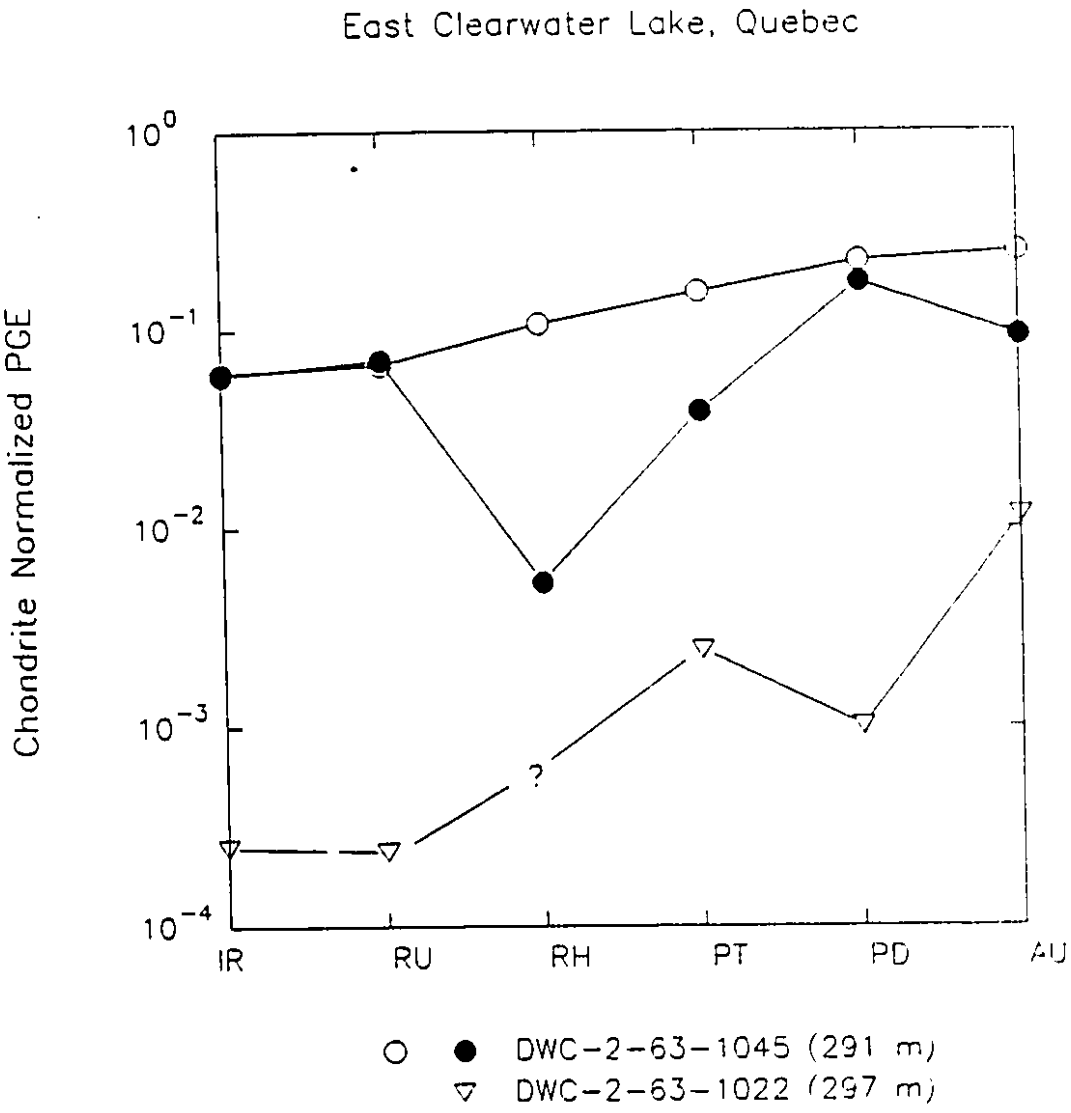

Figure 30. Chondrite normalized PGE plot of impact melt rocks for the East Clearwater Lake Crater.

and Au in the duplicate analysis of DWC-2-63-1045 may be due to loss during analytical preparation procedures as these are the only two elements analysed by external calibration and the same loss is not seen in the other analysis of this sample. The difference in PGE enrichment between the two core samples may be due to concentration of meteoritic components in only some parts of the otherwise homogeneous melt sheet. The likely PGE carrier is a heterogeneously distributed sulphide phase (Palme et al., 1979). Siderophile-rich Fe-Ni particles in the melt rocks are PGE-enriched and are assumed to indicate a C2- or C3-chondrite impactor because C1-chondrites do not contain Fe-Ni metal (Grieve et al., 1980). Unfortunately, C2 and C3 chondrites have similar PGE abundances and ratios (e.g., Ehmann et al., 1970) and the PGE, therefore, cannot be used to identify a specific type of carbonaceous chondrite impactor.

Brent Crater

The Brent structure was formed by a L- or LL-chondrite impacting into mesoperthite gneiss (Palme et al., 1981). Samples of the melt sheet from the core of drill hole BI-59 were analyzed for PGE (Table 21). No published PGE data exists for the samples analyzed here, but Pd, Ir and Au concentrations for samples from comparable depths have been reported by Palme et al. (1981) and are listed in Table 22. The PGE concentrations are lower than in the melt rocks at East Clearwater, with considerably lesser variation with depth. The present results agree well with those of Palme et al. (1981), except for Au (Tables 21, 22). Gold values presented here are not only higher, but their reproducibility was poor (a factor of 4 difference between duplicate analyses of BI-59-2781.0; Table 21), suggesting that the Au is heterogeneously

distributed throughout the sample. Gold leaching during alteration of the Brent melt rocks has previously been suggested to account for the low values (Palme et al., 1981). This could explain the observed large variations in Au content, but not the higher absolute abundances found in the samples analyzed in this study. Comparison of Pd/Ir ratios between the two studies gives an agreement within a factor of 2 (Tables 23, 24). All other ratios determined in this work are consistent between samples and for duplicate analyses (Au being the exception) (Table 23). The Rh depletion observed in the duplicate analysis of BI-2-63-2781 (Table 21) may be due to analytical loss since Au is also depleted in this analysis compared to the other analysis of this sample. The PGE abundances and interelement ratios (Tables 21-24) correspond poorly with those of L-chondrites (Table 19, 20), and the lack of data for LL-chondrite precludes comparison with this meteorite-type (Tables 19, 20). The Ru/Ir ratios for the Brent crater correspond more closely to an enstatite chondrite, whereas the Pt/Ir ratios could be that of virtually any meteorite type (c.f., Tables 20 and 23). The reported Cr content (73-103 ppm; Palme et al., 1981) and the Ni/Cr ratio (2.9; Palme et al., 1981), however, argue against an enstatite chondrite or an iron impactor. This, and the Ni-Cr correlation has been the basis for identification of the projectile as L- or LL-chondrite (Palme et al., 1981). The deviation of the PGE ratios from the L- or LL- values may be a result of fractionation of meteoritic components, perhaps due to alteration (Palme et al., 1981). The chondrite normalized plot for the Brent melt rocks is relatively flat (Figure 31), consistent with a chondrite impactor. Detailed study of the chondrite normalized pattern (c.f., Figure 29 and Figure 31) may indicate a L-chondrite impactor but given the uncertainties discussed above, it would be tenuous to attempt a fine classification.

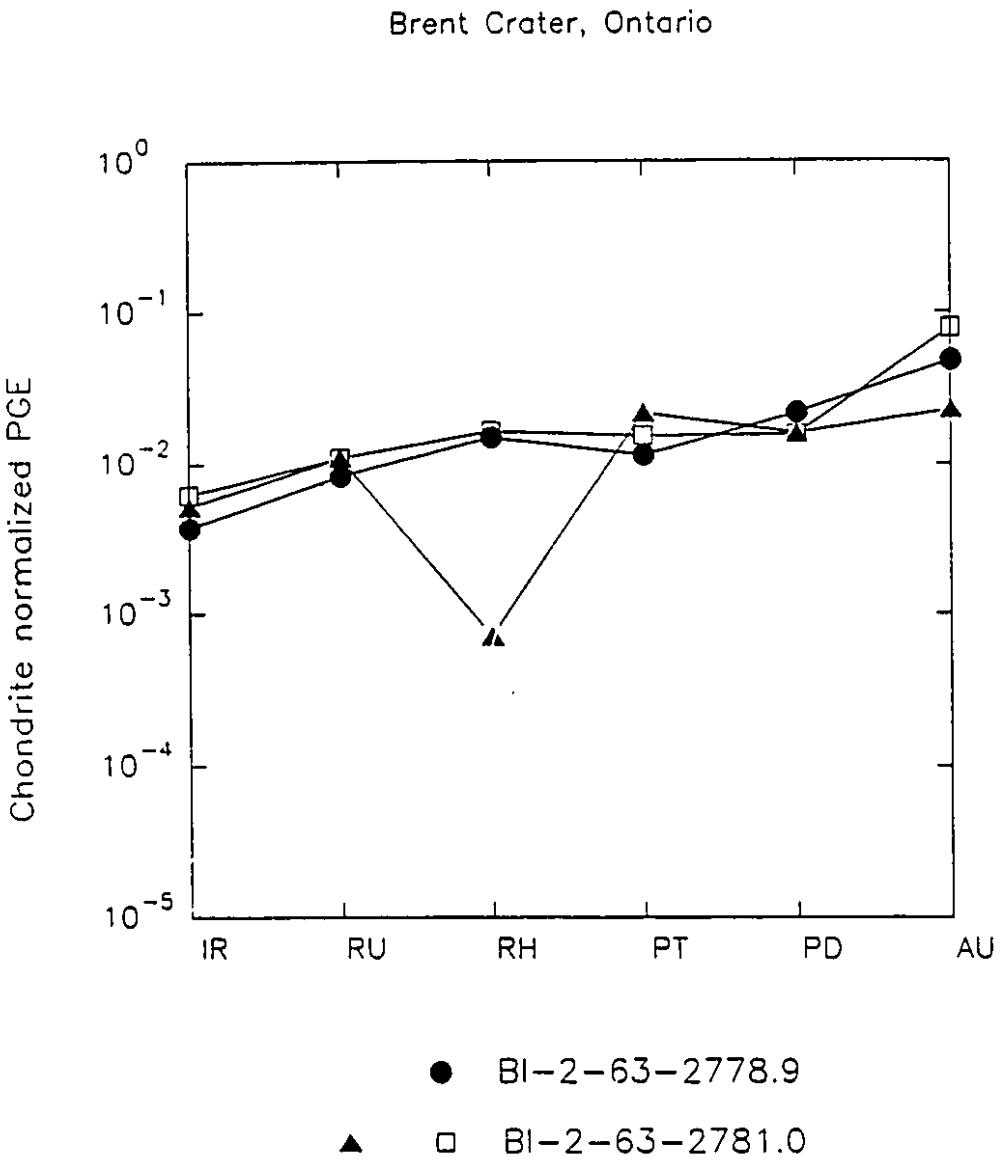

Figure 31. Chondrite normalized PGE plot of impact melt rocks for the Brent Crater.

New Quebec Crater

The New Quebec crater is situated in predominantly granitic Archean gneiss of the Ungava Peninsula of northern Quebec (Figure 28). Pebble samples of impact melt rock were found in glacial sediments within 4 km of the impact structure (Grieve et al., 1991). The impactor is thought to be a chondrite based on Ni, Co and Cr abundances and siderophile interelement ratios (Grieve et al., 1991). The concentrations of all PGE (Tables 21, 22) are consistent between different samples and duplicates of the same sample, and agree with published data (Grieve, et al., 1991). The Ir analyses reported previously for all three samples were too low to provide a good Ni-Ir correlation (Grieve et al., 1991). The Ir values determined here are comparable, suggesting that the Ir depletion is a real feature. RANQ-3c seems to have a somewhat higher Pt, Pd, Ru, Ir and Rh content and a lower Au content than the other two sample sets (Table 21). Interelement ratios (Tables 23) agree within a factor of 2 with the limited data available in the literature (Table 24), but are not chondritic, due to the Ir depletion. Pt/Au ratios (Table 23) are compatible with an enstatite chondrite (Table 20), but the low Cr content (72-120 ppm; Grieve et al., 1991) of the New Quebec melt rocks precludes such an impactor. The only ratio that is close to that of C1-chondrites is Pd/Au for RANQ-3C, a value distinct from all other Pd/Au ratios (c.f., Tables 20 and 23). A depletion of Ir, and possibly Ru, may have raised the other ratios for New Quebec melt rocks, making impactor identification using these ratios impossible. The chondrite normalized plot for New Quebec (Figure 32) indeed shows depletion of Rh and, to a lesser extent, Ir and Pd, but is relatively flat and very similar to the plot for the Brent samples. Because of relatively low Rh and Pd values, the New Quebec projectile is unlikely to have been an

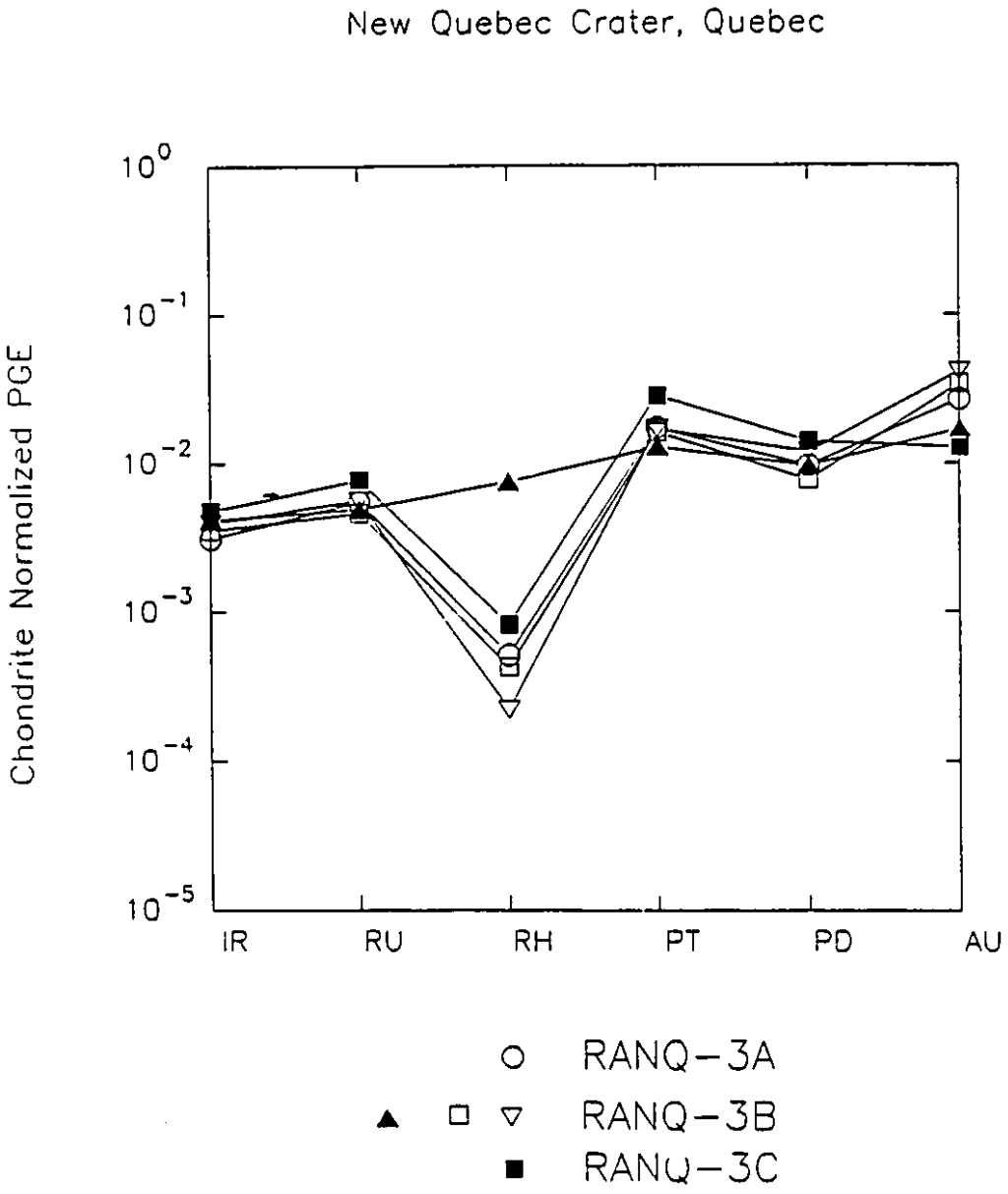

Figure 32. Chondrite normalized PGE plot of impact melt rocks for the New Quebec crater.

iron meteorite (Figure 29). A chondritic impactor is therefore suggested. The Rh concentrations are very low (0.066 ± 0.033 excluding RANQ-3B) for a reason which is not clear at this time. It is difficult to attribute the low Rh values to analytical error since it does not correspond to a depletion of Au. The lack of Ni-Ir correlation (Grieve et al., 1991) may suggest that all the IPGE and Rh have been depleted by an unknown process. Samples are fresh to slightly altered (Grieve et al., 1991) so post-depositional leaching or redistribution of PGE is unlikely. The average Ni/Ir ratio, corrected for target rock contribution, is 5-6 times that in chondritic meteorites. A similar situation exists at Sääksjärvi, where the Ni/Ir ratio is ≈ 3 times chondritic (Palme, 1980). No explanation is available in either case. Perhaps an as yet unidentified meteorite type formed these craters.

Wanapitei Lake

Wanapitei Lake was interpreted to have formed by the impact of a chondrite meteorite into Archean gneiss, Huronian sediments and minor diabase (Wolf et al., 1980). Samples analyzed are glacial float samples of glassy melt rock. All melt rock samples are enriched in PGE (Table 21). Previous analysis (Pd, Ir, Au; Wolf et al., 1980) give comparable values for Pd, but a factor of 2 to 10 lower concentrations for Ir and Au (c.f., Tables 21 and 22). The Ir values from this work agree well in duplicate, but Au values do not. A component of Au may have been added to the melt from the basement Huronian quartzite, which have known Au association (Wolf et al., 1980 and references therein). This factor may preclude the usefulness of Au for meteorite identification at Wanapitei. The interelement Pd/Ir ratios do not agree well with previous determinations (c.f., Table 23 and Table 24) as the present values are a factor of 2-4

higher. The difference in Ir determinations may be a result of inhomogeneous distribution of the Ir carrier phase(s). Radiochemical neutron activation analysis by Wolf et al. (1980) yielded 27% error for Ir determination, however, even with this correction, the Ir data from this work are still much lower than those of the previous study. Compared to known meteorite-types (Table 20), the Ru/Ir ratio is high but within a factor of 2 for most types of chondrite and irons. The Pt/Ir ratio corresponds most closely to an LL-, H- or enstatite chondrite. The Pd/Ir ratio is similar to an enstatite chondrite, but the Pt/Ru ratio matches equally well with any chondrite or iron. The Pd/Ru ratio indicates a C1- or enstatite chondrite. Obviously the impactor can not be classified beyond "chondrite", utilizing the PGE interelement ratios. The high Co/Cr (≈ 100) and Ni/Cr ($\approx$ 4000) ratios of iron meteorites, compared to those of the melt rocks (Co/Cr$\approx$4, Ni/Cr$\approx$2; Wolf et al., 1980) precludes this type of impactor. The lack of Rh enrichment also argure against an iron projectile. On the basis of Ni/Cr ratios, an LL-chondrite has been suggested as the closest match for the impacting body (Wolf et al., 1980). The chondrite normalized plot for Wanapitei (Figure 33) is generally flat, with a slight Ir and Ru depletion in MSWX-154-70. The elemental abundances are not as consistent for this sample as for other samples from Wanapitei, but no duplicate analysis was performed due to sample size limitations. Comparison of the chondrite normalized PGE plot for Wanapitei with the pattern for iron meteorites (c.f., Figure 33 and Figure 29) indicates the impactor was not likely an iron. The low Rh value for the duplicate analysis of MSWX-200-70 may be due to Rh loss during wet chemical preparation as there is also a corresponding depletion of Au for this analysis (Table 21).

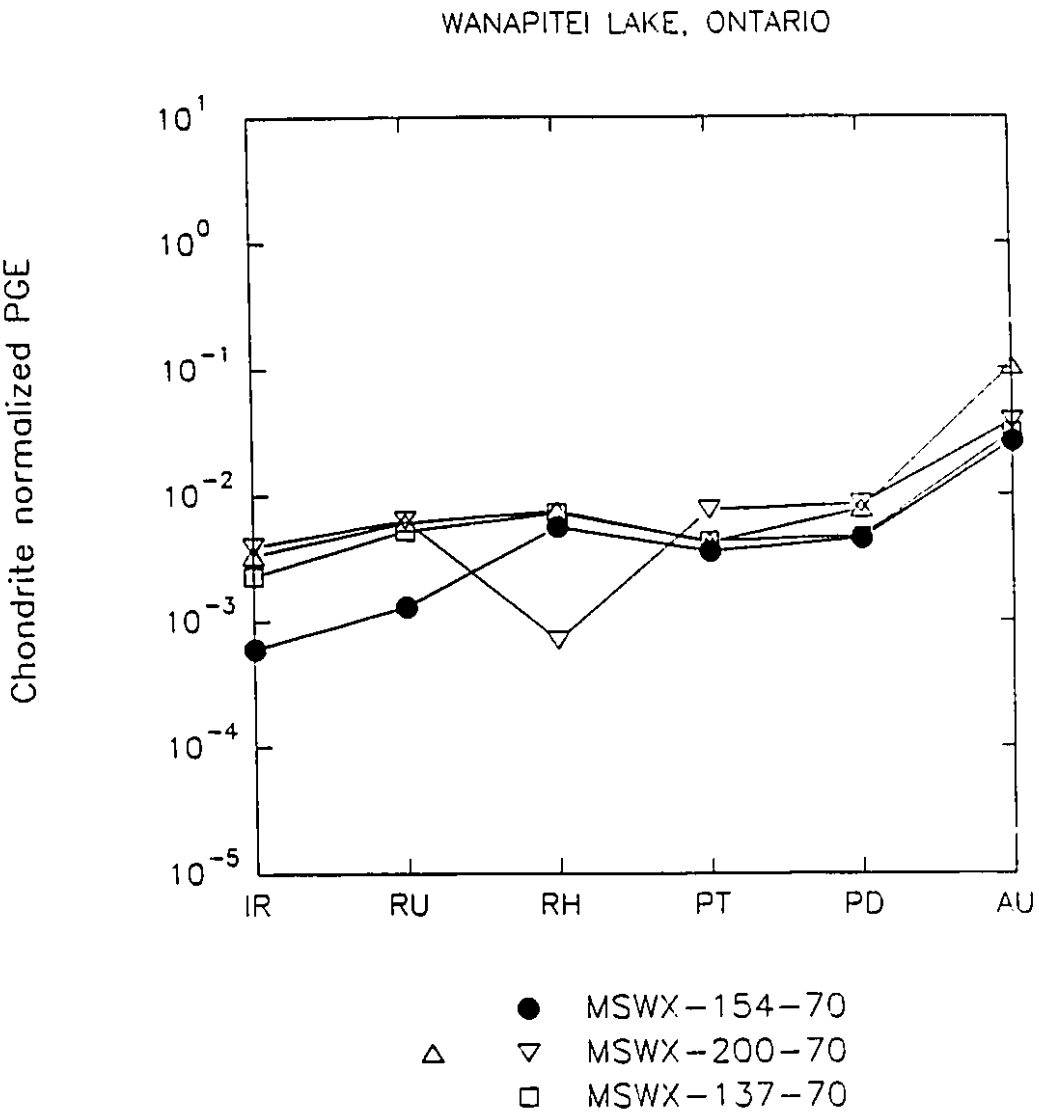

Figure 33. Chondrite normalized PGE plot of impact melt rocks for Wanapitei Lake.

Discussion

The application of PGE concentrations and interelement ratios to impactor identification of melt rocks is limited. Where fresh, unaltered melt rocks were analysed, PGE results can substantiate impactor classification based on other refractory and siderophile elements. If the degree of alteration is high, there is a possibility that redistribution of some or all of the PGE may occur, thereby obscuring the original meteoritic signatures. This is also the difficulty when PGE are concentrated in a heterogeneously distributed, minor carrier phase. Even in the best possible situation (homogeneous distribution of PGE in an unaltered melt sheet), PGE cannot be readily used to identify a meteorite beyond a major group, such as a chondrite or iron. This is often more easily done with elements such as Ni, Co and Cr. Considering these limitations, it is unlikely that the impactor at the K-T boundary can be identified beyond a major meteorite group using PGE.

K-T Boundary Projectile

Recent attempts to locate the K-T boundary impact crater may have met with some success. The Chicxulub crater on the south coast of Mexico's Yucatan Peninsula is the most promising candidate (Hildebrand and Boynton, 1990; Smit, 1991), although dating and analysis of melt rocks have not yet been completed. Before Chicxulub's recent discovery, physical and chemical signatures of the boundary clay were used to distinguish between oceanic and meteoritic impact sites (Shaw and Wasserberg, 1982; Turpin et al., 1988; Hildebrand and Boynton, 1990). Low rare-earth element contents, clinopyroxene within spherules and possible shocked chromite grains in the boundary clay

all suggest an oceanic component (Smit et al., 1988; Bohor et al., 1987a). In contrast, the large shocked quartz grains in North America and the felsic nature of most shocked and unshocked clastic material in the boundary clay suggest that the impact also had a continental component (Izett, 1990) derived from near North America. Recent work on Haitian tektite-like spherules argues for a continental shelf target as well (Sigurdsson et al., 1990). It is also possible that simultaneous multiple impacts occurred, one on land and one off the continental shelf. Binary projectiles have formed 2% of the known impacts on Earth (R.A.F. Grieve pers. comm., 1991). It should be noted, however, that the contribution of PGE from the target material to the K-T boundary clay would likely be inconsequential if compared to that from a large chondritic impactor. The amount of target rock vaporized and ejected is 10-100 times the mass of the bolide, depending on impact velocity (Schmidt and Holsapple, 1982). Nevertheless, a chondritic bolide contains over 10,000 times more Ir than the average crustal rock and the bolide PGE contribution is thus at least two orders of magnitude greater than that of the target material.

Since PGE contamination from target material is of little consequence for a large impact, the major impediments for impactor identification in the K-T boundary clay using PGE are uncertainty in the following: 1) the degree of PGE fractionation on impactor volatilization and condensation, 2) the quantity of projectile PGE distributed globally in the early-time high speed ejecta, 3) the degree of post-depositional alteration and redistribution and the behavior of PGE during those processes. The first process has not yet been quantified. Grieve (1982) established that the bulk of the projectile is unaccounted for, even in complex craters, and has likely been removed in early ejecta.

Since the K-T boundary clay is an ejecta deposit, it may prove more useful than melt rocks from the elusive K-T crater for projectile identification, depending on the amount of melt formed. This work has quantified the mobilization potential of all PGE, at least into organic phases and above/below the boundary layer, and has allowed some constraints to be placed on their redistribution (Chapter 4).

K-T projectile identification using PGE

Previous workers have suggested that the K-T projectile was chondritic based on siderophile abundance (Ir, Os, Au, Pt, Co, Ni, Pd, Ru, Re; Ganapathy, 1980), interelement ratios (Pt/Ir, Au/Ir; Kastner et al., 1984). The low Cr content and Ni/Co ratio ($\approx$31 versus chondrite ratio of 21) of magnesioferrite (a globally distributed, high-temperature relict of the event; Bohor et al., 1986; Zhou et al., 1991) also suggest a chondritic impactor. Ruthenium has not been utilized for projectile identification, because its immobile nature and coherence to Ir in the K-T boundary clay was not recognized previously. The Ru/Ir values may prove to be of greater value for projectile identification than the previously quoted Pt/Ir or Au/Ir ratios (Alvarez et al., 1982; Kastner et al., 1984; Tredoux et al., 1989).

The chondrite normalized plot for marine and terrestrial sites (Figure 34) displays some of the features characteristic to the two environments. Comparison with meteoritic trends presented in Figure 29 show that chondrite normalized plots for all sites are inconsistent with an iron impactor. The flatness of the normalized profiles between Ru and Ir is an indication of the consistency of the Ru/Ir ratio in marine sites and the high coherence of these elements; this argues further against an iron projectile (c.f., Figures

Figure 34. Chondrite normalized PGE plot for marine and terrestrial K-T boundary sites. Elements are presented in order of decreasing melting point. Bulk values for each site were used. Chondrite values are from Anders and Grevesse, 1989.

Marine sites
Open circle = Petriccio; closed circle = Knappengraben; open triangle = Elendgraben; closed triangle = Woodside Creek; open square = Stevns Klint; closed square = Agost.

Terrestrial sites
Open circle = Berwind Canyon; closed circle = Starkville South; open triangle = Clear Creek North; closed triangle = Red Deer Valley; open square = Morgan Creek; closed square = Lance Creek.

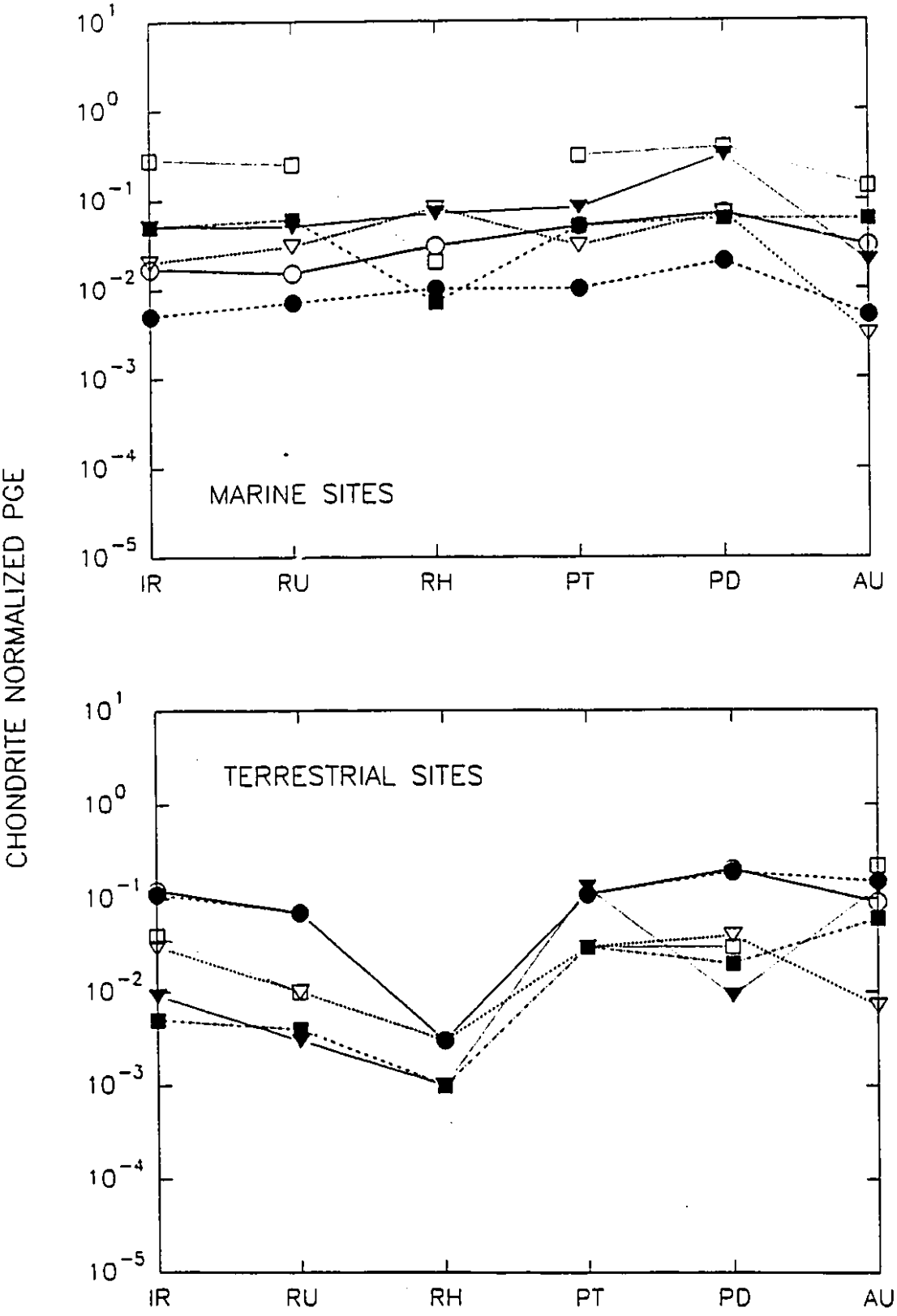
CHONDRITE NORMALIZED PGE
10^{1}
10^{0}
10^{-1}
10^{-2}
10^{-3}
10^{-4}
10^{-5}
MARINE SITES
IR
RU
RH
PT
PD
AU
TERRESTRIAL SITES

29 and 34). Profiles for K-T samples from Petriccio and Knappengraben are also generally flat, and indicative of a chondritic impactor. The trend at Elendgraben is very similar to that of Knappengraben but with higher values overall (Figure 34). The depletion of Au at these sites is not due to loss during analytical preparation as a corresponding loss of Rh would likely be seen and samples were analysed over an extended period of time in many experiments. It is possible that Au has been leached from the boundary clay and fixed in organic matter.

Stevns Klint is the most PGE-enriched site (Figure 34). It is unlikely that the depletion of Rh and Au apparent in the normalized plot of Stevns Klint is due analytical error (e.g., fluctuation in mass-spectrometer sensitivity) since the values are not close to the detection limit for either element (Table 9). Because each size-fraction of SK 1, SK 2 and SK 3 was analysed in different experiments, over a three month period, it is unlikely that the relative depletion of Rh and Au are due to precipitation during analytical preparation. The Rh and Au depletion at Stevns Klint and Agost may reflect loss due to remobilization. Palme (1982) proposed the original meteoritic signature in the Stevns Klint boundary clay had been affected by the same processes of fractionation during impactor volatilization and recondensation as are believed to have occurred at East Clearwater. The chondrite normalized PGE profile for the duplicate analysis of DWC-2-63-1045 (East Clearwater; Figure 30) and for Stevns Klint correspond quite well, although the low Rh and Au in this melt rock sample may be due to the partial precipitation of Rh and Au during analytical preparation. Other samples from East Clearwater display chondrite normalized patterns that do not correspond closely to samples from Stevns Klint and, therefore, the contention of Palme (1982) cannot be

supported by PGE determinations of this work.

The chondrite normalized pattern for Woodside Creek shows a slightly positive slope with a marked peak at Pd (Figure 34). The depletion of Au may be due to secondary remobilization. The PGE pattern for Woodside Creek is comparable to patterns for other marine K-T sites (e.g., Knappengraben, Petriccio), although it is generally more PGE-rich (Figure 34). The chondrite normalized PGE profiles determined here contrast with those previously determined for several marine K-T sites, including three from New Zealand (Tredoux et al., 1989; PGE determined by NiS fire assay with neutron activation analysis). Non-chondritic, steep slopes and a Pd-depletion were observed for the New Zealand sites analysed by Tredoux et al. (1989). Table 25 provides a comparison of Woodside Creek PGE abundances analysed in this work with those of Tredoux et al. (1989). Figure 35 shows comparative chondrite normalized profiles.

Table 25. PGE determinations (in ppb) for Woodside Creek and other New Zealand K-T boundary sites.

	Woodside Creek (this work)	Woodside Creek[1]	Needles Point[1]	Chancet Rocks[1]
Ir	26	37	6.4	4.6
Ru	51	58	19	11
Rh	9.4	nd	nd	nd
Pt	75	236	172	120
Pd	172	56	46	24
Au	2.2	35	7	7
Ru/Ir	2.0	1.6	3.0	2.4

[1] Tredoux et al. (1989).

Figure 35. Chondrite normalized PGE plot for New Zealand K-T sites. Woodside Creek (this work) = open circle; Woodside Creek (Tredoux et al., 1989) = closed circle; Needles Point (Tredoux et al., 1989) = open triangle; Chancet Rocks (Tredoux et al., 1989) = closed triangle. Data of Tredoux et al. (1989) has been recalculated using chondrite values of Anders and Grevesse, 1989.

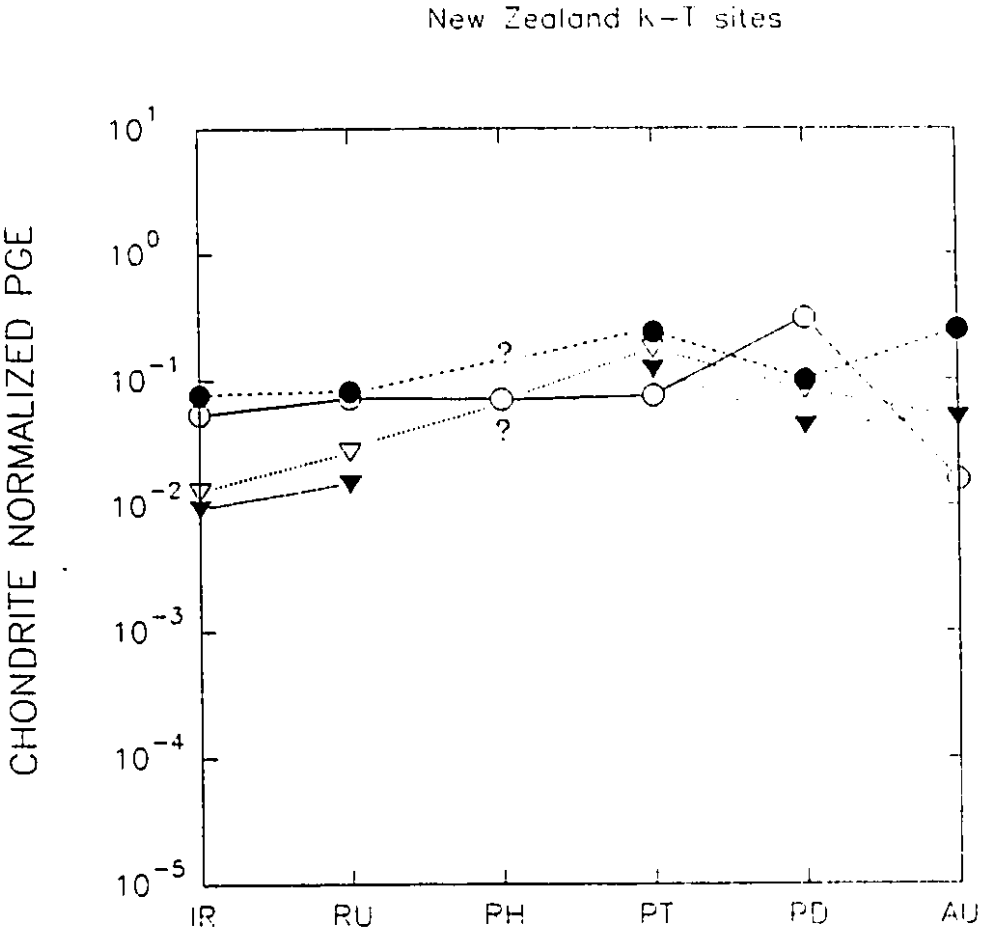
New Zealand K–T sites
CHONDRITE NORMALIZED PGE
10^{1}
10^{0}
10^{-1}
10^{-2}
10^{-3}
10^{-4}
10^{-5}
IR
RU
PH
PT
PD
AU
?
?

For Woodside Creek, Ru and Ir values from this study and those of Tredoux et al. (1989) compare well, as do Ru/Ir ratios. Ru/Ir ratios for Needles Point and Chancet Rocks are higher than those of Woodside Creek (Table 25). The chondrite normalized PGE profiles for all New Zealand sites determined by Tredoux et al. (1989) (Figure 35) are similar, however, neither the Pd peak or the Au depletion shown in the profile for Woodside Creek determined from this study, are evident (Figure 35). Possible explanations for the differences include different analytical methods applied or different locations sampled. The NiS fire assay procedure utilized by Tredoux et al. (1989) requires 50 grams of material, whereas only 5 grams of sample was analysed in this study. The precise location of the samples may be of great importance if winnowing and redeposition occurred during/after deposition of the boundary clay (Bohor, 1990b). Clearly, without analyses of Needles Point and Chancet Rocks by ICP-MS and analysis of exchanged sample splits, the discrepancy between studies cannot be resolved.

Terrestrial chondrite normalized profiles (Figure 34) show a depletion of Ru, making the trace between Ru and Ir negative in comparison to marine sites. This may be the result of illitization of the smectite carrier or fractionation of Ru and Ir during condensation of SCEG (strasospheric condensed ejecta glass; see Chapter 8). Rhodium is consistently near or below the detection limit in terrestrial sites (Table 13a) which is reflected in the low chondrite normalized values in Figure 34. Palladium is relatively depleted at Red Deer Valley and, to a lesser extent, at Lance Creek, perhaps due to remobilization. A similar process may be responsible for Au depletion at Clear Creek North, Starkville South and Berwind Canyon. The PGE traces for Berwind Canyon and Starkville South are almost identical (Figure 34). Clearcreek North has lower PGE

abundances but displays a trend similar to other Raton Basin sites. With these factors taken into consideration, the normalized traces from terrestrial sites are also relatively flat, indicating the possibility of a chondritic impactor.

In summary, the marine and terrestrial K-T sites have statistically different Ru/Ir values. The marine values are chondritic, within error, but cannot be used to classify the projectile beyond the broad chondrite group. The terrestrial Ru/Ir ratios do not correspond to any known PGE-enriched meteorite. This, however, may be an artifact of fractionation during condensation of ejecta or of clay alteration (Chapter 8).

If the K-T impactor was chondritic in composition, there is the possibility of cometary impact. Cometary nuclei contain not only ice, but also a mineralogical component which is thought to deviate little from chondrite in composition (Nazarov et al., 1990). Evidence from the 1908 Tunguska event, suggests that cometary impacts may be accompanied by the influx of cosmic dust particles, of chondritic composition (Nazarov et al., 1990). However, the evidence presented here cannot differentiate between cometary and asteroidal impact.

CHAPTER EIGHT
INTERPRETATION: TOWARDS THE GLOBAL NATURE OF THE K-T EVENT

The K-T impact was an event which left global signatures. This being so, it is important to reconcile the differences between terrestrial and marine sites. The presently assembled geochemical and mineralogical information from marine and terrestrial sites that must be explained by a working hypothesis of global dimensions is as follows:

1) An organic host exists for PGE in both marine and terrestrial sites.

2) Smectite is a probable host to PGE in marine sites.

3) I/S mixed layer clay is a probable host to PGE in terrestrial sites.

4) PGE concentrations in coarse size fractions in terrestrial sites exceed those in their marine counterparts.

5) The Ru/Ir ratio for marine sites is higher than in chondrites.

6) The Ru/Ir ratio for terrestrial sites is lower than in chondrites.

Two hypotheses may account for the observations made in this study. The assumption inherent to both is that there was a single impact of a chondritic body (Ru/Ir = 1.48) at the K-T boundary. 1) Original PGE interelement ratios in the K-T boundary clay, globally, were chondritic. Post-depositional alteration of original stratospheric condensed ejecta glass (SCEG) to clay minerals, PGE remobilization and possible addition of terrestrially-derived PGE subsequently altered the original chondritic ratios. 2) The original PGE ratios in SCEG were not chondritic due to fractionation of PGE during impactor volatilization and condensation. Different ratios in the marine and terrestrial boundary clay resulted from temperature variation in the ejecta cloud with

distance from the impact site.

Discussion

Statistically, the Ru/Ir ratios of the marine and terrestrial K-T boundary clays are distinct at the 99.9% confidence level, a difference which shows up clearly in Figure 36. The marine sites are chondritic within error whereas the terrestrial sites are not. However, if taken as a single group, all sites show a ratio statistically identical to the chondritic value (1.45). The question remains as to whether this shift from chondritic values at terrestrial sites is due to post-depositional or pre-depositional processes.

Post-depositional Processes

Remobilization

The shift of the Ru/Ir ratios cannot be due to remobilization alone. In marine sections there is, on average, 21% Ru and 12% Ir remobilized and fixed in organic phases. If the original values in the impact layer were chondritic just after deposition of the SCEG, the chondrite ratio can be corrected to account for remobilization out of the mineral host. This calculation is likely valid if the remobilized PGE were fixed in organic matter and if the boundary layers behaved as a closed system. The relationship is:

chondrite Ru/Ir - organic Ru/Ir = corrected chondritic Ru/Ir

(712-(712x0.21)) ÷ (481-(481x0.12) = 1.33

The corrected chondrite value (1.33) is farther away from the measured value of 1.77 than the uncorrected chondrite ratio of 1.48. Therefore, organic fixing of Ru and Ir in the marine K-T boundary clay does not fractionate the elements enough to raise a

Figure 36. Iridium versus Ru/Ir ratio for all K-T sites. Note that values for marine and terrestrial sites plot in different fields. Chondrite Ru/Ir is 1.48 ± 0.09. Where the boundary impact layer was subdivided for analysis, total abundance for the layer is plotted for each site. Where more than one section was sampled at a given location, means are plotted for that site.

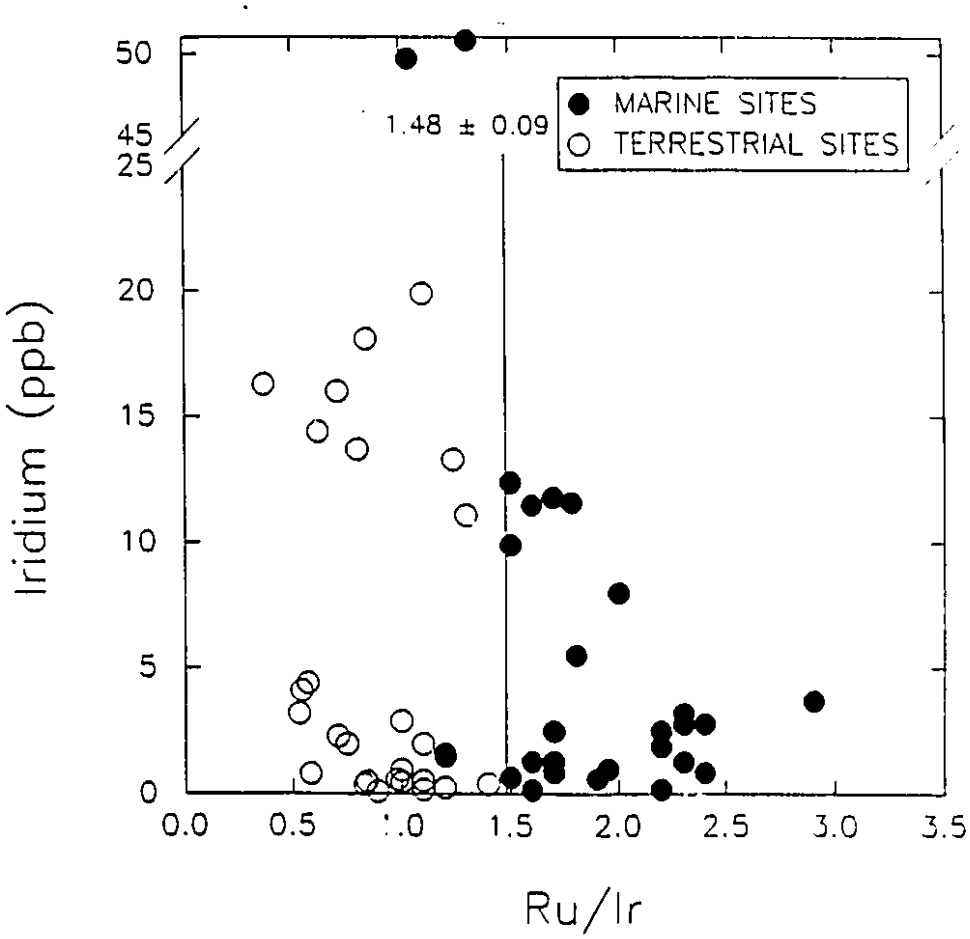
50
45
25
20
15
10
5
0
0.0
0.5
1.0
1.5
2.0
2.5
3.0
3.5
Iridium (ppb)
Ru/Ir
1.48 ± 0.09
MARINE SITES
TERRESTRIAL SITES

chondritic ratio to 1.77. In terrestrial sections the Ru/Ir ratio is lower than chondrite. The degree of organic-association is less than at marine sites (9% for Ru and 6% for Ir). The relationship is:

chondrite Ru/Ir - organic Ru/Ir = corrected chondritic Ru/Ir

(712 - (712x0.09)) ÷ (481 - (481x0.06) = 1.43

Terrestrial values are 0.92, still lower than the corrected chondrite value. For the Raton Basin sites, data is available from layers surrounding the impact layer, but integration of the Ru/Ir ratio across the section does not significantly change the value.

It has been postulated here that the organic-PGE association developed upon illitization (terrestrial sites) and/or smectite formation (terrestrial and marine sites). It cannot be proven whether some remobilization and fixing of Ru and Ir in organic phases occurred millions of years after the K-T boundary clay layer was deposited, however, the coherence of these elements may suggest the effect was minor. It is also possible that some marine PGE were incorporated into settling organic matter during formation of the clay layer. Platinum, Pd, Rh and Au have a higher propensity for PGE-inorganic/organic complex formation (Chapter 4). The large ranges in their interelement ratios indicates they were more greatly affected by redistribution processes, either during or after K-T clay deposition.

Preferential Precipitation in the Marine Environment

On a purely speculative note, it is possible that preferential precipitation under local reducing conditions ("Strangelove ocean"; Hsü and MacKenzie, 1985) may be partially responsible for the marine Ru/Ir ratio being slightly higher than chondrite. Studies of platinum and palladium in the ocean waters indicate an increased tendency

toward formation of stronger halide complexes with increased atomic weight (Hodge et al., 1985). It is expected that platinum forms stronger complexes with chloride and bromide and that palladium is more readily fixed in sediments by scavenging reactions on inorganic and biological phases (Hodge et al., 1985). Although iridium marine chemistry follows that of palladium more than platinum (Goldberg et al., 1986), no data for Ru are available in the literature. If the trend of stronger halide complexing with increasing atomic weight can be extended to Ir and Ru, Ir would complex more strongly in seawater and Ru would be more quickly deposited in the seafloor sediment as organic or inorganic complexes. This is a mechanism by which Ru and Ir may be fractionated in the marine environment and by which the original chondritic marine Ru/Ir ratio could have been slightly raised. The higher degree of organic association displayed by Ru over Ir in the marine sites (Table 4) lends support to this theory.

Terrestrial Input

It is not possible for the Deccan Trap volcanism to be the sole source of the K-T PGE (Chapter 6). However, the fact remains that massive effusion of basalt was occurring contemporaneous with K-T boundary. The Ru/Ir ratio of the Deccan Trap basalt is high (3.42 ± 1.96) and it is possible that a certain amount of Deccan Trap PGE ended up in the nearby marine K-T clay layer and raised the Ru/Ir ratio above chondrite values. Calculations using the Ru/Ir ratios of Deccan Trap volcanic rocks and chondrite indicate that $\approx 15\%$ of Deccan Trap material with $\approx 85\%$ chondrite PGE would give the marine K-T value (Appendix II). Assumptions inherent in such a calculation are that Ru and Ir enter the volatile fluoride phases in the same ratio as they are present in the rock and that the elements can be launched high enough in the atmosphere to spread to

proximal marine K-T boundary sites. There is no data for Ru in hot spot volcanic gasses so the hypothesis is not testable at this time. Other studies (Bhandari et al., 1988) have indicated that the Deccan Trap PGE contribution to the K-T marine clay is negligible. Furthermore, terrestrial sites have not been affected by the Deccan volcanism because the terrestrial Ru/Ir ratios are lower (0.92 $\pm$ 0.28) and statistically different (99.9 % confidence level) to the 3.42 $\pm$ 1.96 Deccan Trap value.

Manson Input

It may also be possible that, if the Manson impact was synchronous with the large K-T impact ($\approx$ 66 Ma; Izett, 1990), some contribution from the Manson impact has affected terrestrial PGE ratios. The identity of the Manson projectile has not yet been established. Original chondritic Ru/Ir ratios have been lowered at terrestrial K-T sites which requires an input of material from the Manson projectile with a Ru/Ir ratio lower than chondrite. It is difficult to conceive of a meteoritic body enriched in PGE that could have this effect (Table 20). All meteorites enriched in PGE have Ru/Ir ratios higher than 1.

Removal of PGE during Clay Alteration

Preferential solubilization of Ru over Ir may have resulted in removal of the former from the terrestrial clays and lowered the Ru/Ir ratio at some sites. Table 15 shows the mean Ru values are lower in terrestrial sites than at marine. Illitization may be the mechanism for Ru removal from terrestrial K-T boundary clays. Illitization is most prevalent in the Raton Basin sites, but extends as far as the Red Deer Valley site in Alberta. Some support for illitization being responsible for the change in terrestrial Ru/Ir ratios is seen upon close study of the Red Deer Valley mineralogy-to-PGE correlation

(c.f., Table 13a and Table 14a). In fine clay and silt size-fractions, I/S clay and kaolinite dominate the clay mineralogy and the Ru/Ir ratio is low (0.75). In coarser fractions, smectite is detected, I/S clay is not found and the Ru/Ir ratio is higher (1.1 - 1.25) and closer to chondrite (1.48 $\pm$ 0.09). This may indicate that alteration of smectite to illite causes solubilization of Ru over Ir, expulsion of the interlayer cations and a lowering of the Ru/Ir ratio. Accumulation of K at the soil surface by biocycling has been documented (Nettleton et al., 1973), as has the process of illitization under high pH, high K^+ conditions (Fanning et al., 1989). It should be noted, however, that although it is structurally possible for PGE to be located in interlayer cation sites, their actual location in/on the clay has not been established. Although illitization has occurred at some sites, it has not been noted at others (e.g., Lance Creek). Illitization , therefore, cannot account for the differences in the Ru/Ir ratio within the group of terrestrial sites studied (e.g., Lance Creek has a Ru/Ir ratio of 1.2 while the Raton Basin ratio is 0.86) and it seems doubtful that the ratio could be lowered from 1.48 (chondrite) to 0.86 by illitization alone.

Pre-depositional Processes

Although post-sedimentary alteration, remobilization or input from terrestrial sources are mechanisms that could alter Ru/Ir ratios to some degree, it seems unlikely that they could lead to the differences observed between marine and terrestrial sites. It is possible, however, that the terrestrial and marine K-T sites had different Ru/Ir ratios at the time of deposition. The degree of PGE fractionation during impactor volatilization and condensation has not been established. Some insight into this process can be obtained from the global trend of Ru/Ir ratios in the K-T boundary clay. The K-T

boundary clay at terrestrial sites has a lower Ru/Ir ratio (Figure 36), a greater content of PGE in coarse size-fractions and larger shocked quartz grains than the marine counterpart (Figure 37). As discussed, shocked quartz size has been used to indicate the location of the K-T impact, since large grains would be expected to settle first, closest to the impact site. Iridium and Ru have vaporization temperatures of 5017°C and 3900°C, respectively, a difference of 1127°C (Table 3). It can be assumed that the impact site is, or is near to, the Chicxulub structure of Mexico's Yucatan Peninsula. After impact, the temperature in the ejecta cloud would be hottest close to the impact site (Melosh, 1982) and Ir would condense while Ru was still in vapour form. The first condensates would, therefore, be more enriched in Ir than Ru and would have a low Ru/Ir ratio. The SCEG falling on areas closer to the impact site will be relatively large as evidenced by shocked quartz and tektite size-distribution patterns, and the higher content of PGE in coarse grain-size particles in terrestrial K-T sites. By the time the stratospheric ejecta cloud expands to pass over European and New Zealand marine K-T sites, the ejecta cloud will have cooled (Melosh, 1982) and incorporated more Ru into condensates, resulting in SCEG with a higher Ru/Ir ratio.

The marine ratio is slightly higher than chondrite, a fact which might be reconciled by this model since more Ir than Ru would be removed from the ejecta cloud early, close to the impact site. Finer SCEG would settle over the locations farther from the impact site. This fractionation of Ru and Ir during condensation may explain the broad differences between the Ru/Ir ratio in each environment (Figure 36, Figure 37). The correlation of Ru/Ir ratio and size of shocked quartz grains (Figure 38) indicates that closer to the impact site, where the shocked quartz size is largest, the Ru/Ir ratio is low.

Figure 37. Maximum size of shocked quartz grains in millimeters (Izett, 1990; Preisinger, 1986) and Ru/Ir ratios for each site studied, plotted on a map with continental configuration 65 Ma. Maximum size of shocked quartz grains has been used to indicate approximate location of the impact site (Izett, 1990). Shocked quartz size decreases and Ru/Ir ratio increases with increasing distance from the proposed K-T impact site ("*"; Chicxulub crater, Yucatan Peninsula; Hildebrand and Boynton, 1990). Sample locations as in Figure 2a with the exception of 8; Caravaca, Spain (instead of Agost). In this case shocked quartz size data was unavailable for Agost and Ru/Ir ratios were unavailable for Caravaca, so the data was combined. No shocked quartz size data has been reported for Knappengraben, Austria. Ru/Ir ratios listed are mean values for each site.

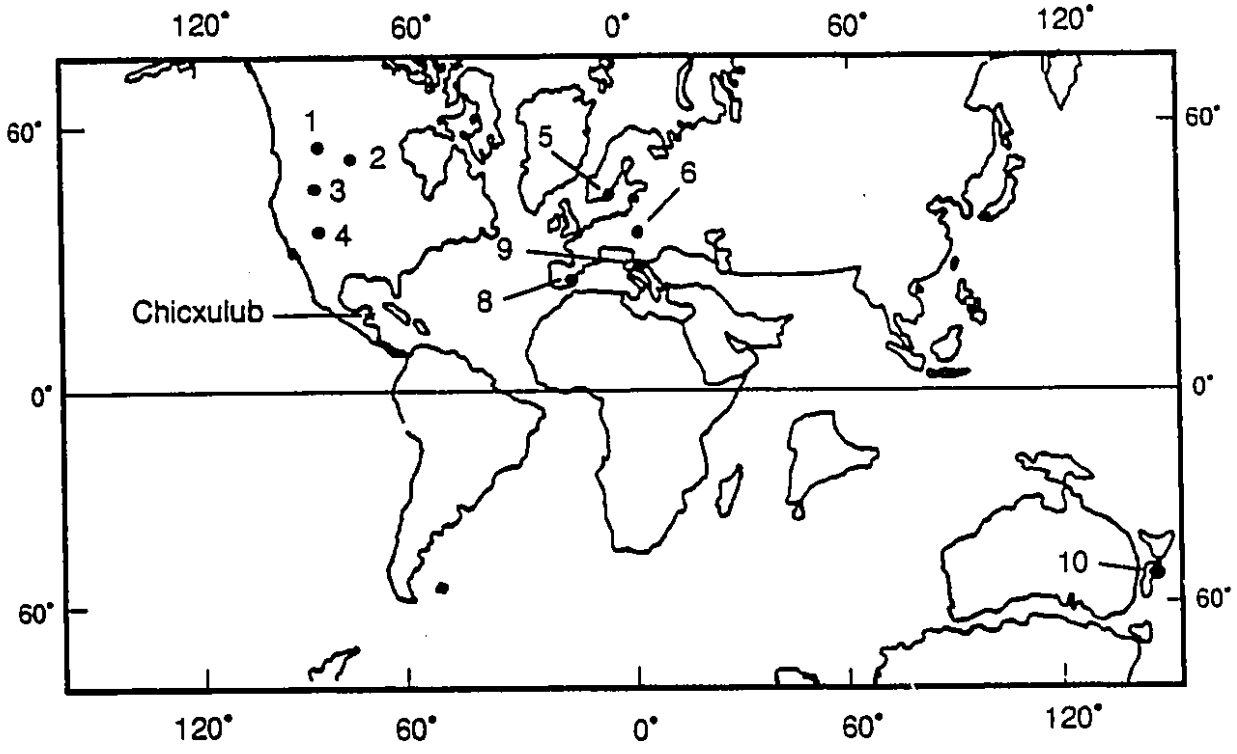

SITE	✱
Red Deer Valley	1. 0.55, 0.82
Morgan Creek	2. 0.53, 0.96
Lance Creek	3. 0.56, 1.2
Raton Basin	4. 0.64, 0.86
Stevns Klint	5. 0.15, 1.5
Elendgraben	6. 0.02, 2.1
Caravaca	8. 0.19, 2.0
Petriccio	9. 0.12, 1.5
Woodside Creek	10. 0.11, 2.0

Maximum shocked quartz size

Ru/Ir ratio

Figure 38. Maximum Shocked quartz grain size (in mm) versus Ru/Ir ratio for all K-T sites studied. A negative correlation exists between these parameters. The increase in Ru/Ir ratio with increasing distance from the impact site may support fractionation of PGE within the ejecta cloud, before deposition in the K-T boundary clay. Ru/Ir ratios plotted are mean values for each site.

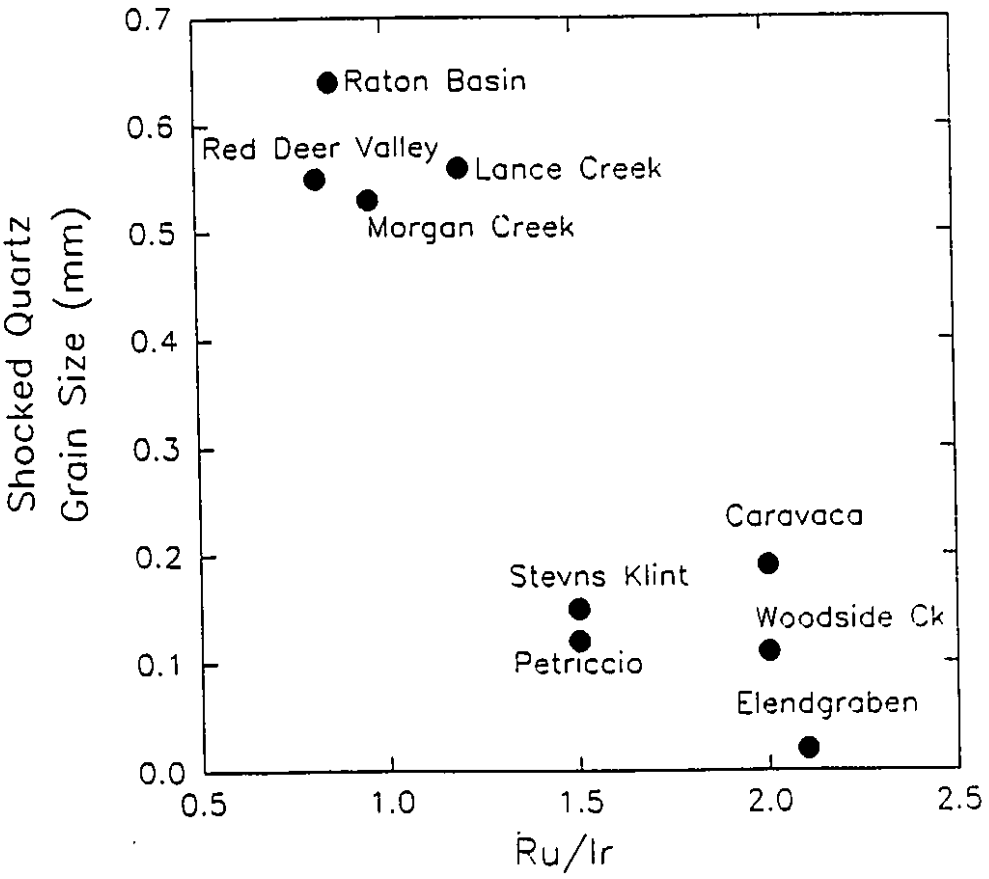
Shocked Quartz
Grain Size (mm)
0.7
0.6
0.5
0.4
0.3
0.2
0.1
0.0
0.5
1.0
1.5
2.0
2.5
Ru/Ir
Raton Basin
Red Deer Valley
Lance Creek
Morgan Creek
Caravaca
Stevns Klint
Woodside Ck
Petriccio
Elendgraben

Figure 39. Iridium versus Ru/Ir ratio for meteorites, marine and terrestrial K-T boundary impact layers and crustal and mantle-derived rocks. Ir values for the K-T boundary are presented as ranges based on the bulk content at each site. Open circle = limestone 1-3 from Table 5; open square = Petriccio and Elendgraben background samples from Table 8; filled square = Ordovician-Silurian black shale from Goodfellow et al., 1991.

The Ru/Ir ratios used for comparing various sample sets (e.g., Deccan Trap basalt, marine K-T boundary sites and terrestrial K-T boundary sites) are arithmetic means. The use of arithmetic mean Ru/Ir values is justified, since the ratios are normally distributed within each population and the median closely matches the mean.

Statistical data for Ru/Ir ratios.

	Deccan Trap basalt	Marine K-T	Terrestrial K-T
Mean	3.42	1.77	0.92
Standard Deviation	1.96	0.53	0.28
Median	3.1	1.7	0.89
Range	0.46-7.4	1.1-2.9	0.37-1.6
n	24	29	29

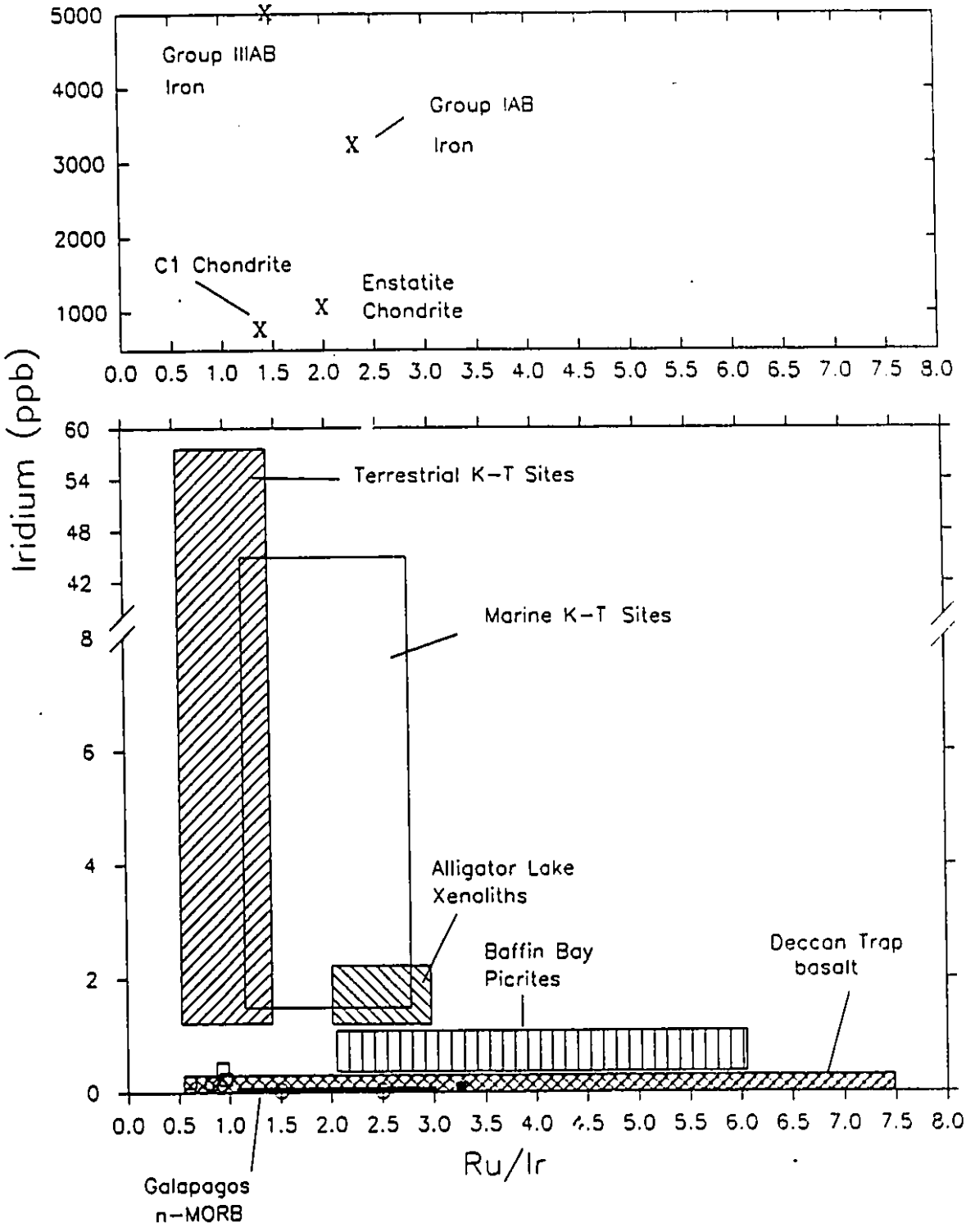
5000
4000
3000
2000
1000
Group IIIAB
Iron
Group IAB
Iron
C1 Chondrite
Enstatite
Chondrite
0.0 0.5 1.0 1.5 2.0 2.5 3.0 3.5 4.0 4.5 5.0 5.5 6.0 6.5 7.0 7.5 8.0
Iridium (ppb)
60
54
48
42
8
6
4
2
0
Terrestrial K-T Sites
Marine K-T Sites
Alligator Lake
Xenoliths
Baffin Bay
Picrites
Deccan Trap
basalt
0.0 0.5 1.0 1.5 2.0 2.5 3.0 3.5 4.0 4.5 5.0 5.5 6.0 6.5 7.0 7.5 8.0
Ru/Ir
Galapagos
n-MORB

Farther from the impact site, shocked quartz is smaller and the Ru/Ir ratio is higher. Considering the possibility that the original Ru/Ir ratios in the marine and terrestrial boundary clay were different at the time of deposition, variation of the Ru/Ir ratio within the groups of terrestrial and marine sites studied may then be attributed to clay alteration, remobilization or terrestrial imput. In the light of this discussion, it should be reiterated that the use of PGE interelement ratios in ejecta blankets for identifying impactors may be hampered by the lack of quantification of PGE fractionation during ejecta condensation.

On a global scale, the PGE data may support the proposed Chicxulub impact site. Terrestrial sites in North America show a greater enrichment of PGE in coarse fractions, whereas pristine European marine sites show more PGE in fine fractions. The coarser-grained SCEG (stratospheric condensed ejecta glass) would tend to settle first from the ejecta, on locations proximal to the impact site, whereas the finer aerosol could be carried over larger distances. Alternate explanations have already been provided to explain coarse size-fraction PGE enrichments at anomalous sites such as Stevns Klint and Woodside Creek (Chapter 5). The correlation of grain size and distance from the impact site can also be extended to tektite-like spherules which are from 1-6 mm in size at the Haitian site (Sigurdsson et al., 1991) and considerably smaller in European K-T boundary clay (0.1-0.8 mm at Caravaca; Smit, 1990, 0.05 mm at Petriccio; Montanari et al., 1983).

Figure 39 provides a summary of all materials analysed for PGE in this work. The large spread in Ir abundances for the K-T sites representing marine and terrestrial

environments is evident, as is the large spread in Ru/Ir values for terrestrial rocks. PGE results for various meteorite types are also plotted. It is clear that, based on the Ru/Ir ratio alone, any one of the various meteorite types shown in Figure 39 could be the source of the K-T PGE. Group IIIAB irons and C-1 chondrites are most similar to both marine and terrestrial Ru/Ir ranges, and iron meteorites can be eliminated on the basis of other evidence (Chapter 7). Partial Ru/Ir ratio overlap of samples from the K-T marine sites with those of volcanic rocks from the Deccan Trap suggest the Deccan Trap volcanism may have contributed to PGE content in the boundary layer. However, it should be noted that only Deccan Trap emissions with Ru/Ir ratios higher than the mean value (3.42) would contribute to raising the marine Ru/Ir ratio. This makes it even less likely that the Deccan Trap basalt effusions were a source of PGE in the K-T boundary clay. The Ru/Ir ratio overlap of the Deccan Trap basalt and Tertiary mantle rocks is evident. The terrestrial sites show lower Ru/Ir values than most meteorite types and all mantle-derived rocks for reasons summarized earlier. Background limestone samples have low Ir abundances and Ru/Ir ratios which range from < 1.0 to 2.5 (Table 8), while the black shale sample has a considerably higher ratio. If these are typical values for crustal rocks, Ru/Ir ratio alone does not provide an indication of extraterrestrial input. The low Ir concentrations, however, indicate a crustal source (Figure 35). The Ru/Ir ratio indicates cosmic flux (source of most PGE in sediments; Alvarez, 1986) may be of chondritic or iron meteorite composition. In fact, cosmic dust is of chondritic composition (Nazarov et al., 1990). Samples from above and below the Petriccio and Elendgraben sites have lower Ru/Ir ratios and slightly higher Ir concentrations than other background samples. Post-depositional enhancement by carbonate dissolution (Rocchia et

al., 1990) may account for the higher values, but mobilization out of the impact layer or continuous input of PGE-rich sediment from continents to the ocean are also possible sources for the anomaly. The importance of generating more background data of this type cannot be overemphasized in order that the behavior of PGE in the sedimentary cycle can be fully understood.

CHAPTER NINE
CONCLUSIONS AND FUTURE WORK

Clearly, there is complexity inherent in considering a global catastrophic event which occurred 65 million years ago. However, the interpretations of this work attempt a global perspective on K-T events, taking into consideration many variables in PGE geochemistry and clay mineralogy.

Inductively coupled plasma mass spectrometry has afforded a detailed look at the geochemistry of PGE in the K-T boundary clay. The low detection limits for small samples makes it possible to provide new, detailed K-T boundary clay analyses, even on relatively PGE-poor sites, and also much needed data for crustal and mantle-derived rocks. Anomalous PGE concentrations of extraterrestrial origin cannot be identified if background PGE values and those characteristic of terrestrial sources are not clearly defined.

The PGE are now hosted mainly by clay minerals and organic phases. Ruthenium and iridium have undergone the smallest degree of redistribution and by fixing in organics. This work may encourage a change in focus for future PGE work on impact melt rocks and at extinction horizons, since most PGE are shown here to be too mobile to retain original signatures. The discovery of Ru as an important indicator element in the K-T clay allows interelement ratios of Ru and Ir to be used for the first time in PGE cycling models, in estimates of possible volcanic input and for impactor identification.

Worldwide dispersal of PGE in condensed ejecta glass and the subsequent alteration of this original host to smectite have provided the first opportunity to study the effects of PGE mobilization in the terrestrial and marine realm. In terrestrial sites,

subsequent alteration of smectite to I/S mixed layer clay in an organic, high K^+ activity, high pH environment may have resulted in expulsion of interlayer cation PGE and water and caused further remobilization of PGE. Ruthenium is more soluble under oxidizing conditions and more likely to be associated with organic phases than Ir, vital facts for the understanding the ratios of these "least mobile" PGE. The redistribution of continental PGE or remobilization of PGE may have played important roles in generating anomalous PGE values above the marine boundary clay layer.

The first evidence to support fractionation of PGE during impact volatilization and condensation is presented here. This will have implications for the use of PGE and their ratios in identifying impactors from ejecta deposits at known impact sites and for identifying geochemical evidence of large impacts in the past.

Studies of mantle-derived rocks with PGE abundances representative of Tertiary mantle compositions are vital in assessing the degree of terrestrial input into the K-T boundary clay. The concentrations and interelement ratios indicate that the mantle was not the primary source of metals for the K-T, but that some input from Deccan Trap volcanism may have affected the PGE in marine sites. The largest PGE database ever compiled for the Deccan Traps is presented here. Addition of $\approx 15\%$ Deccan Trap material to proximal marine sites could have raised the Ru/Ir above chondrite values, although this is still considered unlikely. The Manson impact occurred close in time to the large K-T impact and may have had an effect on the proximal terrestrial sites.

PGE analysis of a terrestrial K-T site in Europe, South America or Australasia would provide an opportunity to test some of the theories presented here. If the Ru/Ir ratios were higher at such a site, fractionation of PGE during condensation in the ejecta

cloud would be given further support and the effect of post-sedimentary alteration could be more firmly established. The analysis of the melt rock from the K-T impact crater (Chicxulub?) may provide some of the answers we can as yet only infer from the ejecta layer.

The use of PGE in impactor identification is limited by the number of variables involved, most of which cannot be determined at present. They can be used to support interpretations made using other evidence and elemental abundances (e.g., Ni, Cr).

This work has provided needed insight into the behavior of PGE in both the marine and terrestrial environments and into PGE mobility under low temperature diagenetic and burial metamorphic conditions. However, the geochemistry of these elements under certain conditions still remains largely unknown. Future work necessary for a better understanding of PGE geochemistry include the following:

1. What are the solubilities of the PGE under varying conditions of temperature, pH, salinity and redox potential? Experimental determinations of such parameters would be fairly simple using analytical procedures such as those utilized here. Such information has applications to studies of PGE in the marine environment, for PGE cycles and for PGE associations in organic and acidic complexes. 2. More analyses of PGE abundances in various crustal rocks will help elucidate the distribution of the elements, their low temperature geochemical affinities and in the identification of true anomalies. Other extinction horizons related to extraterrestrial impact and ancient melt rocks may be identified on the basis of PGE abundances and interelement ratios established here.

3. The fractionation of PGE upon meteorite impact, volatilization and condensation must be clearly understood before these elements may be used in projectile identification of

known craters or horizons such as the K-T. Controlled experimental studies with simulated compositions of known impactors and various targets must be made.

4. New techniques of high resolution electron microscopy are being used to investigate crystalline materials on the atomic scale (von Harrach, 1991). Such technology could be applied to the investigation of where PGE are structurally located in various mineral phases such as clays, organic matter, sulphides and chromite. The location of the metals within these phases directly affects the ease of their removal, and is imperative to understanding potential elemental mobility.

REFERENCES

Ager, D.W. 1973. The Nature of the Stratigraphic Record. New York, MacMillan. 144pp.

Ahrens, L.H. 1954. The lognormal distribution of the elements (a fundamental law of geochemistry and its subsidiary). *Geochim. Cosmochim. Acta* 5: 49-73.

Alexopoulos, J.S., Grieve, R.A.F. and Robertson, P.B. 1988. Microscopic lamellar deformation features in quartz: Discriminative characteristics of shock-generated varieties. *Geology* 16: 796-99.

Alvarez, L.W., Alvarez, W., Asaro, F., and Michel, H.V. 1980. Extraterrestrial cause for the Cretaceous-Tertiary extinction. *Science* 208: 1095-1108.

Alvarez, L.W. and Lowrie, W. 1981. Upper Cretaceous to Eocene limestones of the Scaglia Rossa are not Miocene turbidites. *Nature* 194: 246-48.

Alvarez, W.,L. Alvarez, W., Asaro, F. and Michel, H.V. 1982. Current status of the impact theory for the terminal Cretaceous extinction, In L.T. Silver and P.H. Schultz eds., Geological Implications of Impacts of Large Asteroids and Comets on the Earth. *Geol. Soc. Am. Spec. Pap. 190*: 305-13.

Alvarez, W. 1986. Toward a theory of impact crises. *EOS* Sept. 2: 649-58.

Alvarez, W. and Asaro, F. 1990. An extraterrestrial impact. *Scientific American*, October, 1990: 78-84.

Anders, E. and Grevesse, N, 1989. Abundances of the elements: Meteoritic and solar. *Geochim. Cosmochim. Acta* 53: 2363-80.

Arndt, N.T. and Jochum, K.-P. 1990. Komatiites: unreliable witnesses of the Archean mantle. In S.E. Ho, J.E. Glover, J.S. Myers and J.R. Muhling eds., Excursion Guidebook, Third International Archean Symposium, Perth, 1990: 147-8.

Baragar, W.R.A. and Lamontagne, C.G. 1980. The Circum-Ungava Belt in eastern Hudson Bay: The geology of Sleeper Islands and parts of the Ottawa and Belcher islands. Current Research, Part A, Geological Survey of Canada, Paper 80-1A, p. 89-94.

Baragar, W.R.A. and Scoates, R.F.J. 1987. Volcanic geochemistry of the northern segments of the Circum-Superior Belt of the Canadian Shield. *Geological Society Spec. Pub.* 33: 113-31.

Barnes, S-J., Naldrett, A.J. and Gorton, M.P. 1985. The origin of the fractionation of platinum-group element in terrestrial magmas. *Chem. Geol.* 53: 303-23.

Barnes, S-J., Boyd, R., Korneliussen, A., Nilsson, L-P., Often, M., Pedersen, R.B. and Robins, B. 1988. The use of mantle normalization and metal ratios in discriminating between the effects of partial melting, crystal fractionation and sulphide segregation on platinum-group elements, gold, nickel and copper: examples from Norway. In; H.M. Prichard, P.J. Potts, J.F.W. Bowles and S. Cribb (eds.) Geo-platinum 87, Elsevier, Barking, 113-43.

Birkelund, T. and Bromley, R.G. 1979. Cretaceous-Tertiary boundary events, v. 1, The Maastrichtian and Danian of Denmark: Copenhagen, University of Copenhagen, pp. 210.

Birkelund, T. and Hakansson, E. 1982. The terminal Cretaceous extinction in Boreal shelf areas-a multicausal event, In L.T. Silver and P.H. Schultz eds., Geological Implications of Impacts of Large Asteroids and Comets on the Earth. *Geol. Soc. Am. Spec. Pap. 190*: 373-84.

Blatt, H., Middleton, G. and Murray, R. 1980. Origin of Sedimentary Rocks, Second Edition. Prentice-Hall, Inc., New Jersey. pp.782.

Bohor, B.B., Foord, E.E. and Ganapathy, R. 1986. Magnesioferrite from the Cretaceous-Tertiary boundary, Caravaca, Spain. *Earth. Planet. Sci. Lett.* 81: 57-66.

Bohor, B.F., Modreski, P.J. and Foord, E.E. 1987a. Shocked quartz in the Cretaceous-Tertiary boundary clays: evidence for a global distribution. *Science* 236: 705-9.

Bohor, B.F., Triplehorn, D.M., Nichols, D.J. and Millard, H.T. Jr. 1987. Dinosaurs, spherules and the "magic" layer: A new K-T boundary clay site in Wyoming. *Geology* 15: 896-99.

Bohor, B.F. 1990a. Shocked quartz and more; Impact signatures in K-T boundary clays, In V.L. Sharpton and P.D. Ward, Global Catastrophes in Earth History: An Interdisciplinary Conference on Impacts, Volcanism and Mass Mortality; Abstracts Presented to the Topical Conference. *Geol. Soc. Am. Spec. Pap. 247*: 335-42.

Bohor, B.F. 1990b. Comment on "Origin of microlayering in worldwide distributed Ir-rich marine Cretaceous/Tertiary boundary clays", B. Schmitz, Geology 16: 1068-72. *Geology* 18: 88-89.

Bohor, B.F. 1990c. Shock induced microdeformation in quartz and other mineralogical indications of an impact event at the Cretaceous-Tertiary boundary. *Tectonophysics* 171: 359-72.

Bourgeois, J., Hansen, T.A., Wiberg, P.L. and Kauffman, E.G. 1988. A tsunami deposit at the Cretaceous-Tertiary boundary in Texas. *Science* 241: 567-69.

Bowles, J.F.W. 1986. The Development of Platinum-Group Minerals in Laterites. *Econ. Geol.* 81: 1278-85.

Brooks, R.R. 1983. Biological Methods of Prospecting for Minerals. John Wiley and Sons, New York. 322pp.

Brooks, R.R. 1984. Elemental anomalies at the Cretaceous-Tertiary boundary, Woodside Creek, New Zealand. *Science* 226: 539-41.

Brooks, R.R., Strong, C.P., Lee, J., Orth, C.J., Gilmore, J.S., Ryan, D.E. and Holzbecher, J. 1986a. Stratigraphic occurrences of iridium anomalies at four Cretaceous/Tertiary boundary sites in New Zealand. *Geology* 14: 727-29.

Brooks, R.R., Hoek, P.L., Reeves, R.D. and Strong, C.P. 1986b. Geochemical delineation of the Cretaceous/Tertiary boundary in some New Zealand rock sequences. *New Zealand Journal of Geology and Geophysics* 29: 1-8.

Bunch, T.E. and Olsen, E. 1975. Distribution and significance of chromium in meteorites. *Geochim. Cosmochim. Acta* 39: 911-27.

Campbell, I.H. and Barnes, S.J. 1984. A model for the geochemistry of the platinum group elements in magmatic sulphide deposits. *Can. Mineral.* 22: 151-60.

Campbell, I.H., Griffiths, R.W. and Hill, R.I. 1989. Melting in an Archean mantle plume: heads it's basalts, tails it's komatiites. *Nature* 339: 697-99.

Carter, N.L., Officer, C.B., Chesner, C,A. and Rose, W.I. 1986. Dynamic deformation of volcanic ejecta from the Toba caldera: possible relevance to Cretaceous/Tertiary boundary phenomena. *Geology* 14: 380-83.

Christensen, L., Fregerslev, S., Simonsen, A and Thiede, J. 1973. Sedimentology and depositional environment of Lower Danian fish clay from Stevns Klint, Denmark. Bull. *Geol. Soc. Denmark* 22: 193-212.

Courtillot, V., Besse, J., Vandamme, D., Montigny, R. Jaeger, J.-J. and Capetta, H. 1986. Deccan flood basalts at the Cretaceous/Tertiary boundary. *Earth Planet. Sci. Lett.* 80: 361-74.

Courtillot, V., Feraud, G., Maluski H., Vandamme, D., Moreau, M.G. and Besse, J. 1988. Deccan flood basalts and the Cretaceous-Tertiary boundary. *Nature* 333: 843-46.

Courtillot, V.E. 1990. A volcanic eruption. *Scientific American* October, 1990: 85-92.

Cousins, C.A. 1973. Notes on the Geochemistry of the Platinum Group Elements. *Transactions of the Geological Society of South Africa* 76(1): 77-81.

Cousins, C.A. and Vermaak, C.F. 1976. The contribution of Southern African ore deposits to the geochemistry of the platinum group metals. *Econ. Geol.* 71: 287-305.

Crocket, J.H., Keays R.R. and Hsieh, S. 1967. Precious metal abundances in some carbonaceous and enstatite chondrites. *Geochim. Cosmochim. Acta* 31: 1615-23.

Crocket, J.H. 1981a. Geochemistry of the Platinum-Group Elements. *Can. Inst. Min. and Metall., Spec. Iss.* 23: 47-64.

Crocket, J.H. 1981b. Analytical Methods for the Platinum-Group Elements. *Can. Inst. Min. and Metall., Spec. Iss.* 23: 72-81.

Crocket, J.H. and MacRae, W.E. 1986. Platinum-Group Element Distribution in Komatiitic and Tholeiitic Volcanic Rocks from Munro Township, Ontario. *Econ. Geol.* 81: 1242-51.

Crocket, J.H., Officer, C.B., Wezel F.C. and Johnson, G.D. 1988. Distribution of noble metals across the Cretaceous/Tertiary boundary at Gubbio, Italy: Iridium variation as a constraint on the duration and nature of Cretaceous-Tertiary events. *Geology* 16: 77-80.

Dence, M. R. 1971. Impact melts. J. Geophys. Res. 76, 5552-65

DePaolo, D.J., Kyte, F.T., Marshall, B.D., O'Neil, J.R. and Smit, J. 1983. Rb-Sr, Sm-Nd, K-Ca, O and H isotopic study of Cretaceous-Tertiary boundary sediments, Caravaca, Spain: evidence for an oceanic impact site. *Earth Planet. Sci. Lett.* 64: 356-73.

Dostal. J., Baragar, W.R.A. and Dupuy, C. 1986. Petrogenesis of the Natkusiak continental basalts, Victoria Island, Northwest Territories, Canada. Can. J. Earth Sci. 23, No. 5, 622-32.

Dyer, B.D., Lyalikova, N.N., Murray, D., Doyle, M., Lolesov, G.H. and Krumbein, W.E. 1989. Role for microorganisms in the formation of Ir anomalies. *Geology* 17: 1036-39.

Ehmann, W.D., Baedecker, P.A. and McKown, D.M. 1970. Gold and iridium in meteorites and some selected rocks. *Geochim. Cosmochim. Acta.* 34: 493-507.

Ekdale, A.A. and Bromley, R.G. 1984. Sedimentology and ichnology of the Cretaceous-Tertiary boundary in Denmark: Implications for the causes of the terminal Cretaceous extinctions. *J. Sed. Pet.* 54: 681-703.

Elliot, W.C., Aronson, J.L., Millard Jr., H.J. and Gierlowski-Kordesch, E. 1989. The origin of the clay minerals at the Cretaceous/Tertiary boundary in Denmark. *Geol. Soc. Am. Bull.* 101: 702-10.

Elson C.M. and Chatt, A. 1983. Determination of Gold in Silicate Rocks and Ores by Coprecipitation with Tellurium and Neutron Activation Spectrometry. *Anal. Chim. Acta* 155: 305-10.

Esbensen, K.H., Buchwald, V.F., Malvin, D.J. and Wasson, J.T. 1982. Systematic compositional variations in the Cape York iron meteorite. *Geochim. Cosmochim. Acta.* 46:1913-20.

Fanning, D.S., Keramidas, V.Z. and El-Desoky, M.A. 1989. Micas. In Mineral in Soil Environments, Second Edition, J.B Dixon and S.B. Weed (eds.), Soil Science Society of America, Madison, Wisconsin: 551-634.

Fastovsky, D.E., McSweeney, K. and Norton, L.D. 1989. Pedogenic development at the Cretaceous-Tertiary boundary, Garfield County, Montana. *J. Sed. Pet.* 59: 758-67.

Feather, C.E. 1976. The Mineralogy of Pt-Group Minerals in the Witwatersrand, South Africa. *Econ. Geol.* 71: 1399-1428.

Finnegan, D.L., Miller, T.M. and Zoller, W.H. 1990. Iridium emissions from Hawaiian volcanoes, In V.L. Sharpton and P.D. Ward eds., Global Catastrophes in Earth History: An Interdisciplinary Conference on Impacts, Volcanism and Mass Mortality. *Geol. Soc. Am. Spec. Pap. 247*: 111-16.

Francis, D. 1985. The Baffin Bay lavas and the value of picrites as analogues of primary magmas. *Contrib. Min. Pet.* 89: 144-54.

Francis, D. 1987. Mantle-melt interaction recorded in spinel lherzolite xenoliths from the Alligator Lake volcanic complex, Yukon, Canada. *J. Pet.*, 28, 569-97.

Fritze, K. and Robertson, R. 1969. Precision in the neutron activation analysis for gold in standard rocks G-1 and W-1, In J.R. DeVoe ed. Modern Trends in Activation Analysis. *Natl. Bur. Standards Spec. Pub.* 312: 1279-83.

Fyfe, F.T. 1990. Comment, In Comments and Replies on "Origin of microlayering in worldwide distributed Ir-rich marine Cretaceous/Tertiary boundary clays". *Geology* Jan 1990 18: 87-88.

Ganapathy, R. 1980. A major meteorite impact on the earth 65 million years ago: Evidence from the Cretaceous-Tertiary boundary clay. *Science* 209: 921-23.

Glen, W. 1990. What killed the dinosaurs? *Am. Sci.* 78: 354-70.

Goldberg, E.G., Hodge, V., Kay, P., Stallard, M. and Koideh, M. 1986. Some comparative marine chemistries of platinum and iridium. *Applied Geochemistry* 1(2): 227-32.

Goldberg, E.D., Koide, M., Bertine, K., Hodge, V. and Stallard, M. 1988. Marine geochemistry-2: scavenging redox. *Applied Geochemistry* 3: 561-71.

Goodfellow, W.D., Nowlan, G.S., McCracken, A.D., Lenz, A.C. and Gregoire, D.C. 1991. Geochemical anomalies near the Ordovician-Silurian boundary, Northern Yukon Territory, Canada. *Historical Biology*, in press.

Gostin, V.A., Haines, P.W., Jenkins, R.J.F., Compston, W. and Williams, I.S. 1986. Impact ejecta horizon within late Precambrian shales, Adelaide geosyncline, South Australia. *Science* 233: 198-200.

Gostin, V.A., Keays, R.R. and Wallace, M.W. 1989. Iridium anomaly from the Acramen impact ejecta horizon; Impacts can produce sedimentary iridium peaks. *Nature* 340: 542-44.

Govindaraju, K. (ed. in chief). 1989. *Geostands. Newslett.* vol XIII, Spec Iss. July, 1989.

Gregoire, D.C. 1985. Selective extraction of organically bound gold in soils, lake sediments and stream sediments. *J. Geochem. Expl.* 23: 299-313.

Gregoire, D.C. 1988. Determination of Platinum, Palladium and Iridium in Geological Materials by Inductively Coupled Plasma Mass Spectrometry with Sample Introduction by Electrothermal Vaporization. *J. Anal. At. Spectrocs.* 3: 309-14.

Grieve, R.A.F. and Floran R.J. 1978. Manicouagan impact melt, Quebec II. Chemical interrelations with basement and formational processes. *J. Geophys. Res.* 82, 750-58.

Grieve, R.A.F., Palme, H. and Plant A.G. 1980. Siderophile-rich particles in the melt rocks at the E. Clearwater structure, Quebec: Their characteristics and relationship to the impacting body. *Contrib. Min. Pet.* 75: 187-98.

Grieve, R.A.F. and Robertson, P.B. 1987. Terrestrial Impact Structures. *Geological Survey of Canada Map 1658A*, Scale 1:63,000,000.

Grieve, R.A.F. 1982. The record of impact on Earth: Implications for a major Cretaceous/Tertiary impact event. In L.T. Silver and P.H. Schultz eds., Geological Implications of Impacts of Large Asteroids and Comets on the Earth. *Geol. Soc. Am. Sp. Pap.* 190: 25-37.

Grieve, R.A.F., Bottomly, R.B., Bouchard, M.A., Robertson, P.B., Orth, C.J. and Atrepp, M. Jr. 1991. Impact melt rocks from New Quebec crater, Quebec, Canada. In Press in *Meteoritics*.

Grim, R.E. 1968. Clay Mineralogy, McGraw-Hill, New York. 185-233.

Groot, J.J., de Jonge, R.B.G., Langereis, C.G., ten Kate, W.G.H.Z. and Smit, J. 1989. Magnetostratigraphy of the Cretaceous-Tertiary boundary at Agost (Spain). *Earth Planet. Sci. Lett.* 94: 385-97.

Haas, J.R. and Haskin, L.A. 1991. Compositional variations among whole-rock fragments of the L6 chondrite Bruderheim. *Meteoritics* 26: 13-26.

Håkansson, E., Bromley, R. and Perch-Nielsen, K. 1974. Maastrichtian chalk of north-west Europe-A pelagic shelf sediment. *International Association of Sedimentologists Special Publication* 1: 211-233.

Hamlyn, P.R., Keays, R.R., Cameron, W.E., Crawford, A.J. and Waldron, H.M. 1985. Precious metals in magnesian low-Ti lavas: implications for metallogenesis and sulphur saturation in primary magmas. *Geochim. Cosmochim. Acta* 49: 1797-1811.

Hansen, H.J., Rasmussen, K.L., Gwozdz, R and Kunzendorf, H. 1987. Iridium-bearing carbon black at the Cretaceous-Tertiary boundary. *Bull. Geol. Soc. Den.* 36: 305-14.

Hildebrand, A.R. and Boynton, W.V. 1990. Proximal Cretaceous-Tertiary boundary impact deposits in the Caribbean. *Science* 248: 843-47.

Hsü, K.J. and Mackenzie, J.A. 1985. A "Strangelove" ocean in earliest Tertiary. In E.T. Sunquist, W. Broecker eds, The Carbon Cycle and Atmospheric CO_2: Natural Variations, Archean to Present. Geophys. Monogr.:32 487-92. Washington, D.C.: Am. Geophys. Union.

Huffman, A.R. 1990. An endogeneous mechanism for extinctions. *Geotimes* August, 1990: 16-17.

Izett, G.A. 1987. Authigenic "shpercules" in K-T sediments at Caravaca, Spain and Raton basin, Colorado and New Mexico, may not be impact derived. *Geol. Soc. Am. Bull.* 98: 78-86.

Izett, G.A. 1990. The Cretaceous/Tertiary boundary interval, Raton Basin, Colorado and New Mexico, and its content of shock-metamorphosed minerals: evidence relevant to the K/T boundary impact-extinction theory. *Geological Society of America Special Paper 249*: 100 pp.

Izett, G.A., Maurrasse, F.J-M.R., Lichte, F.E., Meeker, G.P. and Bates, R. 1990. Tektites in Cretaceous-Tertiary boundary rocks on Haiti. *USGS Open File Report* 90-635: 31 pp.

Jackson, M.L. 1973. Soil Chemical Analysis--Advanced Course. Published by the author, Department of Soil Science, University of Wisconsin, 817pp.

Jones, D.S., Mueller, P.A., Bryan, J.R., Dobson, J.P., Chanell, J.E.T., Zachos, J.C. and Arthur, M.A. 1987. Biotic, geochemical and paleomagnetic changes across the Cretaceous/Tertiary boundary at Braggs, Alabama. *Geology* 15: 311-15.

Karkare, S.G. 1985. Potassic volcanism vis-a-vis the Narmada Rift. *IAVCEI Scientific Assembly*, Abstract: 131.

Kastner, M., Asaro, F., Michel, H.V., Alvarez, W. and Alvarez, L.W. 1984. The precursor of the Cretaceous-Tertiary boundary clays at Stevns Klint, Denmark and DSDP Hole 465A. *Science* 226: 137-143.

Kimberlin, J., Charoonratana, C. and Wasson, J.T. 1968. Neutron activation determination of iridium in meteorites. *Radiochim. Acta* 10: 69-76.

Koeberl, C. 1986. Geochemistry of tektites and impact glasses. *Ann. Rev. Earth Planet. Sci.* 14, 323-50.

Kucha, H. 1982. Platinum-group metals in the Zechstein copper deposits, Poland. *Econ. Geol.* 81: 1578-91.

Kyte, F.T., Smit, J. and Wasson, J.T. 1985. Siderophile interelement variations in the Cretaceous-Tertiary boundary sediments from Caravaca, Spain. *Earth Planet. Sci. Lett.* 73: 183-95.

Lerbekmo, J.F., Evans, M.E. and Baadsgaard, H. 1979. Magnetostratigraphy, biostratigraphy and geochronology of Cretaceous-Tertiary boundary sediments, Red Deer Valley. *Nature* 279: 26-30.

Lerbekmo, J.F. and St. Louis, R.M. 1986. The terminal Cretaceous iridium anomaly in the Red Deer Valley, Alberta, Canada. *Can. J. Earth. Sci.* 23: 120-24.

Lerbekmo, J.F., Sweet, A.R. and St. Louis, R.M. 1987. The relationship between the iridium anomaly and palynological floral events at three Cretaceous-Tertiary boundary localities in western Canada. *Geol. Soc. Am. Bull.* 99: 325-330.

Lesher, C.M. and Arndt, N.T. 1990. Geochemistry of komatiites at Kambalda, Western Australia: Assimilation, crystal fractionation and lava replenishment. In S.E. Ho, J.E. Glover, J.S. Myers and J.R. Muhling eds., Excursion Guidebook, Third International Archean Symposium, Perth, 1990: 149-51.

Luck, J.M. and Turekian, K.K. 1983. Osmium-187/osmium-186 in manganese nodules and the Cretaceous-Tertiary boundary. *Science* 222: 613-15.

Malvin, D.J., Wang, D. and Wasson, J.T. 1984. Chemical classification of iron meteorites- X. Multielement studies of 43 irons, resolution of group IIIE from IIIAB, and evaluation of Cu as a taxonomic parameter. *Geochim. Cosmochim. Acta* 48: 785-804.

Margolis, S.V. and Doehne, E.F. 1988. Trace element and isotope geochemistry of Cretaceous-Tertiary boundary sediments: identification of extraterrestrial and volcanic components. In Global Catastrophes in Earth History: An Interdisciplinary Conference on Impacts, Volcanism and Mass Mortality: Abstracts Presented to the Topical Conference: Houston Texas, *Lunar and Planetary Institute*: 113-14.

Mason, B. 1971. Handbook of Elemental Abundances in Meteorites. Gordon and Braeach, New York N.Y. 555 pp.

McHone, J.F., Niema, R.A., Lewis, R.A. and Yates, A.M. 1989. Stishovite at the Cretaceous-Tertiary boundary, Raton, New Mexico. *Science* 243: 1182-84.

McLaren, D.J. and Goodfellow, W.D. 1990. Geological and biological consequences of giant impacts. *Annual Rev. Earth Planet. Sci.* 18: 123-71.

Melosh, H.J. 1982. The mechanics of large meteoroid impacts in the Earth's oceans. In L.T. Silver and P.H. Schultz eds., Geological Implications of Impacts of Large Asteroids and Comets on the Earth. *Geol. Soc. Am. Sp. Pap. 190*: 121-27.

Mitchell, R.H. and Keays, R.R. 1981. Abundance and distribution of gold, palladium and iridium in some spinel and garnet lherzolites: implications for the nature and origin of precious metal-rich intergranular components in the upper mantle. *Geochim. Cosmichim. Acta* 45: 2425-42.

Morgan, J.W. 1978. Lunar crater glasses and high-magnesium australites: Trace element volatilization and meteoritic contamination. *Proc. Lunar Planet. Sci. Conf. 9th*, 2713-30.

Montanari, A., Hay, R.L., Alvarez, W., Asaro, F., Michel, H.V. and Alvarez, L.W. 1983. Spheroids at the Cretaceous/Tertiary boundary are altered impact droplets of basaltic composition. *Geology* 14:668-72.

Montanari, A. 1986. Spherules from the Cretaceous/Tertiary clay at Gubbio, Italy: the problem of outcrop contamination. *Geology* 11: 1024-26.

Mountain B.W. and Wood, S.A. 1988. Chemical Controls on the Solubility, Transport and Deposition of Platinum and Palladium in Hydrothermal Solutions: A Thermodynamic Approach. *Econ. Geol.* 83: 492-510.

Naldrett, A.J., Hoffman, E.L., Green, A.H. Chou, C-L., Naldrett, S.R. and Adcock, R.A. 1979. The composition of Ni-sulphide ores with particular reference to their content of PGE and Au. *Can. Miner.* 17: 403-15.

Napier, W.M. and Clube, S.V.M. 1979. A theory of terrestrial catastrophism. *Nature* 282: 455-59.

Nazarov, M.A., Korina, M.I., Barsukova, L.D., Kolesnikov, Ye. M., Suponeva, I.V. and Kolesov, G.M. 1990. Material traces of the Tunguska bolide. *Geokhimiya* 5: 627-38.

Nettleton, W.D., Nelson, R.E. and Flach, K.W. 1973. Formation of mica in surface horizons of dryland soils. *Soil Sci. Soc. Am. Proc.* 37: 473-78.

Nichols, D.J., Jarzen, D.M., Orth. C.J. and Oliver, P.Q. 1986. Palynological and iridium anomalies at Cretaceous-Tertiary boundary, south-central Saskatchewan. *Science* 231: 714-17.

Nichols, D.J. and Fleming, R.F. 1988. Plant microfossil record of the terminal Cretaceous event in the western United States and Canada. Abstract in *Lunar Planet. Inst./Natl. Acad. Sci.* 1988: 130-1.

O'Keefe J.D. and Ahrens, T.J. 1982. The interaction of the Cretaceous-Tertiary extinction bolide with the atmosphere, ocean and solid earth. In L.T. Silver and P.H. Schultz eds., Geological Implications of Impacts of Large Asteroids and Comets on the Earth. *Geol. Soc. Am. Sp. Pap. 190*: 103-120.

Officer, C.B. and Drake, C.L. 1983. The Cretaceous-Tertiary transition. *Science* 227: 1161-67.

Officer, C.B. and Drake, C.L. 1985. Terminal Cretaceous environmental events. *Science* 227: 1161-67.

Olmez,I., Finnegan, D.L. and Zoller, W.H. 1986. Iridium emissions from Kilauea volcano. *Journal of Geophysical Research* 91: 653-63.

Palme, H., Hanssens, M.-J., Takahashi, H., Anders, E. and Hertogen, J. 1978a. Meteoritic material at five large impact craters. *Geochim. Cosmochim. Acta* 42, 313-23.

Palme, H., Wolf, R. and Grieve, R.A.F. 1978b. New data on meteoritic material at terrestrial impact craters. *Lunar Planet. Sci.* 9, 856-58.

Palme, H., Göbel, E. and Grieve, R.A.F. 1979. The distribution of volatile and siderophile elements in the impact melt of East Clearwater (Quebec). *Proc. Lunar Planet. Sci. Conf. 10th.*, 2465-2492.

Palme, H. 1980. The meteoritic contamination of terrestrial and lunar impact melts and the problem of indigenous siderophiles in the lunar highland. *Proc 11th Lunar Planet. Sci. Conf., Geochim. Cosmochim. Acta Suppl., Vol 1* 14:481-506.

Palme, H., Grieve, R.A.F. and Wolf, R. 1981. Identification of the projectile at the Brent crater, and further considerations of projectile types at terrestrial craters. *Geochim. Cosmochim. Acta,* 45, 2417-24.

Palme, H. 1982. Identification of projectiles of large terrestrial impact craters and some implications for the interpretation of Ir-rich Cretaceous/Tertiary boundary layers. In L.T. Silver and P.H. Schultz eds., Geological Implications of Impacts of Large Asteroids and Comets on the Earth. *Geol. Soc. Am. Sp. Pap. 190*: 223-34.

Pernika, E. and Wasson, J.T. 1987. Ru, Re, Os, Pt and Au in iron meteorites. *Geochim. Cosmochim. Acta* 51: 1717-26.

Ping, K. and Chifang, C. 1990. A new selective chemical dissolution procedure for chemical speciation studies of anomalous iridium in geological samples. *Chem. Geol.* 82: 51-56.

Pollastro, R.M. and Pillmore, C.L. 1987. Mineralogy and petrology of the Cretaceous-Tertiary boundary clay bed and adjacent clay-rich rocks, Raton Basin, New Mexico and Colorado: A comparative study. *J. Sed. Pet.* 57: 456-66.

Preisinger, A., Zobetz, E., Gratz, A.J., Lahodynsky, R., Becke, M., Mauritsch, H.J., Eder, G., Grass, F., Rogl, F., Stradner, H. and Surenian, R. 1986. The Cretaceous-Tertiary boundary in the Gosau Basin, Austria. *Nature* 322,: 794-99.

Raju, D.S.N., Narasimha Rao, C. and Sengupta, B.K. 1965. Paleocurrents in the miocene Rajahmundry formation, Andhra Pradesh, India. *J. Sed. Pet.* 35: 758-62.

Rambaldi, E.R. 1976. Trace element content of metals from L-group chondrites. *Earth Planet. Sci. Lett.* 31: 224-38.

Rambaldi, E.R. 1977a. Trace element content of metal from H- and LL-group chondrites. *Earth Planet. Sci. Lett.* 36: 347-58.

Rambaldi, E.R. 1977b. The content of Sb, Ge and refractory siderophile elements in metals of L-group chondrites. *Earth Planet. Sci. Lett.* 33: 407-19.

Rampino, M.R. 1982. A non-catastrophist explanation for the iridium anomaly at the Cretaceous/Tertiary boundary. In L.T. Silver and P.H. Schultz eds., Geological Implications of Impacts of Large Asteroids and Comets on the Earth. *Geol. Soc. Am. Sp. Pap. 190*: 455-460.

Rampino, M.R. and Reynolds, R.C. 1983. Clay minerals of the Cretaceous-Tertiary boundary clay. *Science* 219: 495-98.

Rasmussen, H.W. 1971. Echinoid and crustacean burrows and their diagenetic significance in the Maastrichtian-Danian of Stevns Klint, Denmark. *Lethaia* 4:191-216.

Robert, C. and Chamely, H. 1990. Paleoenvironmental significance of clay mineral associations at the Cretaceous-Tertiary passage. *Palaeogeography, Palaeoclimatology, Palaeoecology* 79: 205-19.

Robillard, I., Francis, D.M. and Ludden, J.N. 1991. Trace element constraints on the origin of the Baffin Bay lavas. Submitted to Contrib. Min. Pet.

Rocchia, R., Boclet, D., Courillot, V. and Jaeger, J.-J. 1988. A search for iridium in the Deccan Traps and Inter-Traps. *Geophys. Res. Lett.* 15: 812-15.

Rocchia, R., Boclet, D., Bonté, Ph., Jéhanno, C., Chen, Yan, Courtillot, V., Mary, C. and Wezel, R. 1990. The Cretaceous-Tertiary boundary at Gubbio revisited: vertical extent of the Ir anomaly. *Earth Planet. Sci. Lett.* 99: 206-19.

Ross, J.R. and Keays, R.R. 1979. Precious metals in volcanic-type nickel sulphide deposits in Western Australia, I. Relationship with the composition of the ores and their host rocks. *Can. Mineral.* 17: 417-35.

Schmidt, R.M. and Holsapple, K.A. 1982. Estimates of crater size for large-body impact: gravity-scaling results. In L.T. Silver and P.H. Schultz eds., Geological Implications of Impacts of Large Asteroids and Comets on the Earth. *Geol. Soc. Am. Sp. Pap. 190*: 93-102.

Schmitz, B. 1985. Metal precipitation in the Cretaceous-Tertiary boundary clay at Stevns Klint, Denmark. *Geochim. Cosmochim. Acta* 49: 2361-70.

Schmitz, B. 1988. Origin of microlayering in worldwide distributed Ir-rich marine Cretaceous/Tertiary boundary clays. *Geology* 16: 1068-72.

Sears, D.W., Dallemeyn, G.W. and Wasson, J.T. 1982. The compositional classification of chondrites: II The enstatite chondrite groups. *Geochim. Cosmochim. Acta* 46: 597-608.

Sen Gupta J.G. and Gregoire, D.C. 1989. Determination of Ruthenium, Palladium and Iridium in 27 International Reference Silicate and Iron-Formation Rocks, Ores and Related Materials by Isotope Dilution Inductively Coupled Plasma Mass Spectrometry. *Geostds. Newslett.* XIII: 197-204.

Sethna, S.F. and Sethna, B.S. 1990. Petrology of Deccan Trap basalts of the Western Ghats around Igatpuri and their petrogenetic significance. *J. Geol. Soc. India* 35: 631-43.

Seward, T.M. 1984. The transport and deposition of gold in hydrothermal systems, In R.P. Foster, ed., Gold '82: Rotterdam, A.A. Balkema Pub. pp. 165-181.

Shannon, R.D. 1976. Revised effective ionic radii and systematic studies of interatomic distances in halides and chalcogenides. *Acta Crystall.* 32: 751-67.

Sharpton, V.L and Schuraytz, B.C. 1989. On reported occurrences of shock deformed clasts in the volcanic ejecta from Toba caldera, Sumatra. *Geology* 17: 1040-43.

Shaw, D.M., Dostal, J. and Keays, R.R. 1976. Additional estimates of continental surface Precambrian shield composition in Canada. *Geochim. Cosmochim. Acta.* 40: 73-83.

Shaw, H.F. and Wasserburg, W.V. 1982. Age and provenance of the target material for tektites and possible impactites as inferred from Sm-Nd and Rb-Sr systematics. *Earth. Planet. Sci. Lett.* 60: 155-77.

Shazali, I., Van't Dack, L. and Gijbels, R. 1987. Determination of Precious Metals in Ores and Rocks by Thermal Neutron Activation Spectrometry after Preconcentration by Nickel Sulphide Fire Assay and Coprecipitation with Tellurium. *Anal. Chim. Acta* 196: 49-58.

Shoemaker, E.M., Pillmore, C.L. and Peacock, E.W. 1987. Remnant magnetization of rocks of latest Cretaceous and earliest Tertiary age from drill core at York Canyon, New Mexico. *Geol. Soc. Am. Sp. Pap.* 209: 131-50.

Sigurdsson, H, D'Hondt, S., Arthur, M.A., Bralower, T.J., Zachos, J.C., von Fossen, M. and Channell, J.E.T. 1991. Glass from the Cretaceous/Tertiary boundary in Haiti. *Nature*, 349: 482-87.

Smales, A.A., Mapper, D. and Fouché, K.F. 1967. The distribution of some trace elements in iron meteorites as determined by neutron activation. *Geochim. Cosmochim. Acta* 31:673-720.

Smit, J. 1977. Discovery of a planktonic foraminiferal association between the *Abathomphalus mayaronensis* Zone and the "*Globigerina*" *eugubina* Zone at the Cretaceous/Tertiary boundary in the Barranco del Gredero (Caravaca, SE. Spain). *Koninklijke Nederlandse Akademie van Wetenschappen Proceedings, Series B*, 80(4): 280-301.

Smit, J. and Hertogen, J. 1980. An extraterrestrial event at the Cretaceous-Tertiary boundary. *Nature* 285: 198-200.

Smit, J. and Kyte, F.T. 1984. Siderophile-rich magnetic spheroids from the Cretaceous-Tertiary boundary in Umbria, Italy. *Nature* 310: 403-5.

Smit, J., Groot, H., de Jonge, R. and Smit, P. 1988. Impact and extinction signatures in complete Cretaceous Tertiary (KT) boundary sections, In Global Catastrophes in Earth History: An Interdisciplinary Conference on Impacts, Volcanism and Mass Mortality; Abstracts Presented to the Topical Conference: Houston Texas, *Lunar and Planetary Institute*: 182-83.

Smit, J. 1990. Meteorite impact, extinctions and the Cretaceous-Tertiary boundary. *Geologie en Mijnbouw* 69: 187-204.

Smit, J. 1991. Where did it happen? *Nature* 349: 461-62.

Snedcore, G.W. and Cochran, W.G. 1980. Statistical Methods. Iowa State University Press, Ames, Iowa. 507pp.

Strong, C.P. 1977. Cretaceous-Tertiary boundary at Woodside Creek, northeastern Marlborough. *N.Z. Geol. Surv. Rec.* 3: 47-51.

Strong, C.P., Brooks, R.R., Wilson, S.M., Reeves, R.D. and Orth, C.J., Mao, X-Y., Quintana, L.R. and Anders, E. 1987. A new Cretaceous-Tertiary boundary site at Flaxbourne River, New Zealand: biostratigraphy and geochemistry. *Geochim. Cosmochim. Acta* 51: 2769-77.

Tandon, S.N. and Wasson, J.T. 1968. Gallium, Germanium, indium and iridium variations in a suite of L-group chondrites. *Geochim. Cosmochim. Acta.* 32: 1087-1109.

Toon, O.B., Pollack, J.B., Ackerman, T.P., Turco, R.P., McKay, C.P. and Liu, M.S. 1982. Evolution of an impact-generated dust cloud and its effects on the atmosphere, In L.T. Silver and P.H. Schultz eds., Geological Implications of Impacts of Large Asteroids and Comets on the Earth. *Geol. Soc. Am. Sp. Pap. 190*: 187-200.

Toutain, J-P. and Meyer, G. 1989. Iridium-bearing sublimates at a hot-spot volcano (Piton de la Fournaise, Indian Ocean). *Geophys. Res. Lett.* 16: 1391-1394.

Tredoux, M., De Wit, M.J., Hart, R.J., Lindsay, N.M., Verhagen, B. and Sellschop, J.P.F. 1989. Chemostratigraphy across the Cretaceous-Tertiary boundary and a critical assessment of the iridium anomaly. *J. Geol.* 97: 585-605.

Tschudy, R.H. and Tschudy, B.D. 1986. Extinction and survival of plant life following the Cretaceous/Tertiary boundary event, Western Interior, North America. *Geology* 14: 667-70.

Turpin, L., Rocchia, R., Renard, M. and Boclet, D. 1988. Isotopic (Sr, Nd) and chemical variations across the K-T boundary. *Chem. Geol.* 70: 121.

Van Der Flier-Keller, E. and Fyfe, W.S. 1987. Geochemistry of two Cretaceous coal-bearing sequences: James Bay lowlands, Northern Ontario, and Peace River Basin, northeast British Columbia. *Can. Jour. Earth Sci.* 24:1038-52.

van Ophlen, H. and Fripat, J.J. (eds.). 1979. Data Handbook for Clay Materials and other Non-metallic Minerals. Pergammon Press, 346.

von Harrach, S. 1991. Electron microscope reveals chemical secrets of atomic structures. *New Scientist* 1778: 18.

Wallace, M.A., Gostin, V.A. and Keays, R.R. 1990. Acraman Impact ejecta and host shales; Evidence for low-temperature mobilization of iridium and other platinoids. *Geology* 18: 132-35.

Weast, R.C. 1989. CRC Handbook of Chemistry and Physics. R.C. Weast ed., 69th edition, 1988-9. Chemical Rubber Co. Press Inc., Bocaraton, Fld. I39 pp.

Webster, J.G. and Mann, A.W. 1984. The Influence of Climate, Geomorphology and Primary Geology on the Supergene Migration of Gold and Silver. *J. Geochem. Expl.* 22: 21-42.

Westland, A.D. 1981. Inorganic Chemistry of the Platinum-Group Elements. *Can. Inst. Min. Metal. Spec. Iss.* 23: 5-18.

Wetherill, G.W. and Shoemaker, E.M. 1982. Collision of astronomically observable bodies with the Earth. In L.T. Silver and P.H. Schultz eds., Geological Implications of Impacts of Large Asteroids and Comets on the Earth. *Geol. Soc. Am. Sp. Pap. 190*: 1-13.

Wolbach, W.S., Gilmour, I., Anders, I., Orth, C.J. and Brooks, R.R. 1986. Global wildfires at the Cretaceous-Tertiary boundary. *Nature* 334: 665-67.

Wolf, R., Woodrow, A.B. and Grieve, R.A.F. 1980. Meteoric material at four Canadian impact craters. *Geochim. Cosmochim. Acta* 44, 1015-22.

Zhou, L., Kyte, K.T. and Bohor, B.F. 1991. Cretaceous/Tertiary boundary of DSDP Site 596, South Pacific. *Geology* 19: 694-97.

Zoller, W.H., Parrington, J.R. and Kotra, J.M.P. 1983. Iridium enrichment in airbourne particles from Kilauea Volcano: January 1983. *Science* 222: 1118-1121.

Appendix I

What would be the size of a pure Ir nugget if all the Ir from the richest size-fraction sample (1 gram) was contained in one grain?

The Woodside Creek clay size-fraction has 49.4 ppb Ir (raw data, uncorrected for total weight of Woodside Creek sample).

49.4 ng/g in a 1 gram sample = 49.4×10^{-9} g
Density of Ir $\approx$ 22 g/cm^3

Volume = mass/density
$= 49.4 \times 10^{-9}$ g / 22 g/cm^3
$= 2.25 \times 10^{-9}$ cm^3

1 cm^3 = 1×10^{12} μm^3

1×10^{12} μm^3 x 2.25×10^{-9} cm^3 = 2.25×10^{3} μm^3

Therefore, the grain has a volume of 2.25×10^{3} μm^3 with dimensions of approximately 13μm x 13 μm x 13 μm.

Appendix II

PGE contribution of Deccan Trap volatiles to the marine K-T boundary Ru/Ir values

Variables: x = proportion of chondrite Ru/Ir
y = proportion of Deccan Trap Ru/Ir

$$x(Ru/Ir)_{chondrite} + y(Ru/Ir)_{Deccan} = (Ru/Ir)_{marine\ K\text{-}T}$$

$$x + y = 1$$

$$1\text{-}y(Ru/Ir)_{chondrite} + y(Ru/Ir)_{Deccan} = (Ru/Ir)_{marine\ K\text{-}T}$$

$$y[(Ru/Ir)_{chondrite} + (Ru/Ir)_{Deccan}] = (Ru/Ir)_{marine\ K\text{-}T} - (Ru/Ir)_{chondrite}$$

$$y = 0.164 \approx 16\%$$